First-Principles Phase Diagram Calculations for the Rocksalt-Structure Quasibinary Systems TiN-ZrN, TiN-HfN and ZrN-HfN

Z. T. Y. Liu (Terence Liu)[1], B. P. Burton[2], S. V. Khare[1], D. Gall[3]

1. Department of Physics and Astronomy, University of Toledo, Toledo, OH 43606
2. Materials Measurement Laboratory, Metallurgy Division, National Institute of Standards and Technology (NIST), Gaithersburg, MD 20899
3. Department of Materials Science and Engineering, Rensselaer Polytechnic Institute, Troy, NY 12180,

Department of Physics and Astronomy
University of Toledo

Some Driving Questions from MGI

Transition Metal Nitrides (M_xN_y)

- Can we obtain predictive physical understanding of stable, hard and tough materials for coatings from first-principles calculations?
  - Thermodynamically (multiple-phase stability)?
  - Mechanically (single-phase stability)?
- Can we identify trends of properties and possible correlations between them to restrict the parameter search space?
- How much can we reduce the time and expense for discovering new materials with computational work?
- Can we construct T-x phase diagrams from purely *ab initio* techniques?

Outline

- Transition Metal Nitrides, M_xN_y
- Computational Toolset
  - Density Functional Theory
  - Tools Built on Top of it
- Results 1: Single Phase Properties
- Cluster Expansion Formalism
- Results 2: Solid Solutions (TiN-HfN, TiN-ZrN, HfN-ZrN)

Transition Metal Nitrides (TMNs)

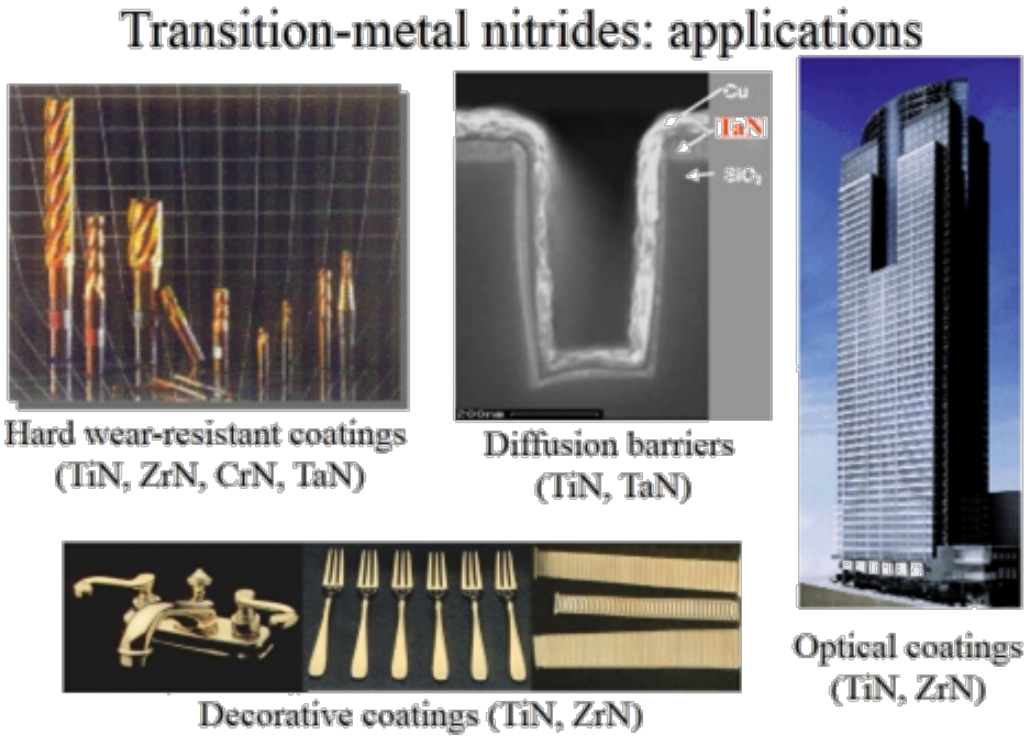

- Wear resistant
- Chemical corrosion and oxidation resistant
- Thermally resistant
- Aesthetically pleasing

Excellent coating materials for multiple purposes. Huge market demand.

Materials Genome Initiative
WWW.MGI.GOV

Computationally achievable on a large scale

Computationally achievable on case by case basis

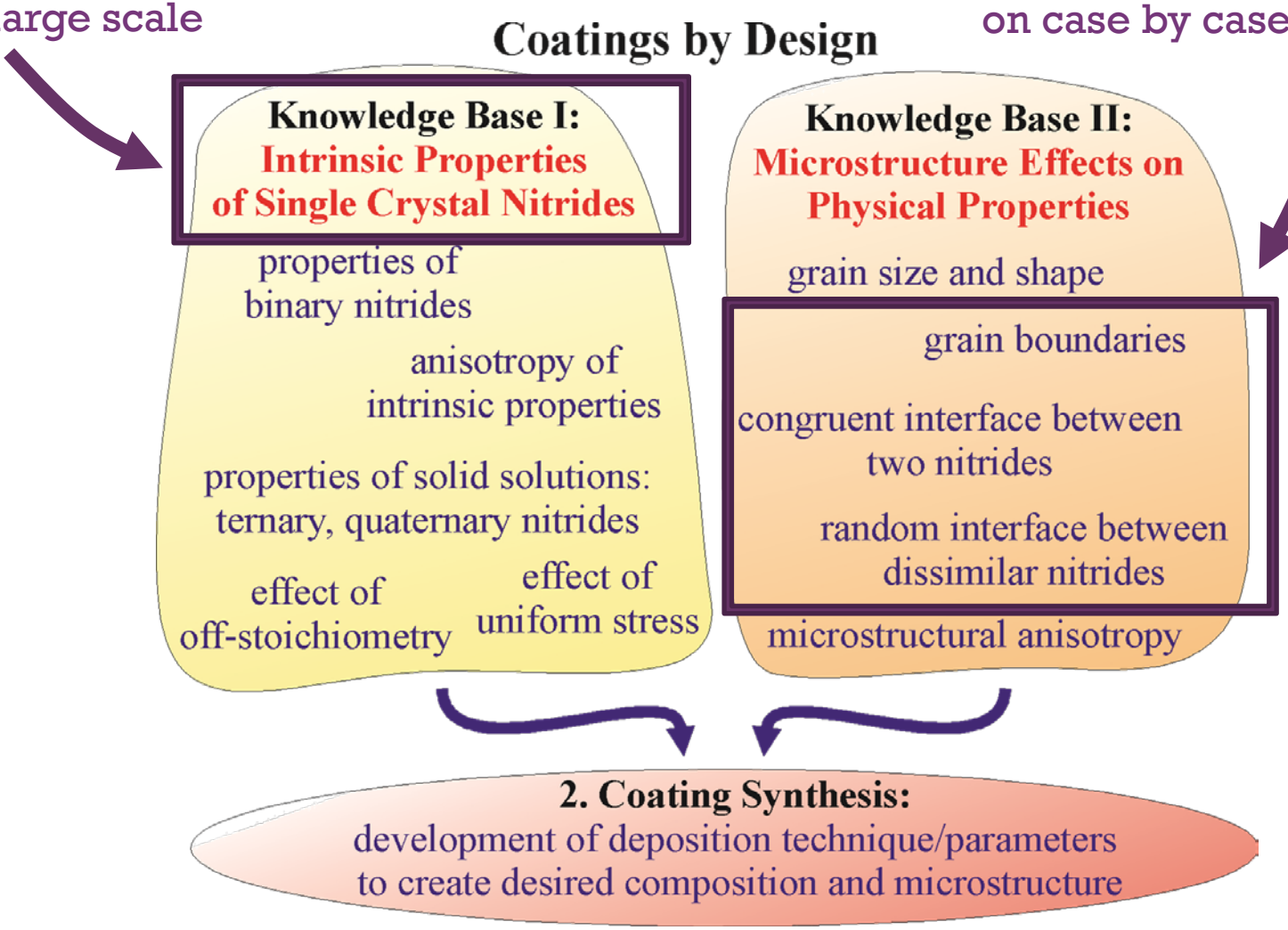

transition metal nitrides

3d
4d
5d

1 H 1.00794																	2 He 4.002602
3 Li 6.941	4 Be 9.012182											5 B 10.811	C 12.0107	7 N 14.00674	8 O 15.9994	9 F 18.9984032	10 Ne 20.1797
11 Na 22.989770	12 Mg 24.3050											13 Al 26.581538	14 Si 28.0855	15 P 30.973761	16 S 32.066	17 Cl 35.4527	18 Ar 39.948
19 K 39.0983	20 Ca 40.078	21 Sc 44.955910	22 Ti 47.867	23 V 50.9415	24 Cr 51.9961	25 Mn 54.938049	26 Fe 55.845	27 Co 58.933200	28 Ni 58.6534	29 Cu 63.545	30 Zn 65.39	31 Ga 69.723	32 Ge 72.61	33 As 74.92160	34 Se 78.96	35 Br 79.504	36 Kr 83.80
37 Rb 85.4678	38 Sr 87.62	39 Y 88.90585	40 Zr 91.224	41 Nb 92.90638	42 Mo 95.94	43 Tc (98)	44 Ru 101.07	45 Rh 102.90550	46 Pd 106.42	47 Ag 196.56655	48 Cd 112.411	49 In 114.818	50 Sn 118.710	51 Sb 121.760	52 Te 127.60	53 I 126.90447	54 Xe 131.29
55 Cs 132.90545	56 Ba 137.327	57 La 138.9055	72 Hf 178.49	73 Ta 180.94.79	74 W 183.84	75 Re 186.207	76 Os 190.23	77 Ir 192.217	78 Pt 195.078	79 Au 196.56655	80 Hg 200.59	81 Tl 204.3833	82 Pb 207.2	83 Bi 208.58038	84 Po (209)	85 At (210)	86 Rn (222)
87 Fr (223)	88 Ra (226)	89 Ac (227)	104 Rf (261)	105 Db (262)	106 Sg (263)	107 Bh (262)	108 Hs (265)	109 Mt (266)	110 (269)	111 (272)	112 (277)		114 (289) (287)		116 (289)		118 (293)

58 Ce 140.116	59 Pr 140.50765	60 Nd 144.24	61 Pm (145)	62 Sm 150.36	63 Eu 151.964	64 Gd 157.25	65 Tb 158.92534	66 Dy 162.50	67 Ho 164.93032	68 Er 167.26	69 Tm 168.93421	70 Yb 173.04	71 Lu 174.967
90 Th 232.0381	91 Pa 231.035888	92 U 238.0289	93 Np (237)	94 Pu (244)	95 Am (243)	96 Cm (247)	97 Bk (247)	98 Cf (251)	99 Es (252)	100 Fm (257)	101 Md (258)	102 No (259)	103 Lr (262)

Published Work

Z. T. Y. Liu, B.P. Burton, S. V Khare, and D. Gall, *J. Phys. Condens. Matter* **29**, 35401 (2017).

Z. T. Y. Liu, D. Gall, and S. V. Khare, *Phys. Rev. B* **90**, 134102 (2014).

Z. T. Y. Liu, X. Zhou, D. Gall, and S. V. Khare, *Comput. Mater. Sci.* **84**, 365 (2014).

Z. T. Y. Liu, X. Zhou, S. V. Khare, and D. Gall, *J. Phys.-Condens. Matter* **26**, 025404 (2014).

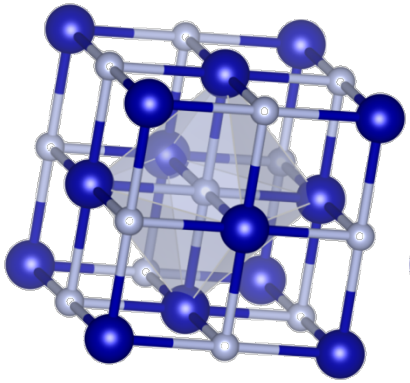

rocksalt (*M*N)

$Fm\bar{3}m$

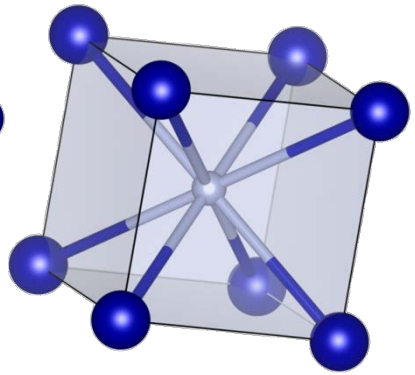

cesium-chloride (*M*N)

$Pm\bar{3}m$

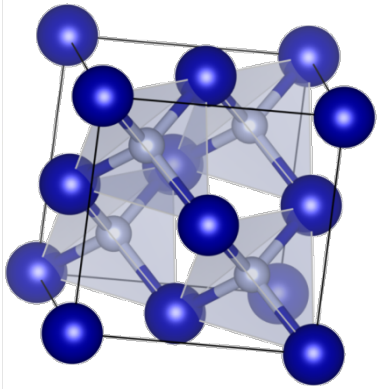

zincblende (*M*N)

$F\bar{4}3m$

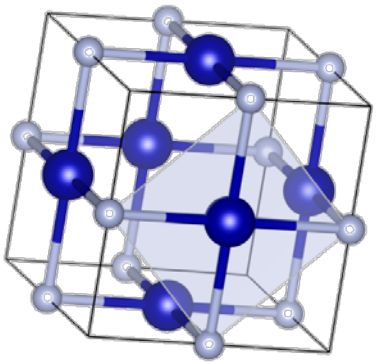

NbO (*M*N)

$Pm\bar{3}m$

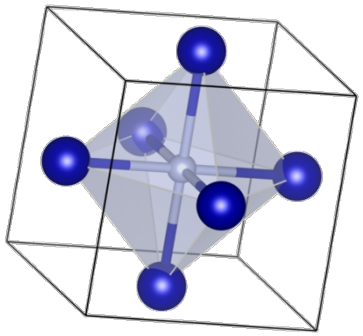

anti-ReO_3 (*M*$_3$N)

$Pm\bar{3}m$

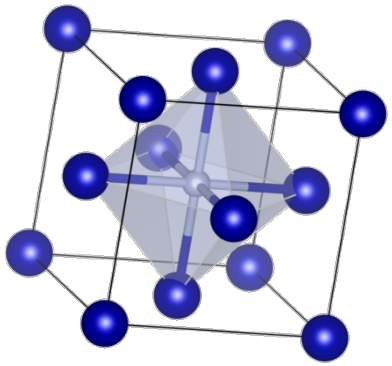

Fe_4N (*M*$_4$N)

$Pm\bar{3}m$

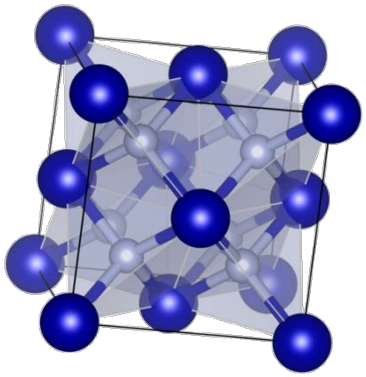

fluorite (*M*N$_2$)

$Fm\bar{3}m$

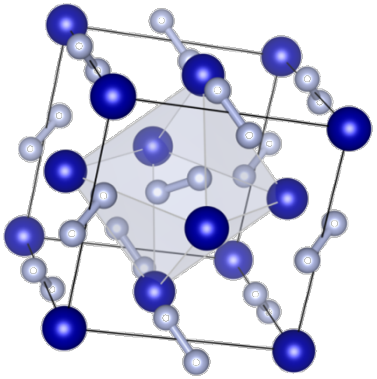

pyrite (*M*N$_2$)

$Pa\bar{3}$

Computed Structures of Transition Metal Nitrides

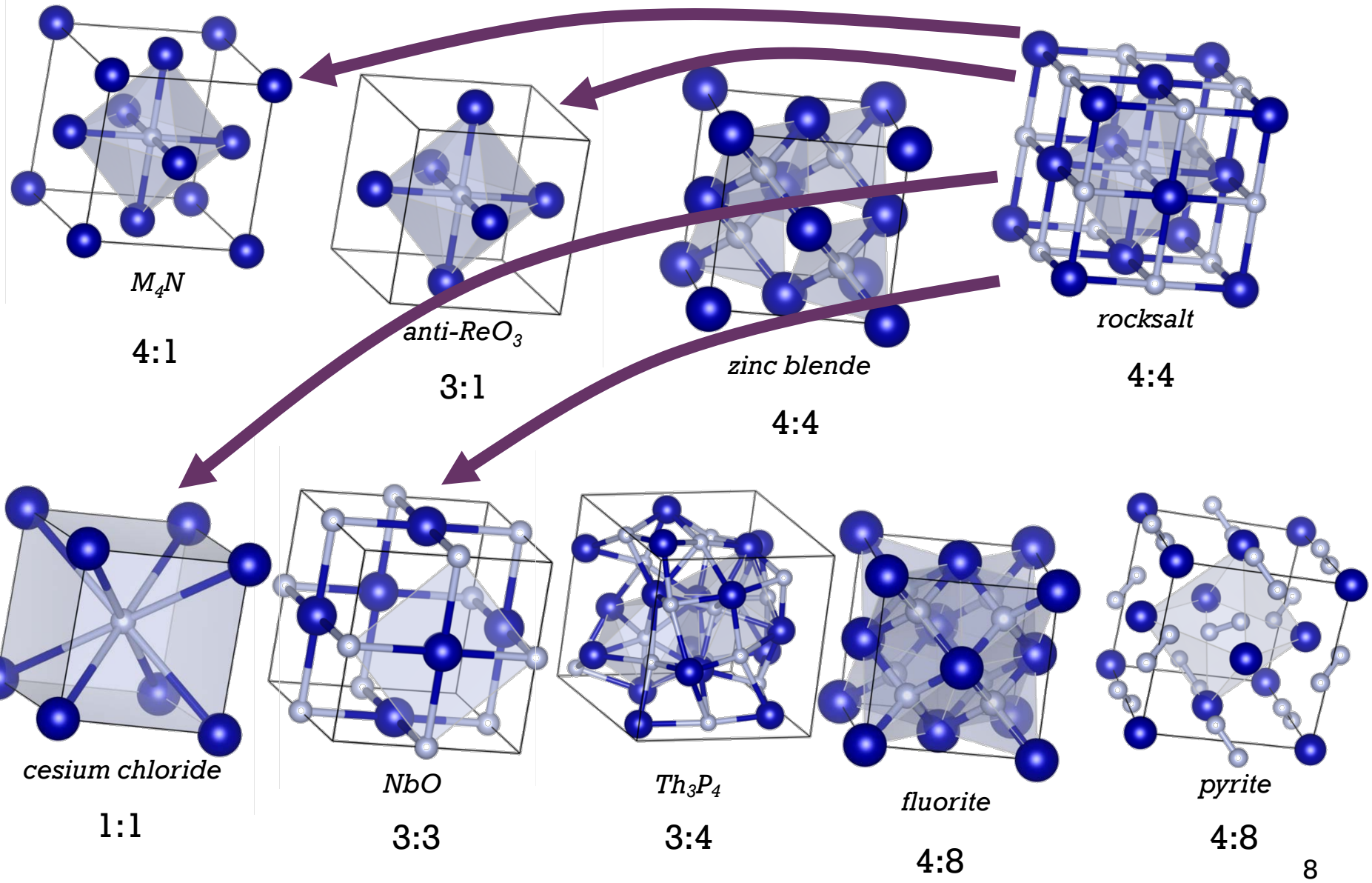

The general procedure

Choice of compositions and structures

DFT program

Obtain single-crystalline properties
e.g. lattice constant, elastic constants, etc.

effective medium theory

Obtain **averaged** poly-crystalline properties
e.g. mechanical moduli, ratios, hardness

visualization

Discover trends and correlations between trends

Identify promising transition metal nitrides and eliminate unfavorable ones

Visualization

Outline

- Transition Metal Nitrides
- Computational Toolset
  - Density Functional Theory
  - Tools Built on Top of it
- Results 1: Single Phase Properties
- Cluster Expansion Formalism
- Results 2: Solid Solutions

- Non-Dissertation Results

Density Functional Theory (DFT)

- The primary feature of DFT is the mapping of a system of N interacting electrons in a given potential $V(\boldsymbol{r})$ to a system of non-interacting electrons acting in an effective potential $V_{eff}(\boldsymbol{r})$.

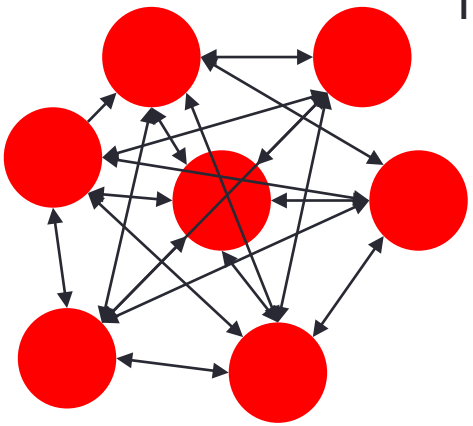

Interacting electrons
+ real potential, $V(\boldsymbol{r})$

Non-interacting fictitious particles + effective potential, $V_{eff}(\boldsymbol{r})$

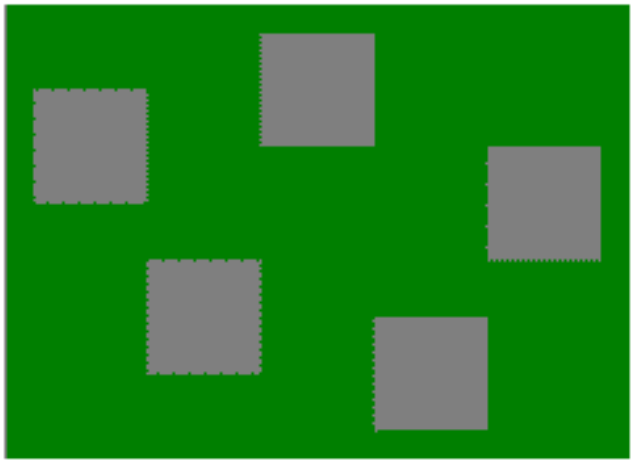

$$\psi\left(\vec{r}_1, \vec{r}_2, ..., \vec{r}_N\right)$$

3N variable

$$\psi\left[n_0\left(\vec{r}\right)\right]$$

3 variable

Figure adapted from http://www.physics.ohio-state.edu/~aulbur/dft.html

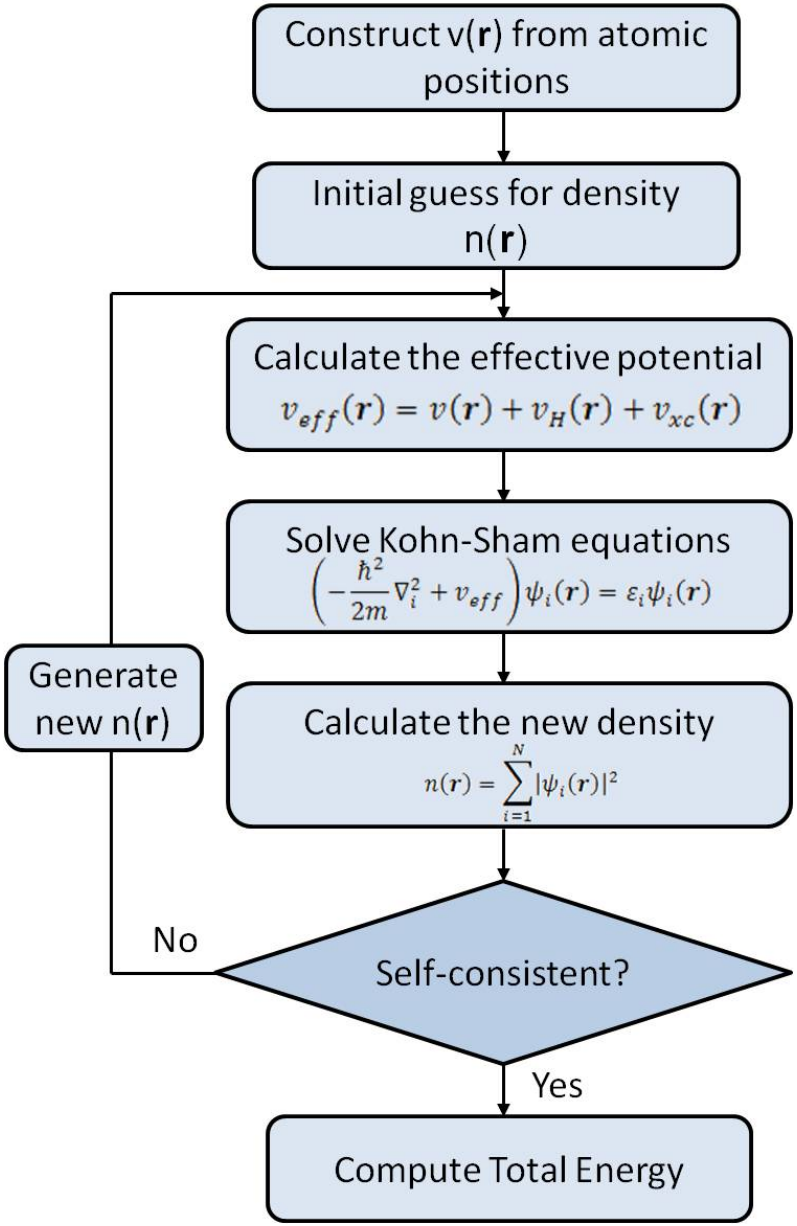

Figure adapted from M. C. Payne *et al.*, *Reviews of Modern Physics*, **64**, 1045, 1992.

Pseudopotentials

- Representation of a pseudopotential V_{pseudo} and pseudo-wavefunction Ψ_{pseudo}.
- Beyond the cutoff radius r_{cutoff}, the pseudopotential and pseudo-wavefunction exactly reproduce the all electron potential and wavefunction.
- Within r_{cutoff}, the 'softer' pseudopotential removes the rapid oscillations of the real, all electron wavefunction as seen by the smooth pseudo-wavefunction.

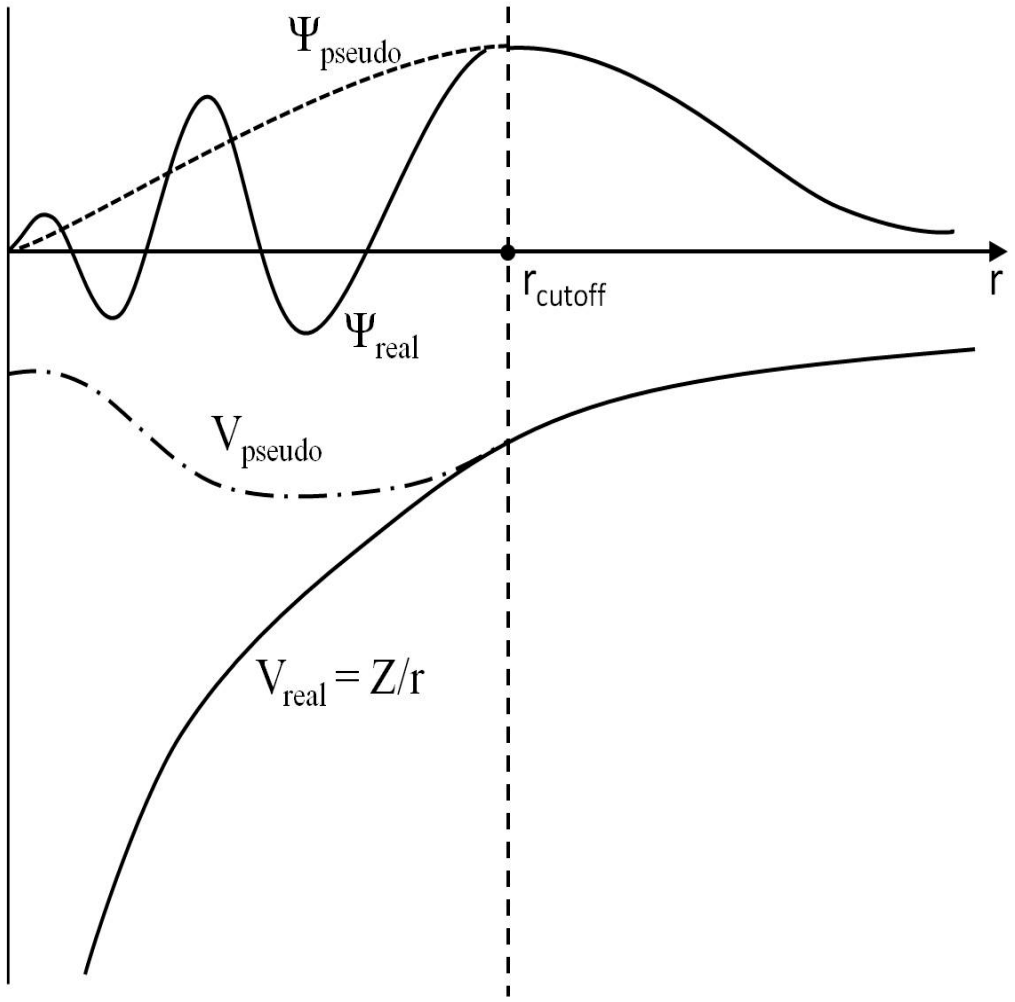

Figure adapted from M. C. Payne *et al.*, Reviews of Modern Physics, vol. 64, no. 4, 1992.

Plane-wave Basis

- Now we can express the wavefunction as

$$\psi_i(\boldsymbol{r}) = \sum_{\boldsymbol{G}} C_{i,\boldsymbol{k}+\boldsymbol{G}} e^{i(\boldsymbol{k}+\boldsymbol{G})\cdot\boldsymbol{r}}$$

- However, a complete expansion with an infinite number of plane-waves is not computationally feasible so we must truncate the expansion
- Since the coefficients of the expansion in equation above decrease rapidly with increasing kinetic energy, the cut off energy for the plane-wave basis set is chosen based on the kinetic energy of the plane-wave.

$$\frac{\hbar^2|\boldsymbol{k}+\boldsymbol{G}|^2}{2m} \leq E_{cut}$$

The Grand Scheme of Things

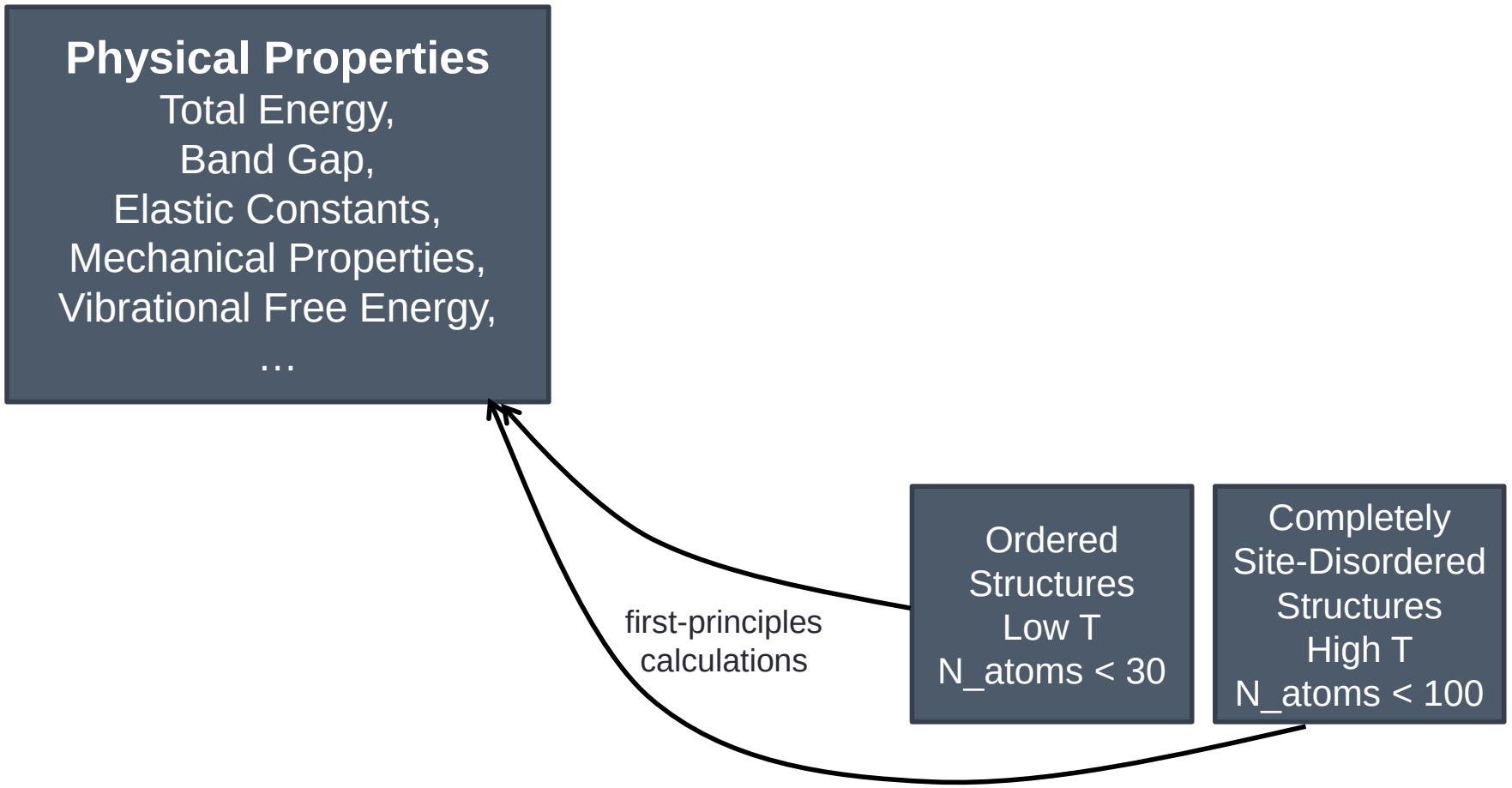

Outline

- Transition Metal Nitrides
- Computational Toolset
  - Density Functional Theory
  - Tools Built on Top of it
- Results 1: Single Phase Properties
- Cluster Expansion Formalism
- Results 2: Solid Solutions

- Non-Dissertation Results

Energy Convex Hull

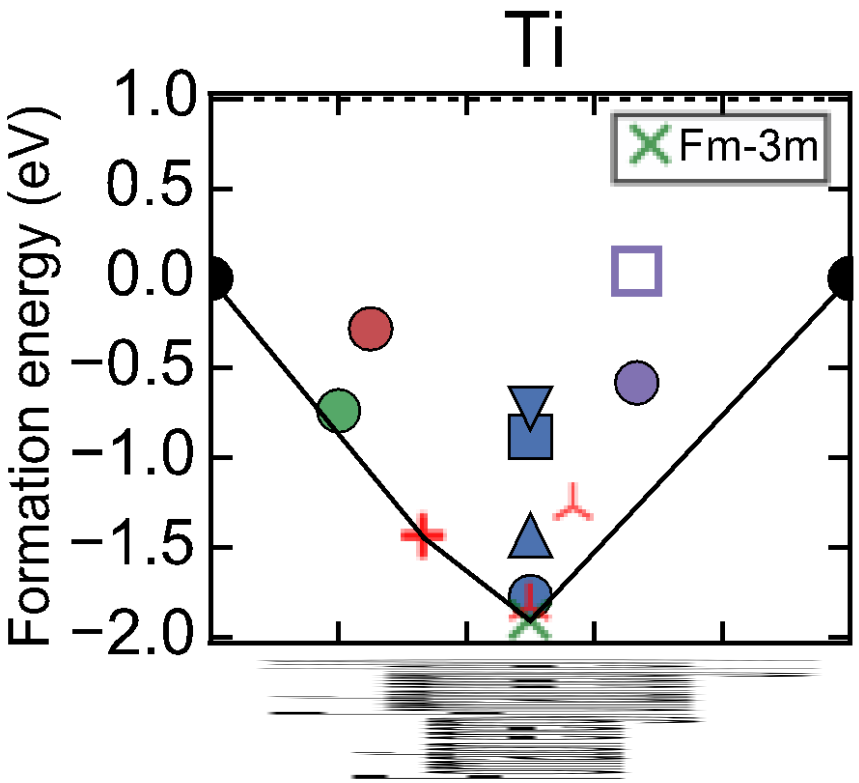

- This describes the energy landscape.
- The values are formation energy per atom, relative to the ground states of the elemental phases at the two ends, denoted by 0.
- The convex vertices are thermodynamically stable members.
- Close to the boundary lines are metastable phases. Metastable phases can still be synthesized through kinetic pathways, e.g. diamond (ΔE_f = 2.4 kJ/mol) vs graphite (0 kJ/mol)

$$\Delta E_f(M_xN_y)/\text{atom} = \frac{1}{x+y}E(M_xN_y) - \frac{x}{x+y}E(M) - \frac{y}{2(x+y)}E(N_2)$$

- Hollow markers are mechanically unstable phases. Criteria for cubic system: $C_{44} > 0$, $C_{11} > C_{12}$, $C_{11} + 2C_{12} > 0$

Energy Convex Hull (Group 3 ~ 7)

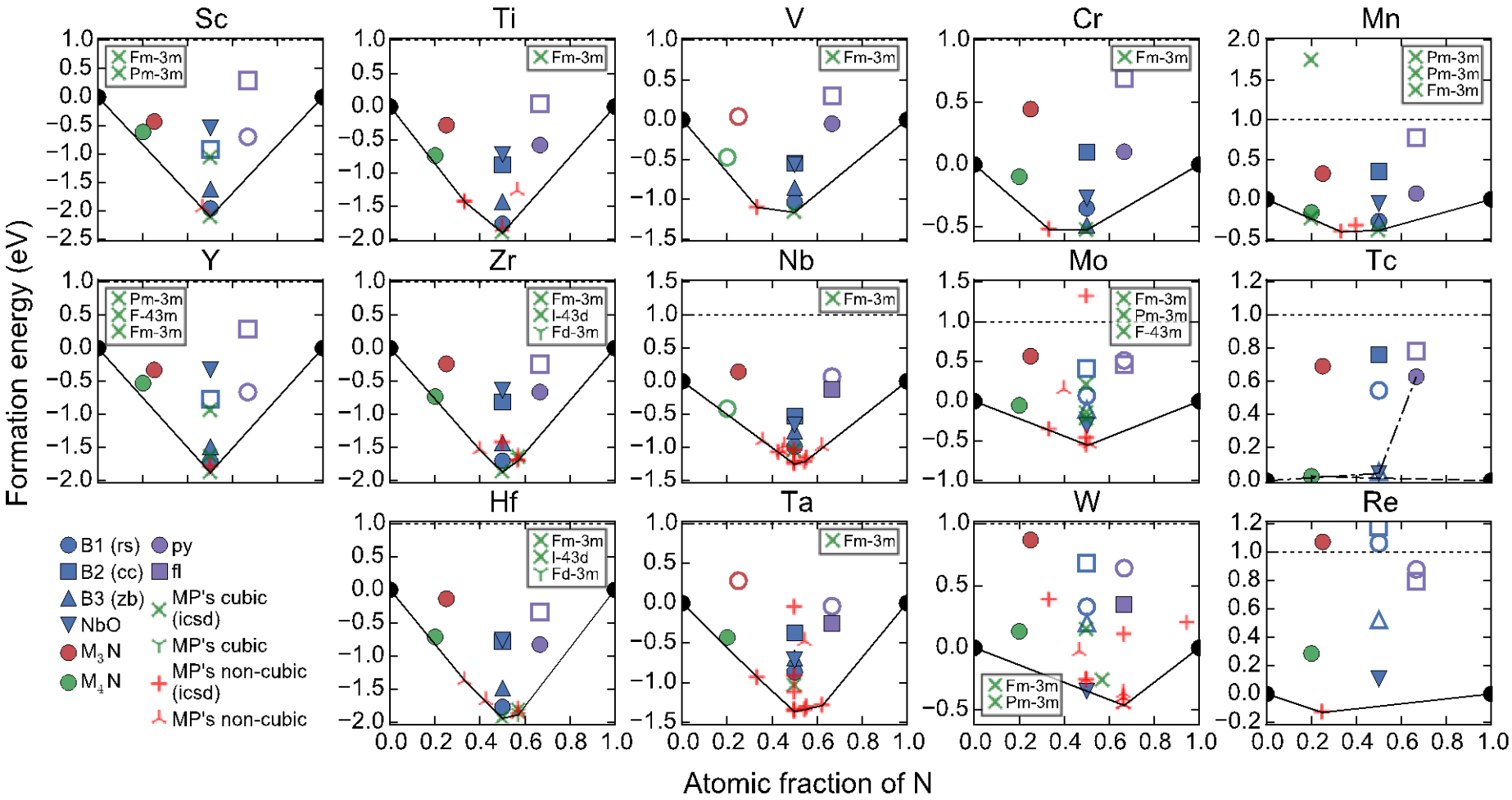

From early to late transition metals, nitrides are increasingly more difficult to form.

Energy Convex Hull (Group 8 ~ 12)

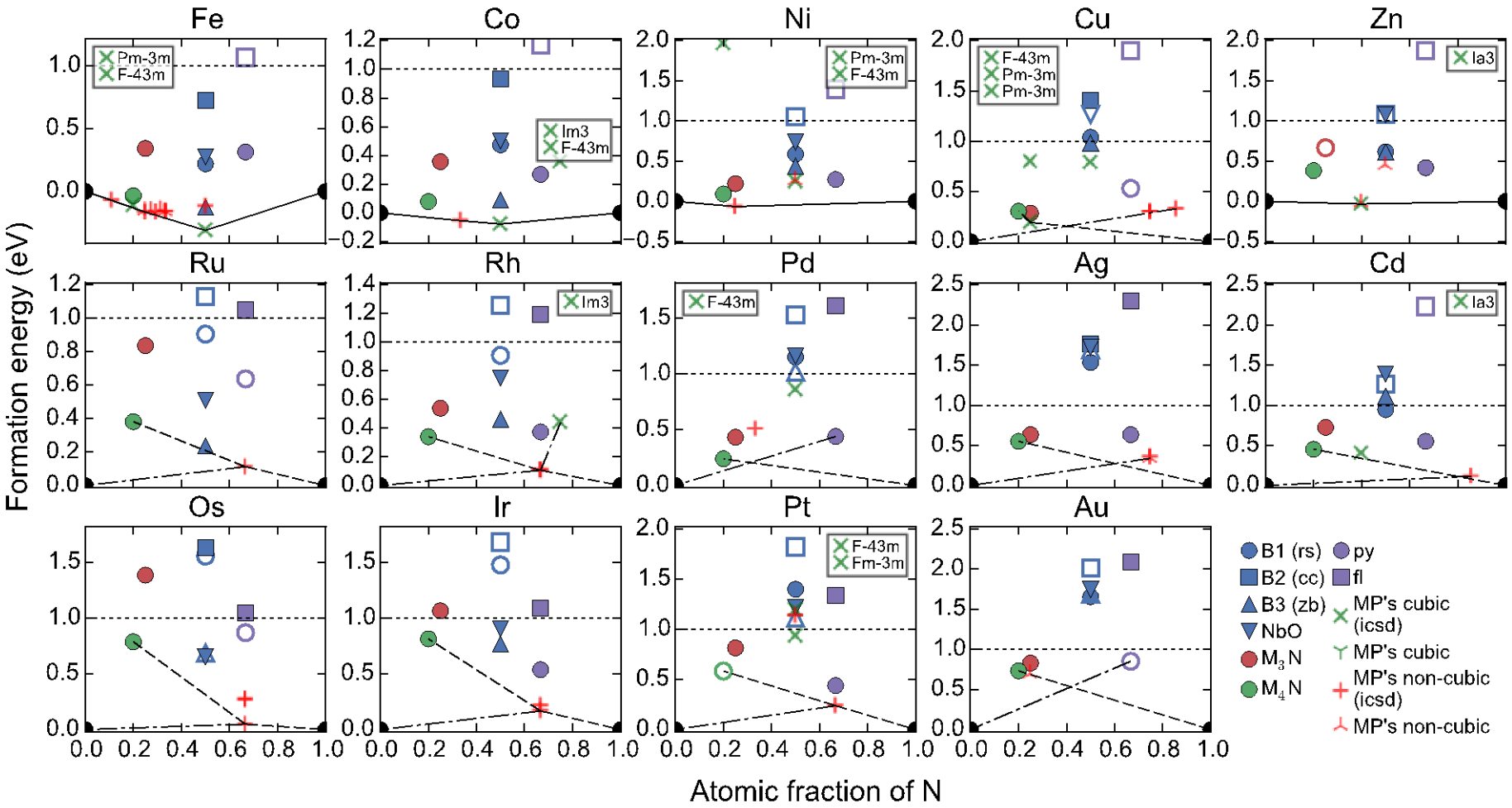

From early to late transition metals, nitrides are increasingly more difficult to form.

Density of States (DOS) and Elastic Constant C_{44}

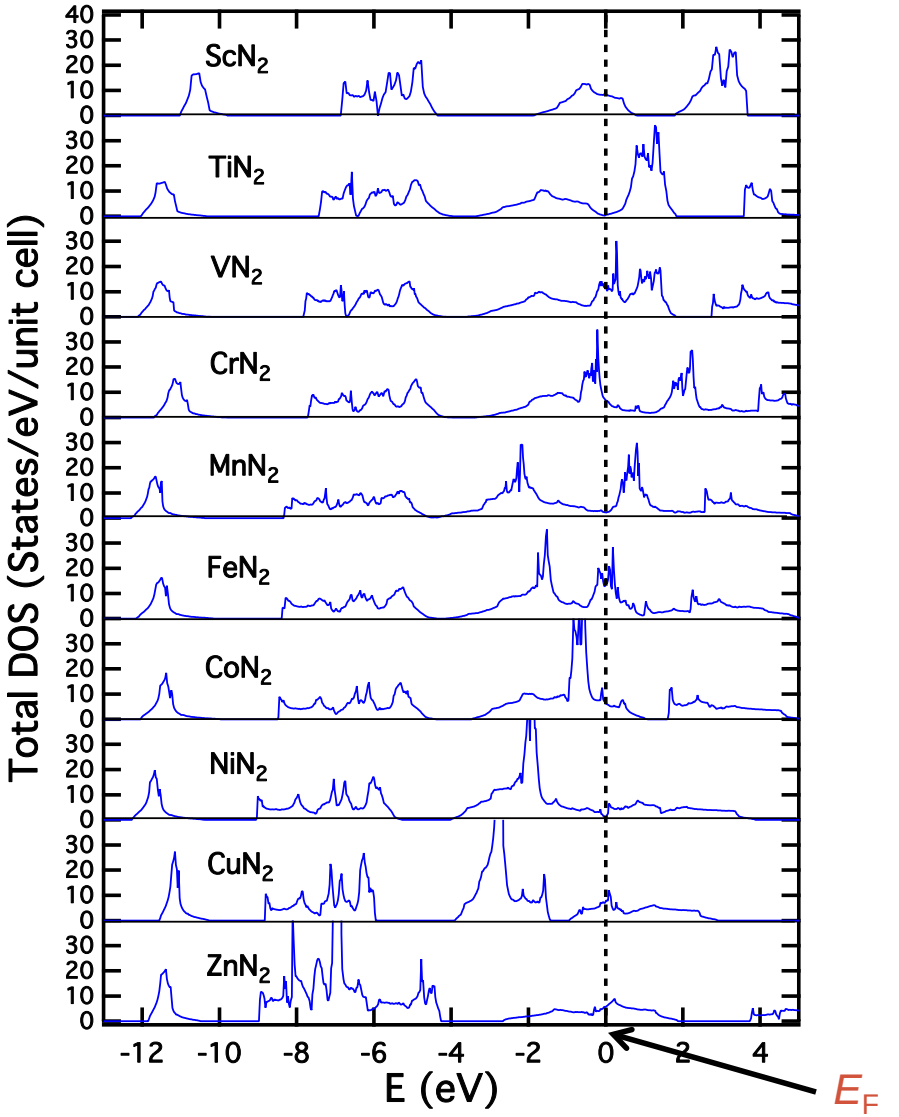

Total DOS of pyrite-structure 3d transition metal pernitrides MN_2.

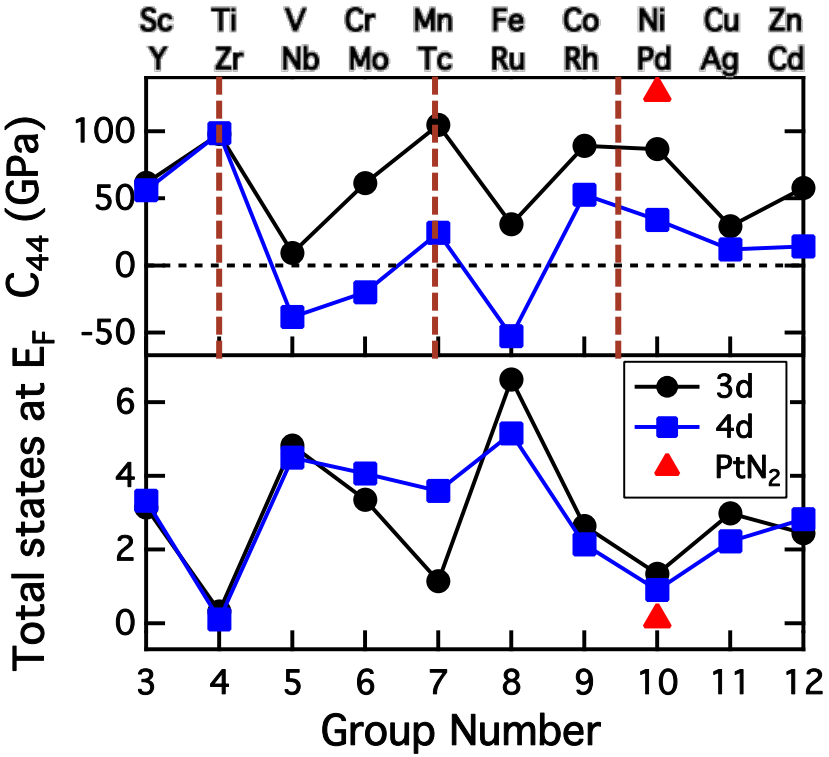

Elastic constant C_{44} and Total DOS at E_F of pyrite-structure 3d, 4d transition metal pernitrides MN_2.

- Left shift and narrowing to accommodate more electrons.
- E_F (Fermi energy) can land on peaks, valleys or plateaus.
- Total DOS at E_F indicates metallicity.
- C_{44} indicates stability and positively correlates with H_V.

Density of States (DOS) and Elastic Constant C_{44}

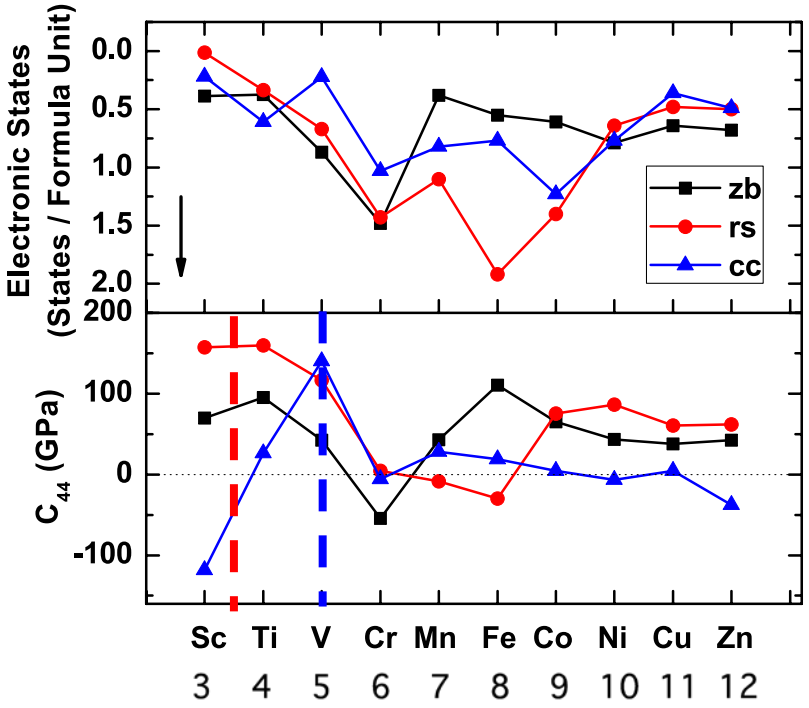

3d transition metal nitrides in zincblende, rocksalt and cesium chloride structures

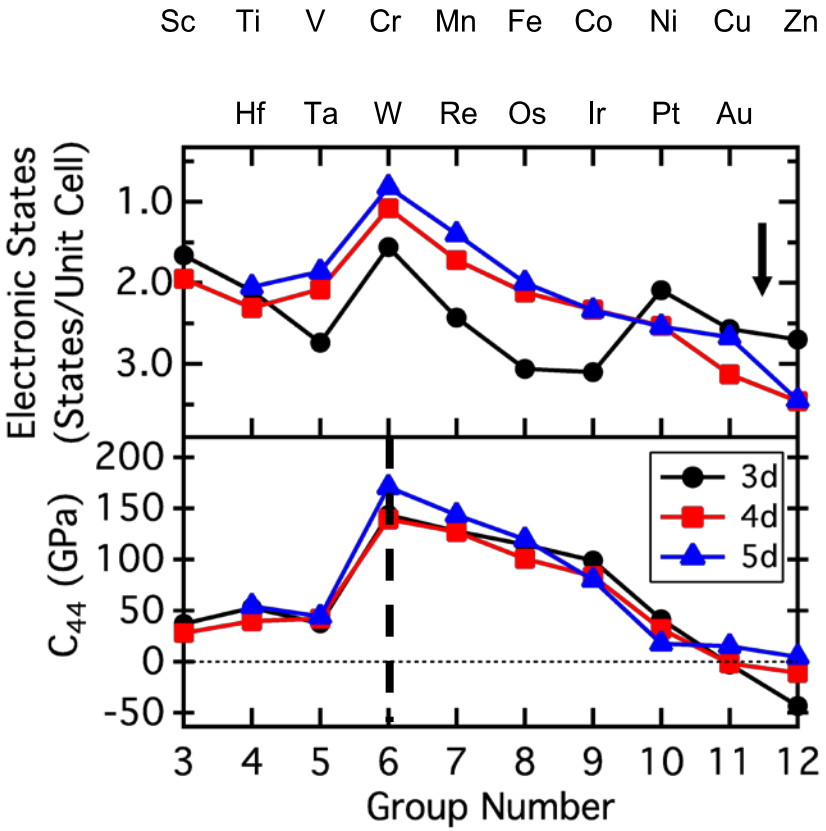

3d, 4d, 5d transition metal nitrides in NbO structure

Z. T. Y. Liu, X. Zhou, D. Gall, and S. V. Khare, *Comput. Mater. Sci.* **84**, 365 (2014).
Z. T. Y. Liu, X. Zhou, S. V. Khare, and D. Gall, *J. Phys.-Condens. Matter* **26**, 025404 (2014).

Difference in B and G
Total pressure vs. shear stress

$B = (C_{11} + 2C_{12})/3$

$G_v = [(C_{11} - C_{12}) + 3C_{44}]/5$

$G_R = [5(C_{11} - C_{12})C_{44}]/[4C_{44} + 3(C_{11} - C_{12})]$

$G = G_{VRH} = (G_v + G_R)/2$

$k = G/B$

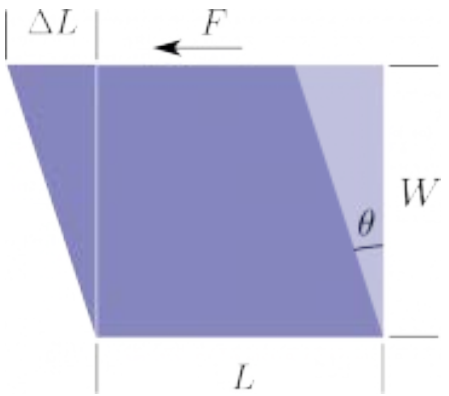

G

Difference in *B* and *G*
An example

Bulk modulus (*B*) only measures the resistance to isotropic hydrostatic pressure, while shear modulus (*G*) measures the resistance to anisotropic shear strain.

TiN (*G*: 187.2 GPa, *B*: 318.3 GPa, H_V: 23 GPa)

β-SiC (*G*: 191.4 GPa, *B*: 224.7 GPa, H_V: 34 GPa)

Gao FM, He JL, Wu ED, Lu SM, Yu LD, Li DC, et al. Phys Rev Lett 2003;91: 015502.
Gou HY, Hou L, Zhang JW, Gao FM. Appl Phys Lett 2008;92:241901.

Tian's alternative for calculating H_V (Vicker's Hardness)

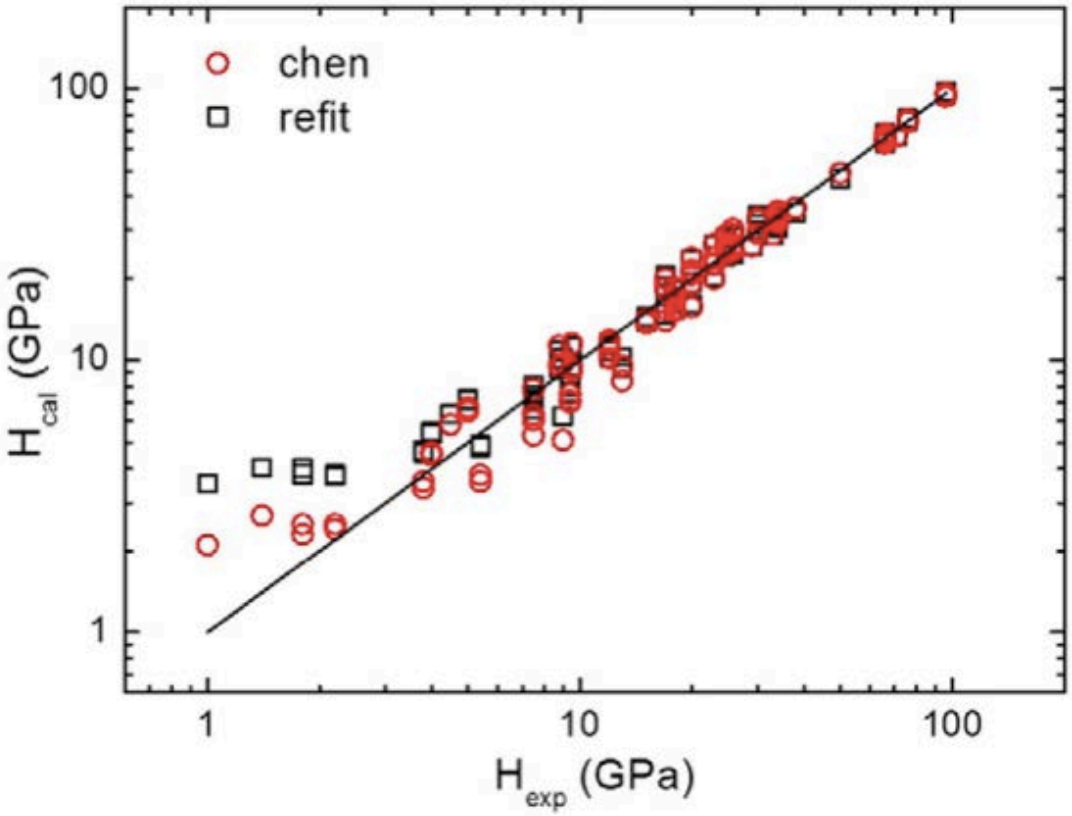

$$B = (C_{11} + 2C_{12})/3$$

$$G_V = [(C_{11} - C_{12}) + 3C_{44}]/5$$

$$G_R = [5(C_{11} - C_{12})C_{44}]/(4C_{44} + 3C_{11} - 3C_{12})$$

$$G = G_{VRH} = (G_V + G_R)/2$$

$$k = G/B$$

Data points (40+ compounds):
Covalent: C, Si, BN…
Ionic: NaCl, KBr…
Metallic glasses

$$H_V = 0.92k^{1.137}G^{0.708}$$

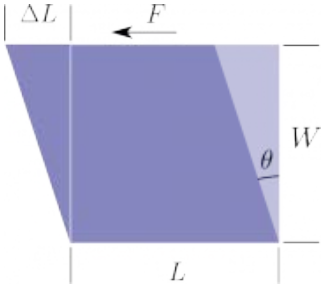

Y. Tian *et al.*, Int. J. Refract. Met. Hard Mater. 33, 93 (**2012**); X. Q. Chen, H. Y. Niu, D. Z. Li and Y. Y. Li, *Intermetallics* 19, 1275 (**2011**).

Crystal	H_{Exp} (GPa)	H_{Tian} (GPa)	$H_{Simunek}$ (GPa)	H_{Xue} (GPa)	H_{Chen} (GPa)
C	96[a]	93.6	95.4[b]	90[e]	94.6[f]
Si	12[a]	13.6	11.3[b]	14[e]	11.2[f]
Ge	8.8[b]	11.7	9.7[b]	11.4[e]	10.4[f]
SiC	31[b]	30.3	31.1[b]	27.8[e]	33.8[f]
BN	63[a]	64.5	63.2[b]	47.7[e]	65.3[f]
BP	33[a]	31.2	26[b]	24.9[e]	29.3[f]
BAs	19[b]	26	19.9[b]	21.1[e]	–
AlN	18[a]	21.7	17.6[b]	14.5[e]	16.8[f]
AlP	9.4[a]	9.6	7.9[b]	7.4[e]	7.2[f]
AlAs	5.0[a]	8.5	6.8[b]	6.3[e]	6.6[f]
AlSb	4.0[a]	4	4.9[b]	4.9[e]	4.4[f]
GaN	15.1[a]	18.1	18.5[b]	13.5[e]	13.9[f]
GaP	9.5[a]	8.9	8.7[b]	8[e]	9.9[f]
GaAs	7.5[a]	8	7.4[b]	7.1[e]	7.8[f]
GaSb	4.5[a]	6	5.6[b]	4.5[e]	5.8[f]
InN	9[a]	10.4	8.2[b]	7.4[e]	7.4[f]
InP	5.4[a]	6	5.1[b]	3.9[e]	3.7[f]
InAs	3.8[a]	3.8	5.7[b]	4.5[e]	3.3[f]
InSb	2.2[a]	4.3	3.6[b]	2.2[e]	2.4[f]
ZnS	1.8[b]	6.8	2.7[b]	2.4[e]	2.4[f]
ZnSe	1.4[b]	5.5	2.6[b]	1.8[e]	2.7[f]
ZnTe	1[b]	4.1	2.3[b]	0.9[e]	2.1[f]
TiC	32[c]	34	18.8[b]	23.9[e]	27[f]
TiN	20.6[c]	21.6	18.7[b]	23.8[h]	23.3[f]
ZrC	25[c]	21	10.7[g]	15.7[h]	27.5[f]

Y. Tian *et al.*, Int. J. Refract. Met. Hard Mater. **33**, 93 (2012).

Crystal	H_{Exp} (GPa)	H_{Tian} (GPa)	$H_{Simunek}$ (GPa)	H_{Xue} (GPa)	H_{Chen} (GPa)
ZrN	15.8[c]	16.7	10.8[g]	15.9[h]	–
HfC	26.1[c]	26.8	10.9[g]	15.6[h]	–
HfN	16.3[c]	18	10.6[g]	15.2[h]	19.2[f]
VC	27.2[c]	23	25.2[g]	17.5[h]	26.2[f]
VN	15.2[c]	14.9	26.5[g]	16.5[h]	–
NbC	17.6[c]	16.1	18.3[b]	12.8[h]	15.4[f]
NbN	13.7[c]	13.6	19.5[b]	12[h]	14.7[f]
TaC	24.5[c]	26	19.9[g]	14.7[h]	–
TaN	22[c]	20	21.2[g]	14.3[h]	–
CrN	11[c]	11	36.6[g]	19.2[h]	–
WC	30[c]	31	21.5[b]	20.6[e]	31.3[f]
Re_2C	17.5[j]	19.7[j]	11.5[g]	16.2[h]	26.4[i]
Al_2O_3	20[c]	18.8	13.5[g]	18.4[h]	20.3[i]
MgO	3.9[d]	4.5	4.4[g]	5.4[h]	24.8[i]
LiF	1[d]	0.8	2.2[g]	–	8.5[i]
NaF	0.6[d]	0.85	1[g]	–	5.7[i]
NaCl	0.2[d]	0.4	0.4[b]	–	2.4[i]
KCl	0.13[d]	0.18	0.2[b]	–	2.3[i]
KBr	0.1[d]	0.23	0.2[g]	–	0.1[i]

[a] Reference [34].
[b] Reference [37].
[c] Reference [32].
[d] Reference [60].
[e] Reference [58].
[f] Reference [30].
[g] Calculated by authors using method [36].
[h] Caculated using [35].
[i] Calculated with [30].
[j] Referenece [52].

Anti-Correlation H_v and TDOS at Fermi Energy E_F

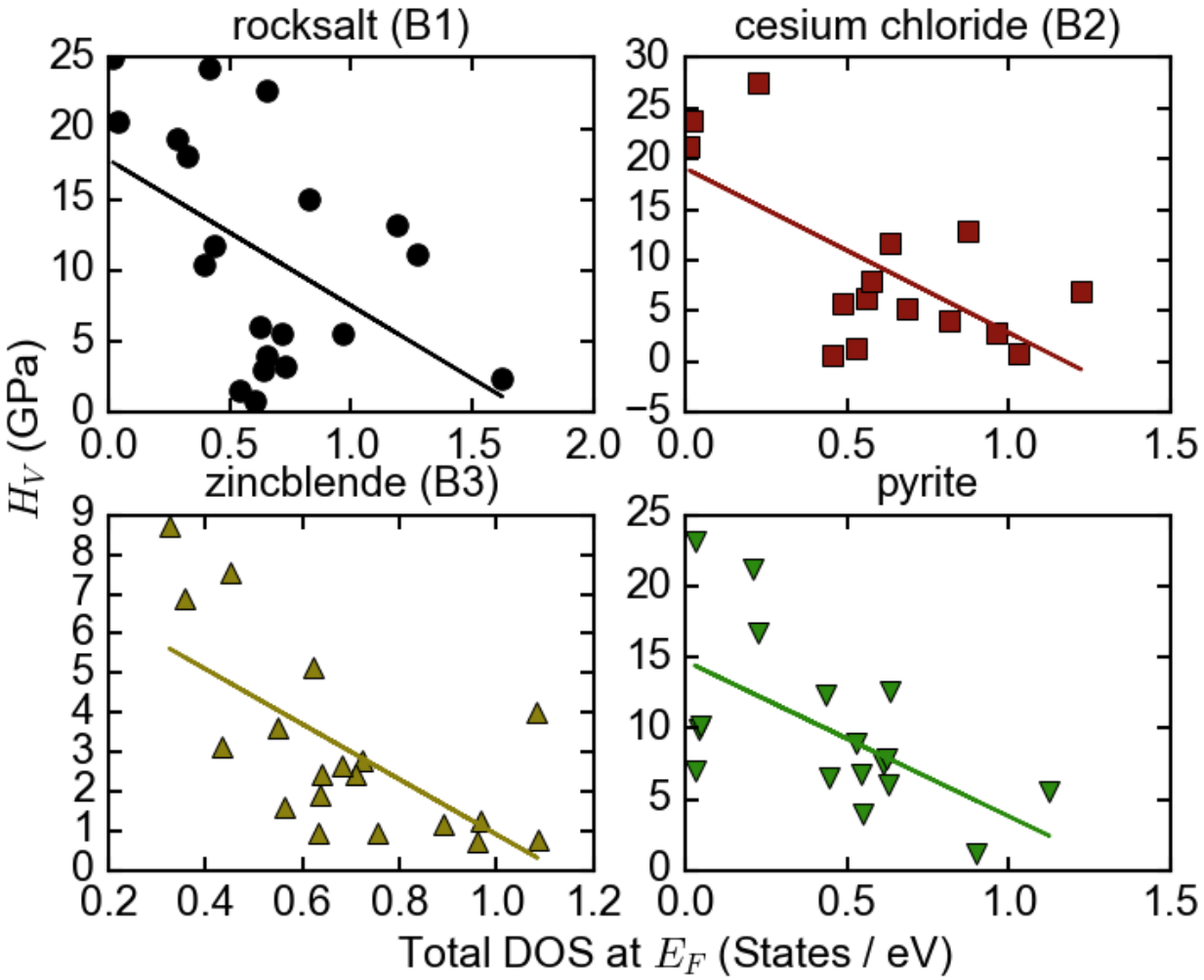

H_V vs k (Pugh's ratio, G/B) x-axis inverted

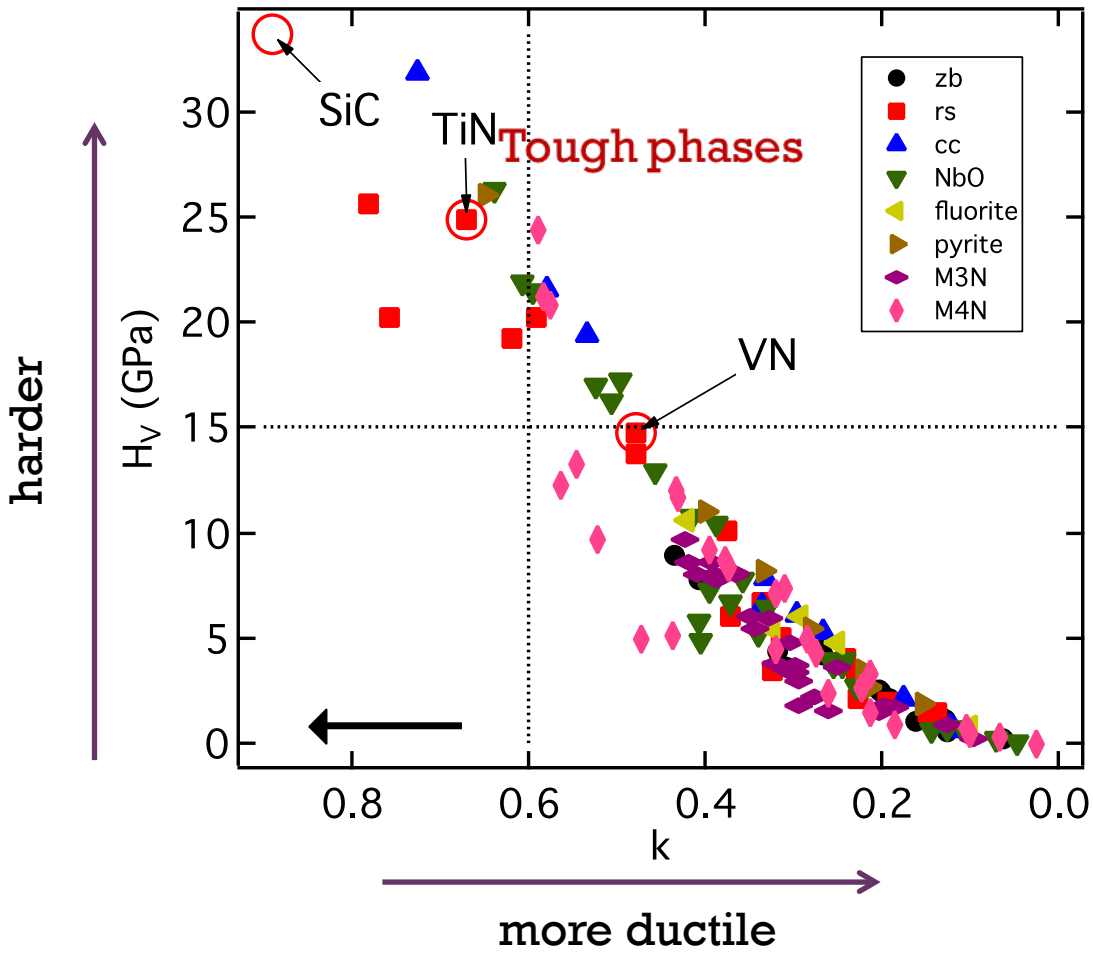

Z. T. Y. Liu, X. Zhou, S. V. Khare, and D. Gall, J. Phys.-Condens. Matter **26**, 025404 (2014).
Z. T. Y. Liu, X. Zhou, D. Gall, and S. V. Khare, Comput. Mater. Sci. **84**, 365 (2014).
S. K. R. Patil, N. S. Mangale, S. V. Khare, and S. Marsillac, Thin Solid Films **517**, 824 (2008).
W. Chen and J. Z. Jiang, J. Alloys Compd. **499**, 243 (2010).
E. J. Zhao, J. P. Wang, J. Meng, and Z. J. Wu, Comput. Mater. Sci. **47**, 1064 (2010).
E. J. Zhao and Z. J. Wu, J. Solid State Chem. **181**, 2814 (2008).

H_{VA} vs P_C (Cauchy's pressure)

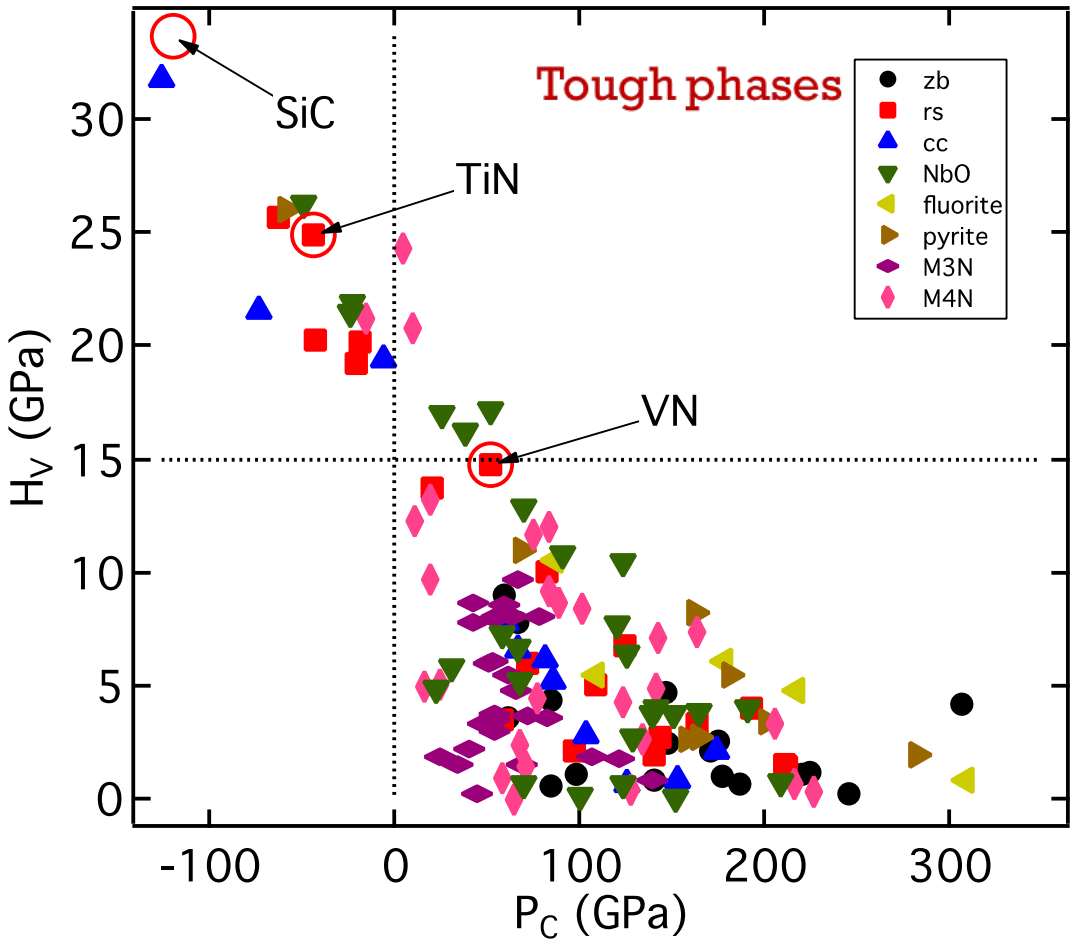

$$Pc = C_{12} - C_{44}$$

Data partly from

W. Chen *et al.*, J. Alloys Compd. **499**, 243 (2010).
E. J. Zhao *et al.*, Comput. Mater. Sci. **47**, 1064 (2010).
E. J. Zhao *et al.*, J. Solid State Chem. **181**, 2814 (2008).

H_{VA} vs ν (Poisson's ratio)

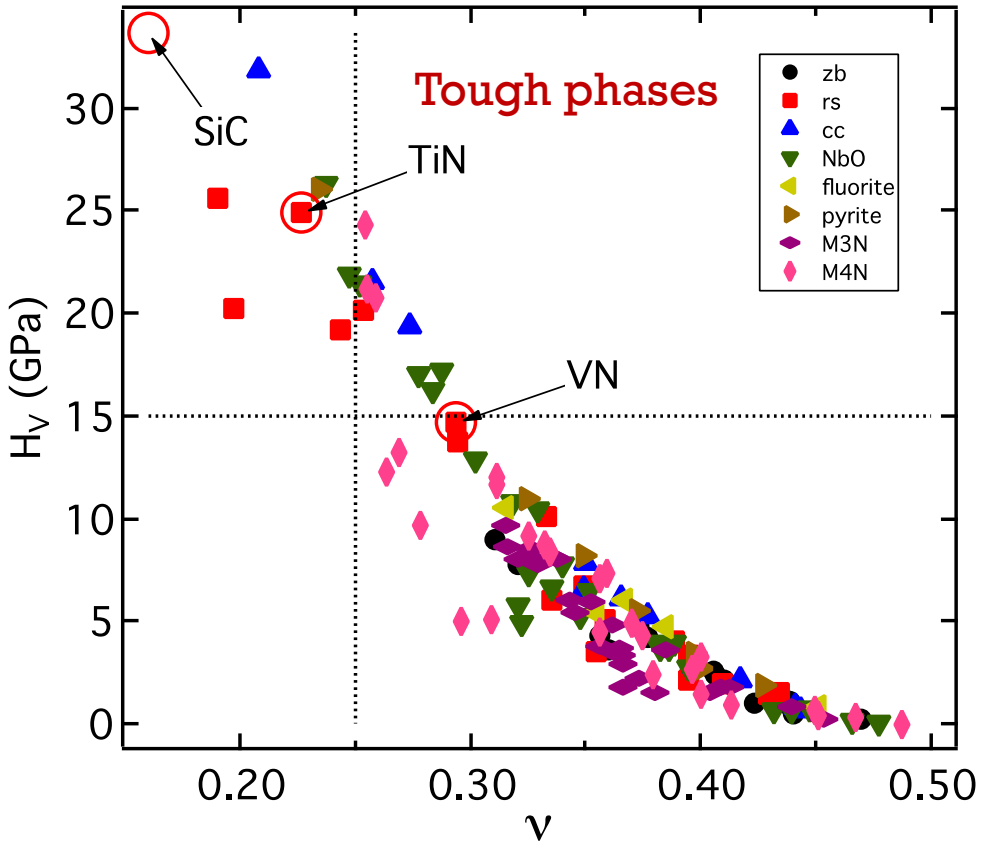

Conclusions for Binary Cubic Phases

- Thermodynamically, energy convex hull draws the energy landscape, and shows a number of insights on the stability of each structural prototypes of TMNs.
- Mechanically, in the cubic structures studied, the anti-correlation between shear-related mechanical properties like H_V and TDOS at E_F is observed for zincblende-, rocksalt-, cesium-chloride-, NbO- and pyrite-structure TMNs in a transition metal period. Structures of other crystallographic systems need to be further studied.
- Hard phases: rocksalt-structure ScN (24.9 GPa), TiN (24 GPa), cesium-chloride-structure VN (29.6 GPa), NbO-structure CrN (21.6 GPa), MoN (21.9 GPa), WN (26.7 GPa), and pyrite-structure MnN_2 (19.9 GPa), PtN_2 (23.5 GPa).
- Several tough phases identified

Published Work

Z. T. Y. Liu, B.P. Burton, S. V Khare, and D. Gall, *J. Phys. Condens. Matter* **29**, 35401 (2017).
Z. T. Y. Liu, D. Gall, and S. V. Khare, *Phys. Rev. B* **90**, 134102 (2014).
Z. T. Y. Liu, X. Zhou, D. Gall, and S. V. Khare, *Comput. Mater. Sci.* **84**, 365 (2014).
Z. T. Y. Liu, X. Zhou, S. V. Khare, and D. Gall, *J. Phys.-Condens. Matter* **26**, 025404 (2014).

astro1.panet.utoledo.edu/ceramicsdb

Community-Based Ceramics Database

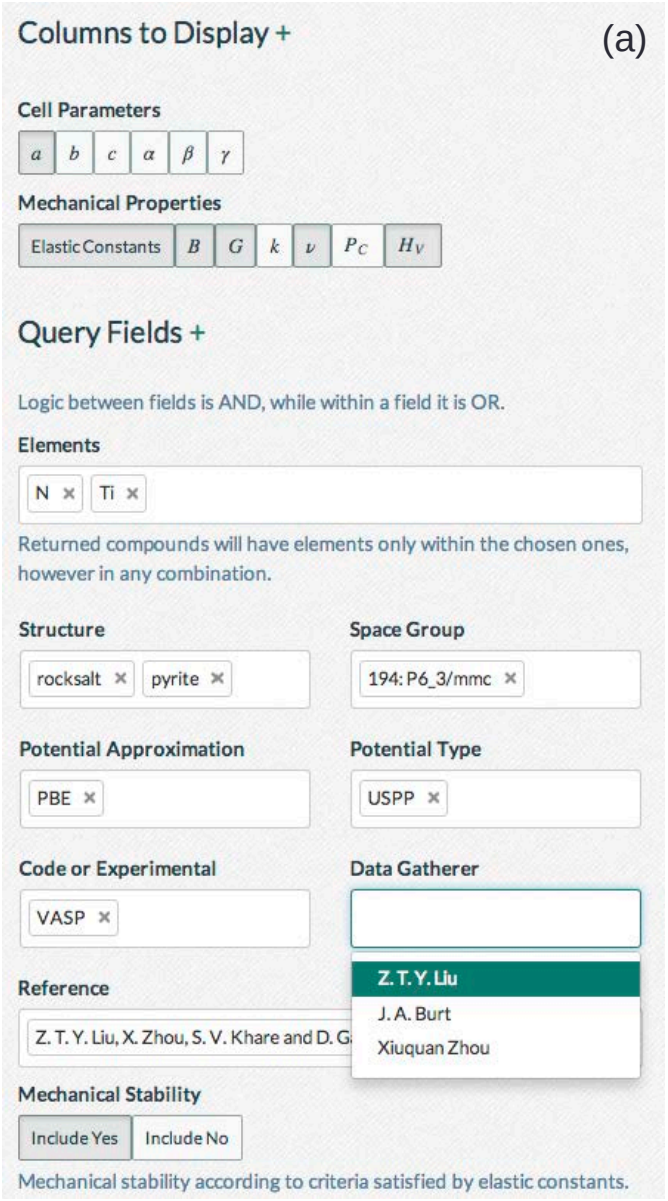

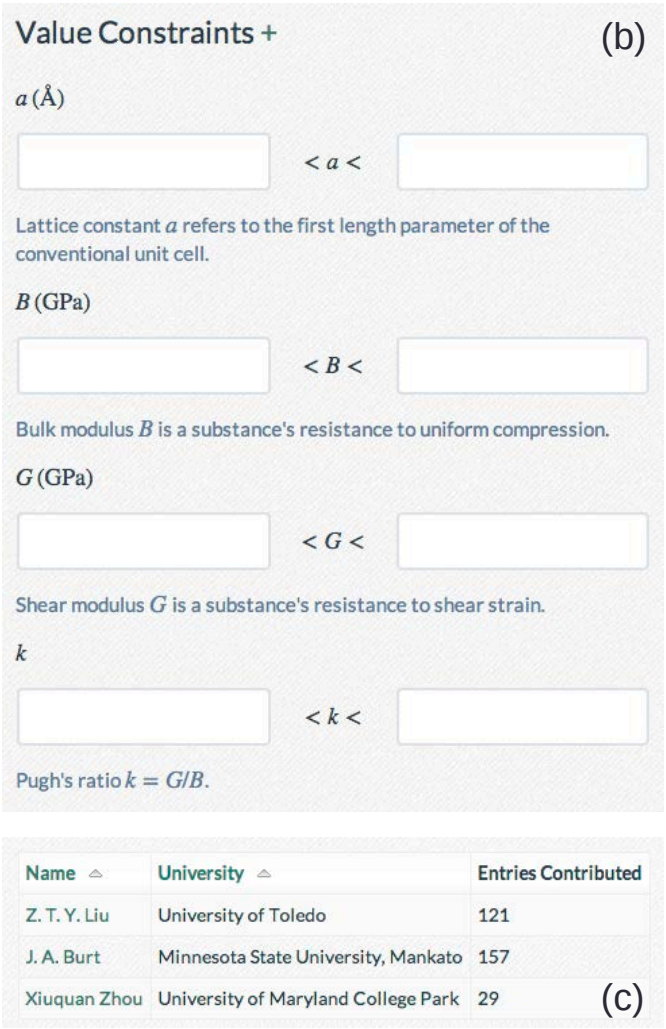

astro1.panet.utoledo.edu/ceramicsdb

Draw Figure

Display

First select rows (by checkbox in the table)

Selected rows (by ID)

1, 2, 3, 4, 5, 6, 7, 8, 9, 10, 11, 12, 13, 14, 15, 16, 17, 18, 19, 20

Now select a column

a | B | G | ν | H_V

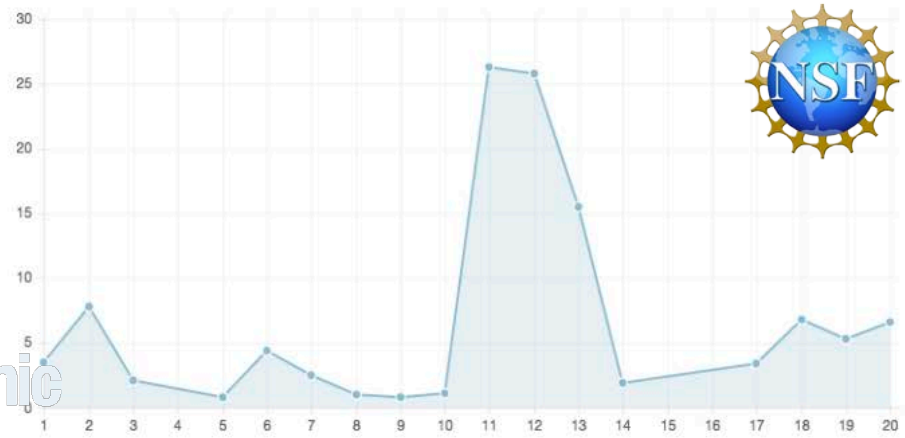

bilbao crystallographic server

www.cryst.ehu.es

ID	Structure	Space Group	Formula	a (Å)	Elastic Constants (GPa)	B (GPa)	G (GPa)	ν	H_V (GPa)	Potential Approx.	Potential Type	Code Package	Reference
1	zinc blende	216: $F\text{-}43m$ Cubic	ScN	4.84	C11 = 186.9, C12 = 140.9, C44 = 73.8	156.2	46.3	0.37	3.5	LDA	USPP	VASP	Z. T. Y. Liu, X. Zhou, S. V. Khare and D. Gall, *Journal of P*
2	zinc blende	216: $F\text{-}43m$ Cubic	TiN	4.529	C11 = 322.2, C12 = 176.4, C44 = 103.1	225.0	89.7	0.32	7.8	LDA	USPP	VASP	Z. T. Y. Liu, X. Zhou, S. V. Khare and D. Gall, *Journal of P*
3	zinc blende	216: $F\text{-}43m$ Cubic	VN	4.368	C11 = 346.8, C12 = 229.4, C44 = 43.2	268.5	48.9	0.41	2.1	LDA	USPP	VASP	Z. T. Y. Liu, X. Zhou, S. V. Khare and D. Gall, *Journal of P*
4	zinc blende	216: $F\text{-}43m$ Cubic	CrN	4.262	C11 = 361.7, C12 = 258.7, C44 = -77.9	–	–	–	–	LDA	USPP	VASP	Z. T. Y. Liu, X. Zhou, S. V. Khare and D. Gall, *Journal of P*
5	zinc blende	216: $F\text{-}43m$ Cubic	MnN	4.188	C11 = 372.7, C12 = 279.7, C44 = 24.0	310.7	31.4	0.45	0.8	LDA	USPP	VASP	Z. T. Y. Liu, X. Zhou, S. V. Khare and D. Gall, *Journal of P*
6	zinc blende	216: $F\text{-}43m$ Cubic	FeN	4.16	C11 = 379.2, C12 = 282.8, C44 = 114.2	314.9	80.8	0.38	4.4	LDA	USPP	VASP	Z. T. Y. Liu, X. Zhou, S. V. Khare and D. Gall, *Journal of P*
7	zinc blende	216: $F\text{-}43m$ Cubic	CoN	4.177	C11 = 347.4, C12 = 266.0, C44 = 71.2	293.1	56.9	0.41	2.5	LDA	USPP	VASP	Z. T. Y. Liu, X. Zhou, S. V. Khare and D. Gall, *Journal of P*
8	zinc blende	216: $F\text{-}43m$ Cubic	NiN	4.241	C11 = 278.1, C12 = 246.2, C44 = 49.9	256.8	31.6	0.44	1.0	LDA	USPP	VASP	Z. T. Y. Liu, X. Zhou, S. V. Khare and D. Gall, *Journal of P*
9	zinc blende	216: $F\text{-}43m$ Cubic	CuN	4.344	C11 = 222.4, C12 = 199.9, C44 = 41.1	207.4	24.5	0.44	0.8	LDA	USPP	VASP	Z. T. Y. Liu, X. Zhou, S. V. Khare and D. Gall, *Journal of P*
10	zinc blende	216: $F\text{-}43m$ Cubic	ZnN	4.472	C11 = 178.0, C12 = 159.4, C44 = 47.4	165.6	25.1	0.43	1.1	LDA	USPP	VASP	Z. T. Y. Liu, X. Zhou, S. V. Khare and D. Gall, *Journal of P*
11	rocksalt	225: $Fm\text{-}3m$ Cubic	ScN	4.463	C11 = 470.1, C12 = 99.4, C44 = 164.3	223.0	172.4	0.19	26.3	LDA	USPP	VASP	Z. T. Y. Liu, X. Zhou, S. V. Khare and D. Gall, *Journal of P*
12	rocksalt	225: $Fm\text{-}3m$ Cubic	TiN	4.184	C11 = 712.3, C12 = 123.2, C44 = 171.1	319.6	213.0	0.23	25.8	LDA	USPP	VASP	Z. T. Y. Liu, X. Zhou, S. V. Khare and D. Gall, *Journal of P*
13	rocksalt	225: $Fm\text{-}3m$ Cubic	VN	4.057	C11 = 751.1, C12 = 178.9, C44 = 126.6	369.6	176.7	0.29	15.5	LDA	USPP	VASP	Z. T. Y. Liu, X. Zhou, S. V. Khare and D. Gall, *Journal of P*
14	rocksalt	225: $Fm\text{-}3m$ Cubic	CrN	3.987	C11 = 702.8, C12 = 227.1, C44 = 9.3	385.7	57.9	0.43	1.9	LDA	USPP	VASP	Z. T. Y. Liu, X. Zhou, S. V. Khare and D. Gall, *Journal of P*
15	rocksalt	225: $Fm\text{-}3m$ Cubic	MnN	3.945	C11 = 682.1, C12 = 241.6, C44 = -13.3	–	–	–	–	LDA	USPP	VASP	Z. T. Y. Liu, X. Zhou, S. V. Khare and D. G *Journal of P*

dx.doi.org/10.1088/0953-8984/26/2/025404

Outline

- Transition Metal Nitrides
- Computational Toolset
  - Density Functional Theory
  - Tools Built on Top of it
- Results 1: Single Phase Properties
- Cluster Expansion Formalism
- Results 2: Solid Solutions

- Non-Dissertation Results

The Grand Scheme of Things

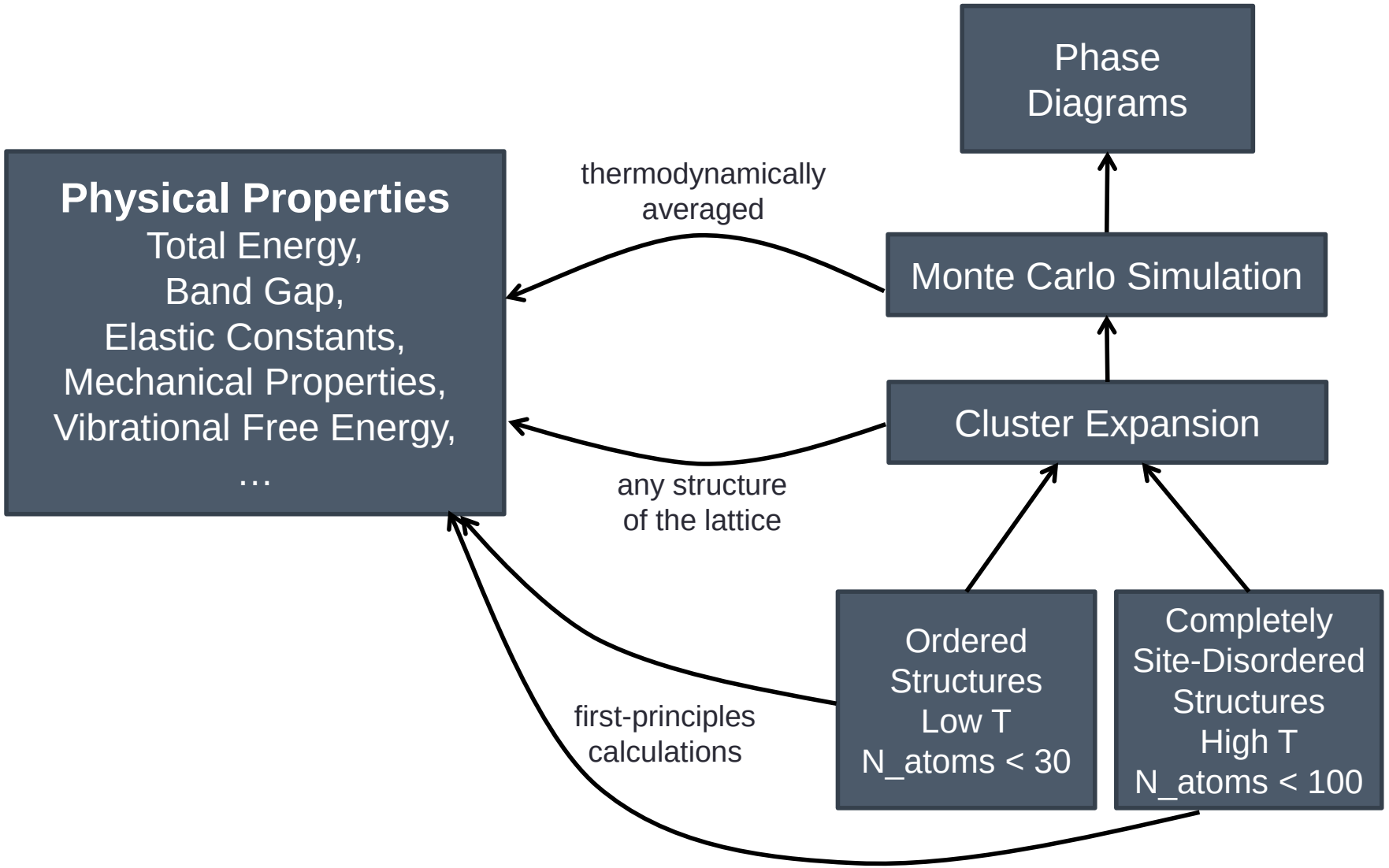

Phase Diagrams

- *T-x* phase diagrams provide the road maps for synthesis of a particular phase or a mixture at a given set of external conditions.
- Common examples are solids with vacancies, interstitials and substitutions.

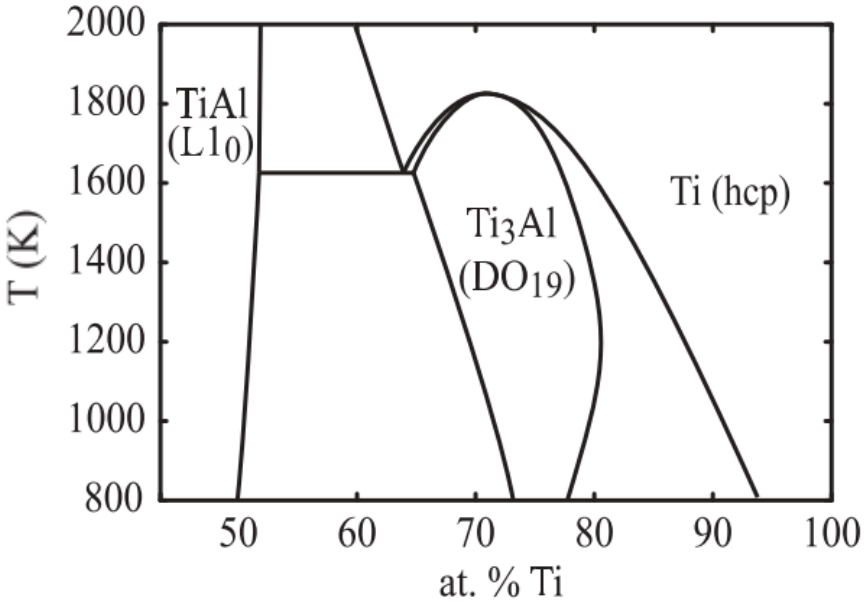

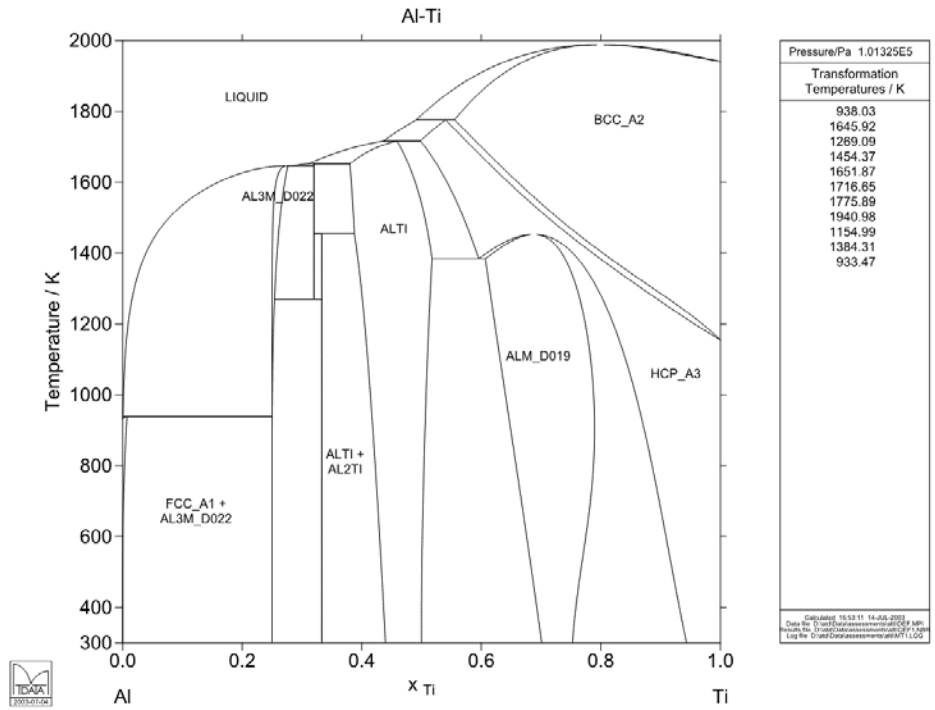

A. van de Walle and M. Asta, *Model. Simul. Mater. Sci. Eng.* **10**, 521 (2002).

http://resource.npl.co.uk/mtdata/phdiagrams/png/alti.png

Phase Diagrams

- It calls for an efficient way of generation and energy prediction of tens of thousands of structures consisting of tens of thousands of atoms, beyond the brute force first-principles calculation of each structure. The cluster expansion formalism offers such a solution.

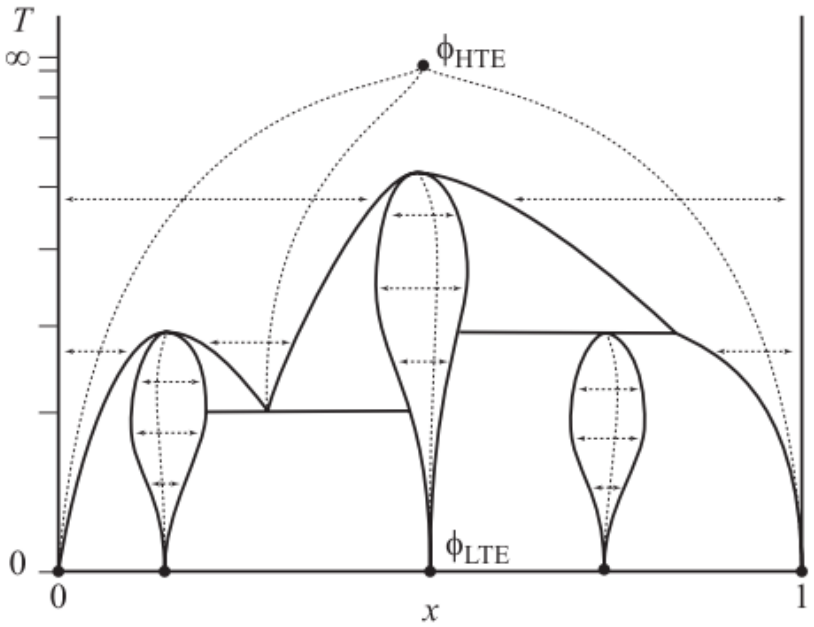

A. van de Walle and M. Asta, *Model. Simul. Mater. Sci. Eng.* **10**, 521 (2002).

Cluster Expansion

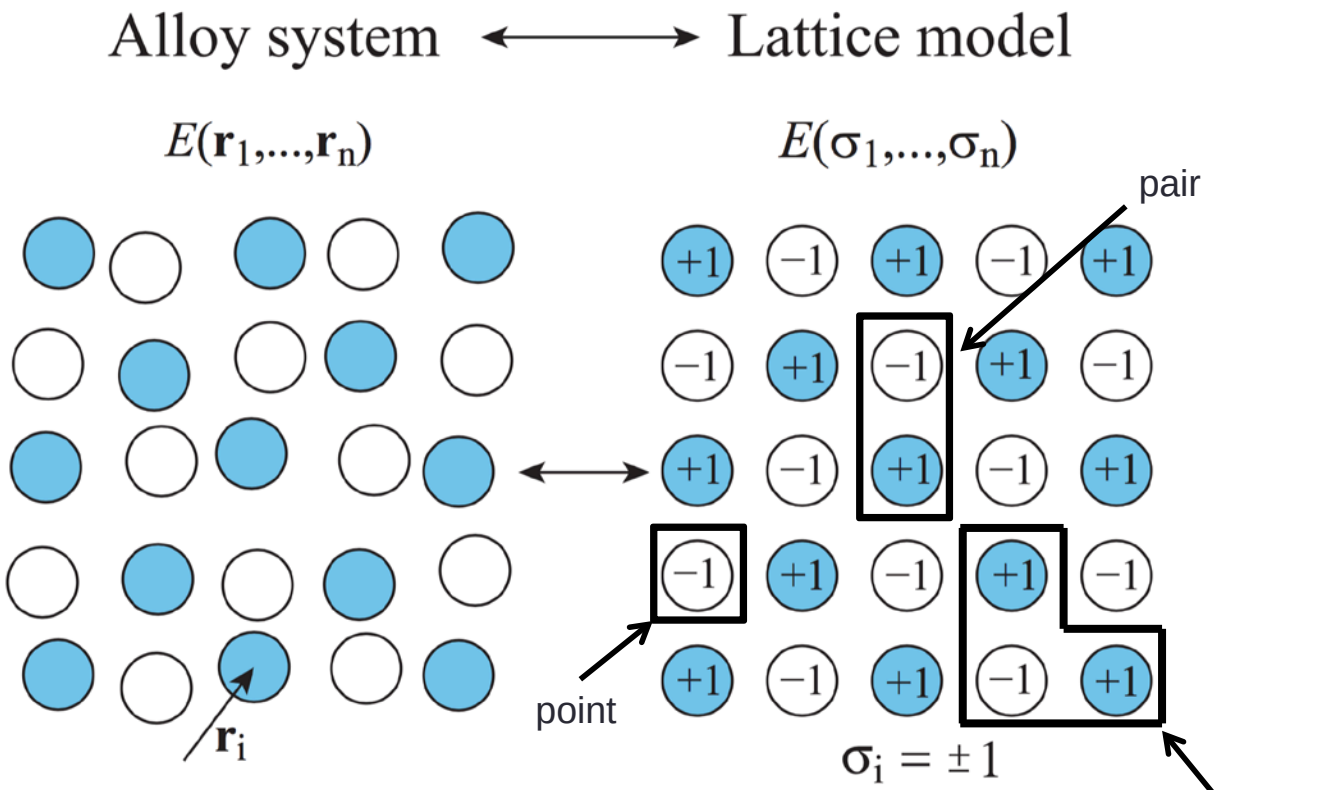

$$E^{(n)}(\sigma) = \sum_{\alpha} J_\alpha \, \sigma_\alpha^{(n)}$$

$$\sigma_\alpha^{(n)} = \prod_{i \in \alpha} \sigma_i^{(n)}$$

Adapted from http://www.brown.edu/Departments/Engineering/Labs/avdw/atat/atattalk.pdf

Cluster Expansion

$$E^{(n)}(\sigma) = \sum_{\alpha} J_{\alpha}\, \sigma_{\alpha}^{(n)}$$

$$\sigma_{\alpha}^{(n)} = \prod_{i \in \alpha} \sigma_{i}^{(n)}$$

- α is a cluster of a set of substitutional sites (i) of the parent lattice, and each substitutional site is assigned a configuration variable σ_i.
- The sum is taken over all the clusters of the parent lattice
- Coefficients J_α are called effective cluster interactions (ECIs).

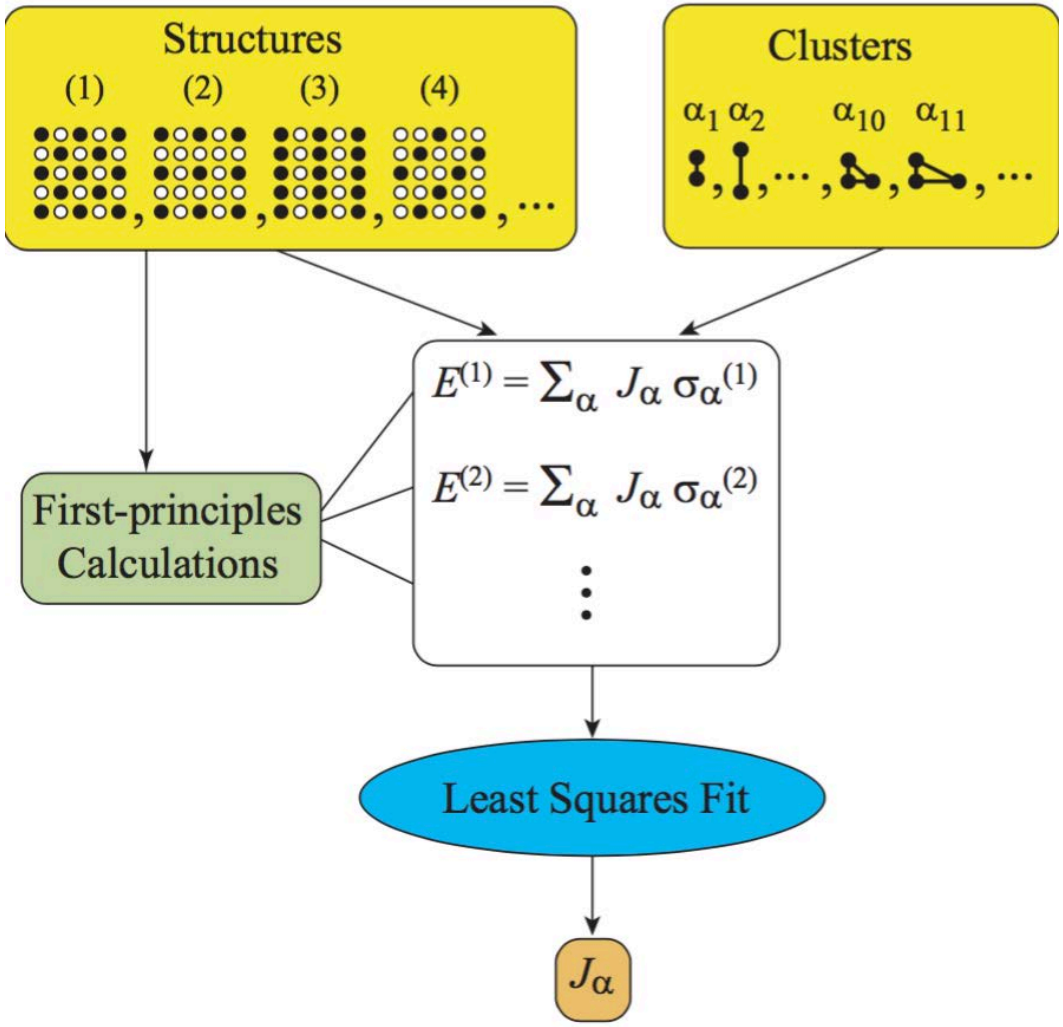

Adapted from http://www.brown.edu/Departments/Engineering/Labs/avdw/atat/atattalk.pdf

- The optimal cluster set and ECIs is selected by minimizing the cross-validation (CV) score,

$$CV = \frac{1}{n}\sum_{i=1}^{n}\left(E_i - \hat{E}_{(i)}\right)^2,$$

where E_i is the first-principles calculated energy of structure i, and $E_{(i)}$ is the "leave-one-out" (without structure i) least-squares fitted energy to prevent over-fitting.

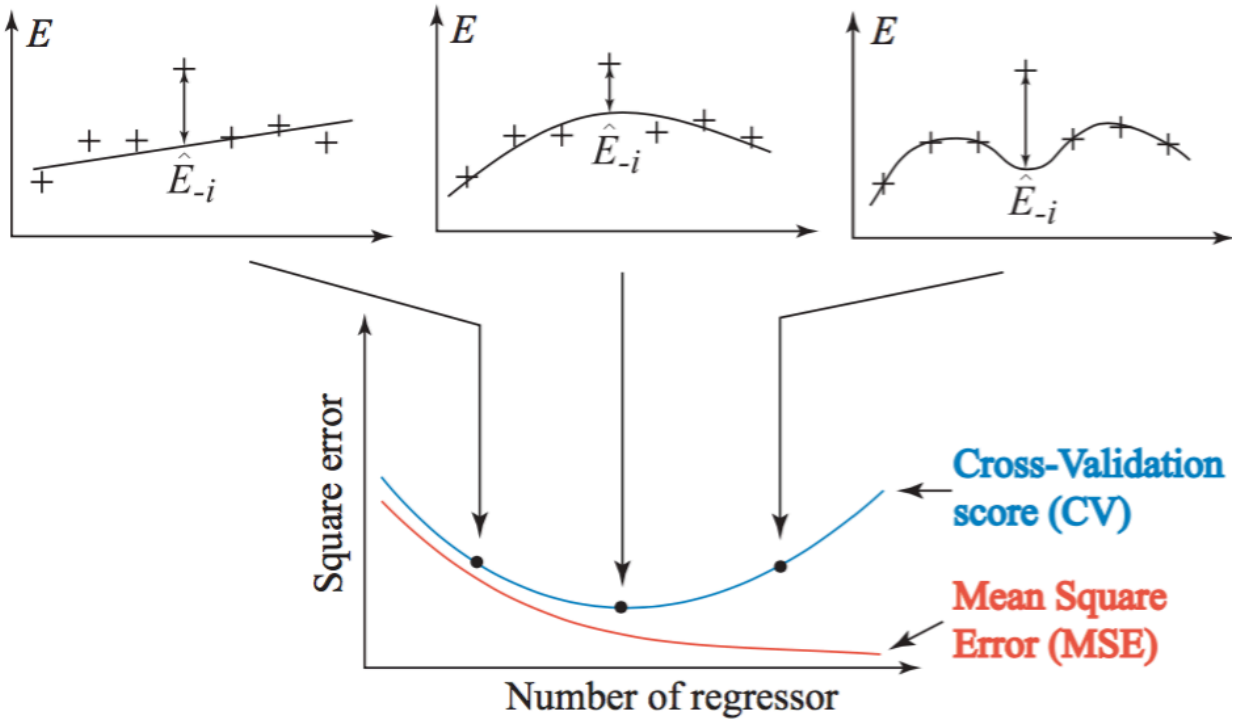

Adapted from http://www.brown.edu/Departments/Engineering/Labs/avdw/atat/atattalk.pdf

Cluster Expansion

- The cluster expansion formalism [1-4] describes an effective representation of the crystalline material system's energy, through a cluster set and their coefficients. Typically, the cluster set need to remain as small as a few pairs and triplets. This compact representation is the key to fast ground state search and statistical sampling of microscopic states.
- It is realized in the open source implementation The Alloy Theoretic Automated Toolkit (ATAT).

[1] van de Walle, A., Asta, M. & Ceder, G. *Calphad-Computer Coupling Phase Diagrams Thermochem.* **26,** 539–553 (2002).
[2] van de Walle, A. *Calphad-Computer Coupling Phase Diagrams Thermochem.* **33,** 266–278 (2009).
[3] van de Walle, A. & Asta, M. *Model. Simul. Mater. Sci. Eng.* **10,** 521–538 (2002).
[4] van de Walle, A. & Ceder, G. *J. Phase Equilibria* **23,** 348–359 (2002).

SQS for Disorder

- A special quasi-random structure (SQS) is a supercell that matches, or very close to the correlations of a random state.
- Inputs are maximum diameter of the pair/triplet/quadruplet clusters to match, and the supercell size.

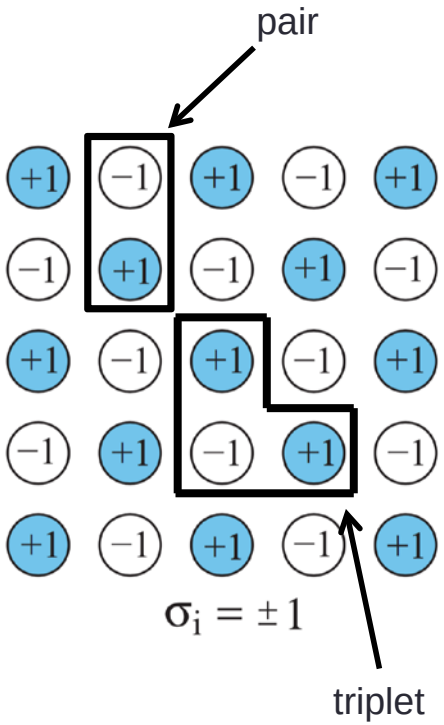

[1] A. van de Walle *et al.*, Calphad-Computer Coupling of Phase Diagrams and Thermochemistry **42**, 13 (2013).
[2] A. van de Walle *et al.*, Calphad-Computer Coupling of Phase Diagrams and Thermochemistry **26**, 539 (2002).
Figure adapted from http://www.brown.edu/Departments/Engineering/Labs/avdw/atat/atattalk.pdf

SQS for Disorder

- The more clusters included, the larger the supercell is needed to perfectly match the random state.
- Usually a small cluster set and small supercell (<50 atoms) is still fine.
- Treating spin-up and spin-down as two different electronic states, SQS can be used to model magnetic disorder with an Ising model.

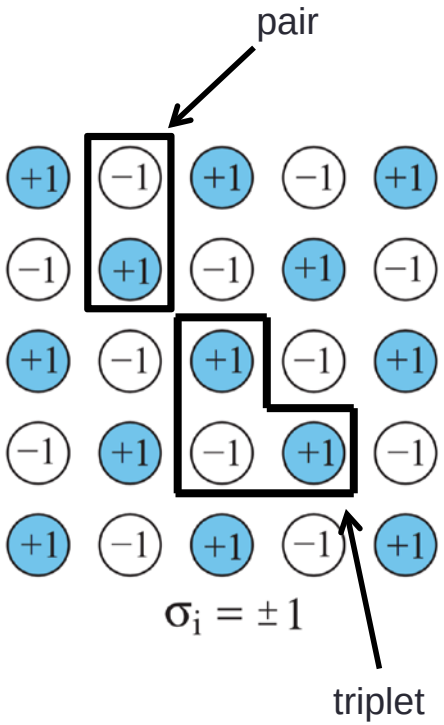

Figure adapted from http://www.brown.edu/Departments/Engineering/Labs/avdw/atat/atattalk.pdf

Outline

- Driving Questions
- Transition Metal Nitrides
- Computational Toolset
  - Density Functional Theory
  - Tools Built on Top of it
- Results 1: Single Phase Properties
- Cluster Expansion Formalism
- Results 2: Solid Solutions

- Answers to Driving Questions

TiN-ZrN, TiN-HfN and ZrN-HfN

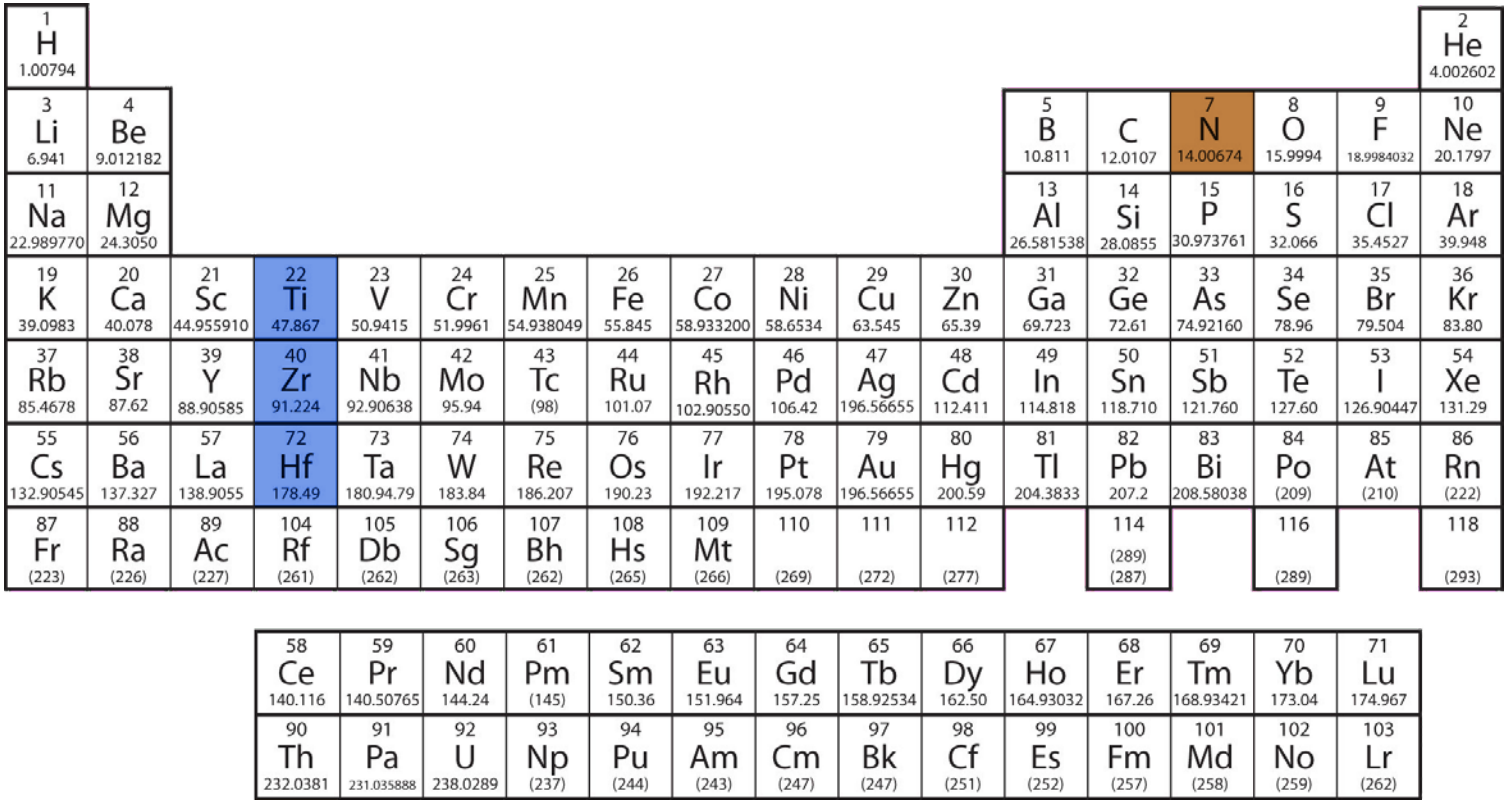

- Can they be mixed? Do their solid solutions phase separate, at what temperature?
- How to model their solid solutions?

Z. T. Y. Liu, B. P. Burton, S. V. Khare, and D. Gall, *J. Phys. Condens. Matter* **29**, 35401 (2017).

Formation Energy Landscapes

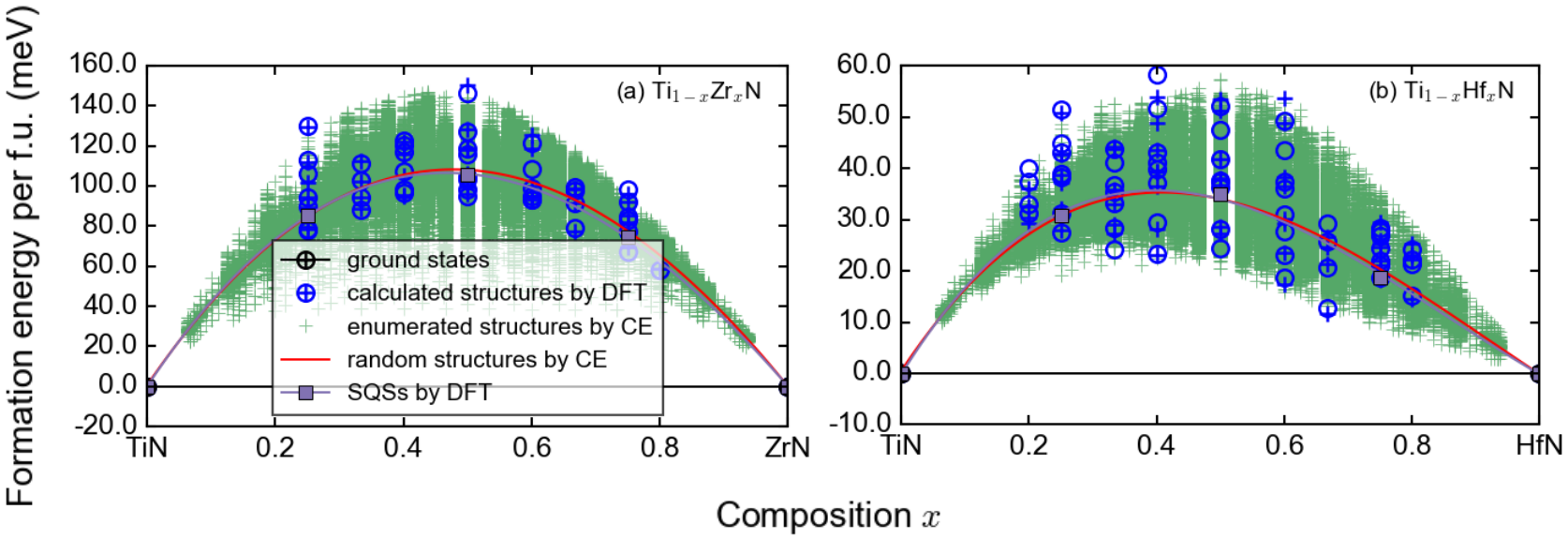

Formation energy landscapes of (a) $Ti_{1-x}Zr_xN$, (b) $Ti_{1-x}Hf_xN$. Energy values are per formula unit, i.e. per exchangeable site. **Black** markers and convex hull lines indicate ground states, **blue** markers indicate the structures calculated with DFT and used to obtain the cluster expansion (CE), and **green** crosses indicate a 16-exchangeable-site ground-state analysis. Among the markers, hollow circles indicate DFT values, and crosses indicate CE-fitted values. **Red** curves indicate CE-fitted values of the random solid solution configurations, while purple squares and lines indicate DFT values and polynomial fit of the SQS's.

Z. T. Y. Liu, B. P. Burton, S. V. Khare, and D. Gall, *J. Phys. Condens. Matter* **29**, 35401 (2017).

Formation Energy Landscapes

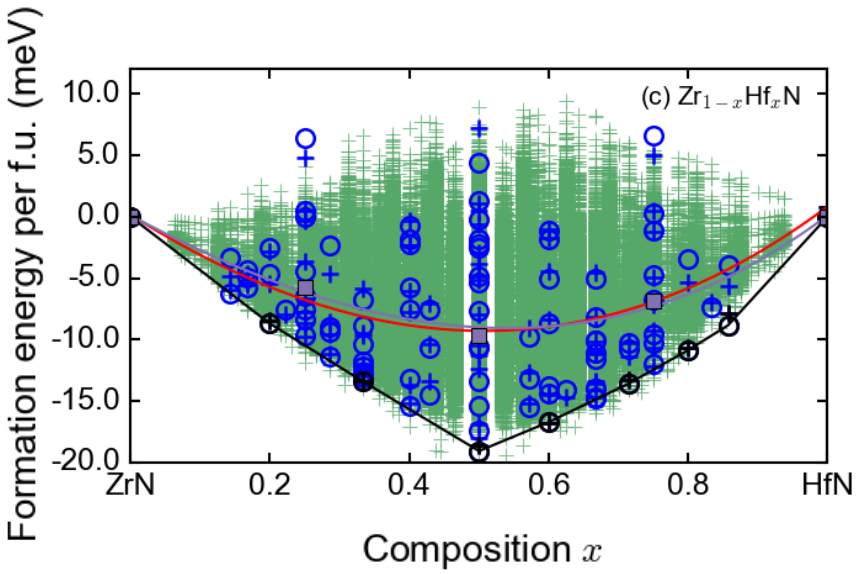

	Num. of structures	Num. of clusters (pair + trip + quad)	CV score (meV)
$Ti_{1-x}Zr_xN$	45	15 + 7	5.2
$Ti_{1-x}Hf_xN$	74	16 + 7	3.8
$Zr_{1-x}Hf_xN$	95	32 + 23 + 3	2.6

Formation energy landscapes of (c) $Zr_{1-x}Hf_xN$. Energy values are per formula unit, i.e. per exchangeable site. **Black** markers and convex hull lines indicate ground states, **blue** markers indicate the structures calculated with DFT and used to obtain the cluster expansion (CE), and **green** crosses indicate a 16-exchangeable-site ground-state analysis. Among the markers, hollow circles indicate DFT values, and crosses indicate CE-fitted values. **Red** curves indicate CE-fitted values of the random solid solution configurations, while purple squares and lines indicate DFT values and polynomial fit of the SQS's.

Z. T. Y. Liu, B. P. Burton, S. V. Khare, and D. Gall, *J. Phys. Condens. Matter* **29**, 35401 (2017).

Thermodynamic Functions, Prefactors and Diffusion Coefficients

- The main quantity for our purposes here is the vibrational contribution to the free energy, which is given by the standard definition

$$F = U - TS$$

  - where U is internal energy, S is entropy and T is temperature

- Both $\boldsymbol{U}$ and $\boldsymbol{S}$ have contributions from atomic configurations and vibrations

$$F = F^{\mathrm{conf}} + F^{\mathrm{vib}}$$

- For each atomic configuration of the system there is a specific vibrational contribution which can be further written as

$$F^{\mathrm{vib}} = U^{\mathrm{vib}} - TS^{\mathrm{vib}}$$

H. Yildirim, A. Kara, S. Durukanoglu, and T. S. Rahman, Surf. Sci. **600**, 484 2006.

Calculated Phase Diagrams

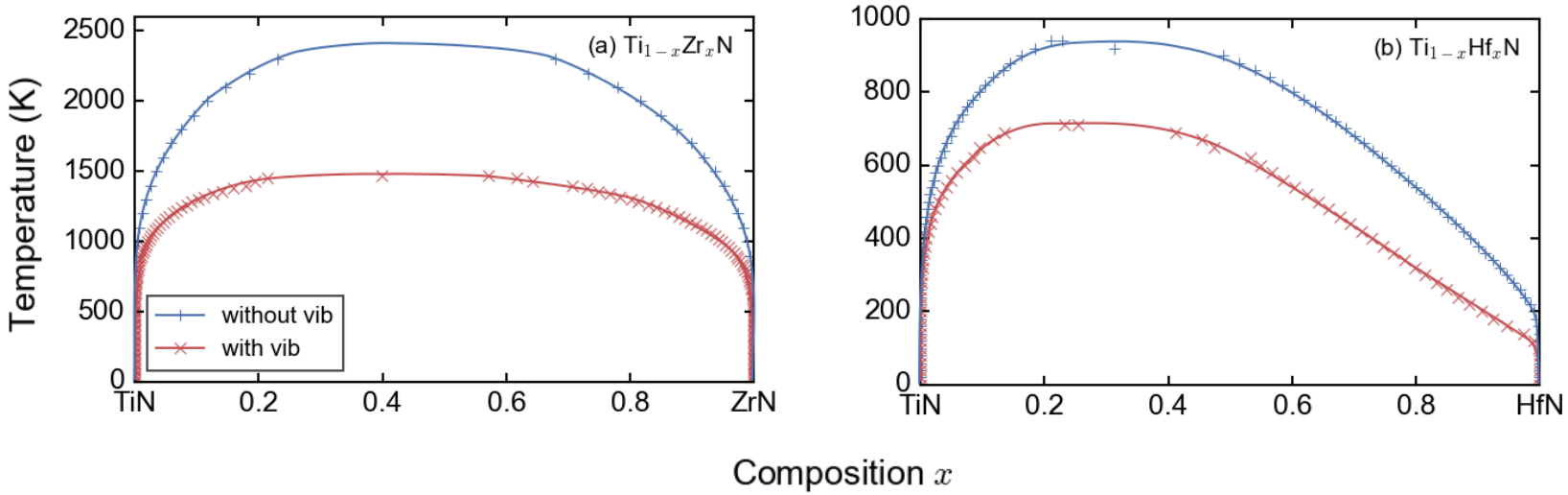

Calculated phase diagrams of (a) $Ti_{1-x}Zr_xN$, (b) $Ti_{1-x}Hf_xN$. Small crosses are raw data points, and curves are interpolations and extrapolations. **Blue** "+" and **red** "×" curves correspond to results without and with the vibrational contribution.

	Ti	Zr	Hf
r of M^{4+} (Å)	0.61	0.72	0.71
V of nitride (Å^3)	19.2	24.3	23.4
B of nitride (GPa)	259	240	247

Z. T. Y. Liu, B. P. Burton, S. V. Khare, and D. Gall, *J. Phys. Condens. Matter* **29**, 35401 (2017).

L. Pauling, *The Nature of the Chemical Bond and the Structure of Molecules and Crystals: An Introduction to Modern Structural Chemistry* (Cornell University Press, 1960).

Calculated Phase Diagrams

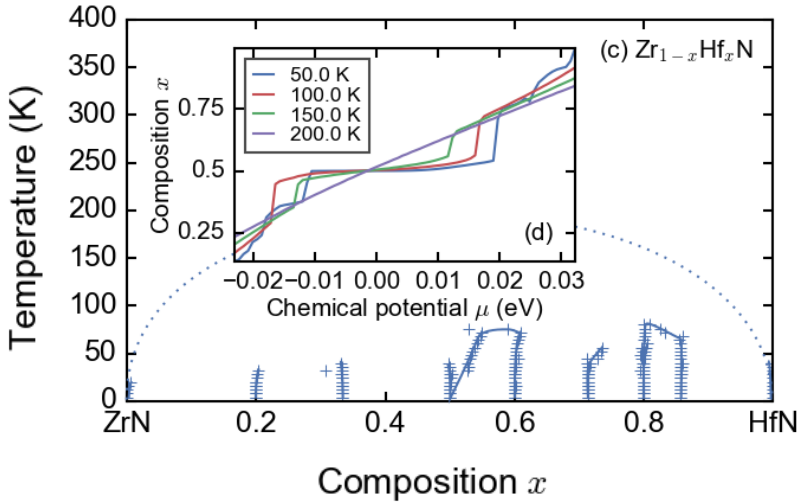

	T_C without vib (K)	T_C with vib (K)	T_C from literature (K)
$Ti_{1-x}Zr_xN$	2400	1400	1850[a], 5000[b] (empirical)
$Ti_{1-x}Zr_xC$	3200	2250	2250 (expt.)[c]
$Ti_{1-x}Hf_xN$	900	700	1300[a]
$Zr_{1-x}Hf_xN$	< 200		

Calculated phase diagrams of (c) $Zr_{1-x}Hf_xN$. Small crosses are raw data points, and curves are interpolations and extrapolations. In (c), the dotted curve indicates the estimated consolute boundary, as demonstrated by the inset (d). In (d), curves indicate compositions with respect to chemical potentials at various temperatures in a semi-grand-canonical ensemble. The abrupt changes disappear above 200 K, marking the consolute boundary.

[a] Holleck, H., *J. Vac. Sci. Technol. A-Vacuum Surfaces Film.* **4,** 2661–2669 (1986).
[b] Hoerling, A. *et al*., *Thin Solid Films* **516,** 6421–6431 (2008).
[c] Kieffer, R. & Ettmayer, P., *Angew. Chemie Int. Ed. English* **9,** 926–936 (1970).

Z. T. Y. Liu, B. P. Burton, S. V. Khare, and D. Gall, *J. Phys. Condens. Matter* **29**, 35401 (2017).

Calculated Phase Diagrams: $Ti_{1-x}Zr_xC$

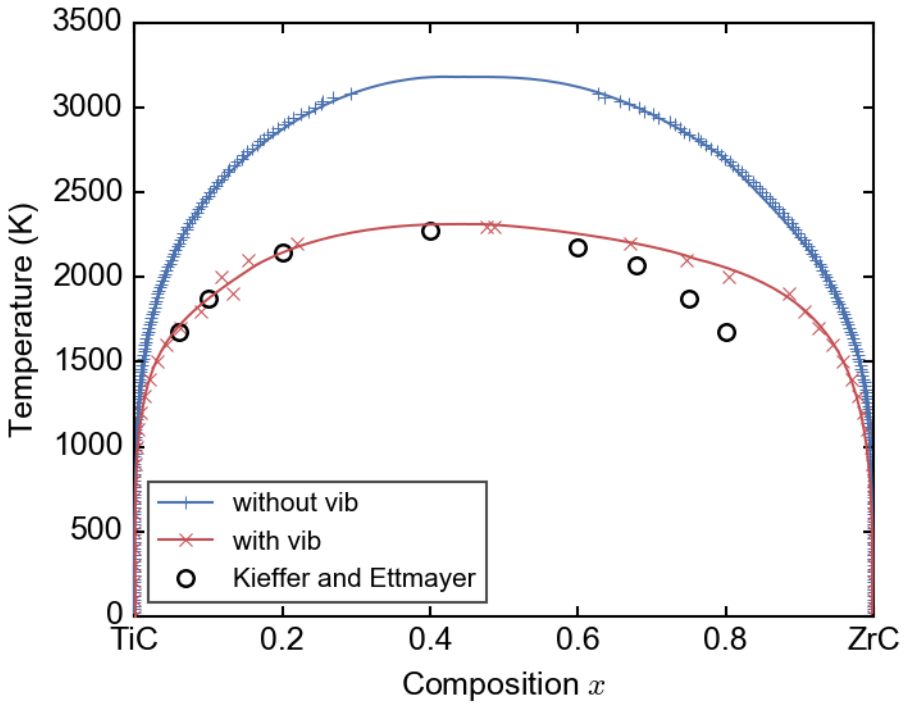

Calculated phase diagrams of (a) $Ti_{1-x}Zr_xC$. Small crosses are raw data points, and curves are interpolations and extrapolations. **Blue** "+" and **red** "×" curves correspond to results without and with the vibrational contribution.

Z. T. Y. Liu, B. P. Burton, S. V. Khare, and D. Gall, *J. Phys. Cond. Matt.* **29**, 35401 (2017); Kieffer, R. & Ettmayer, P. Principles and Latest Developments in the Field of Metallic and Nonmetallic Hard Materials. Angew. Chemie Int. Ed. English 9, 926–936 (1970).

Monte Carlo Simulation Cells

12 x 12 x 12 sites

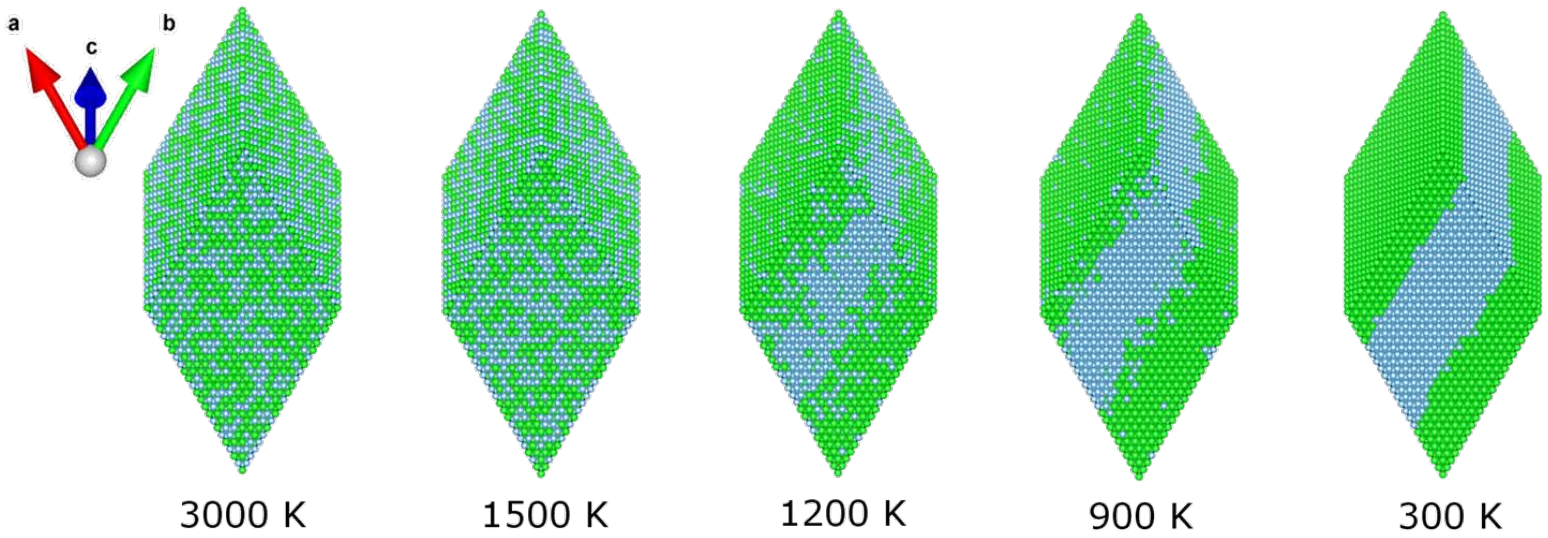

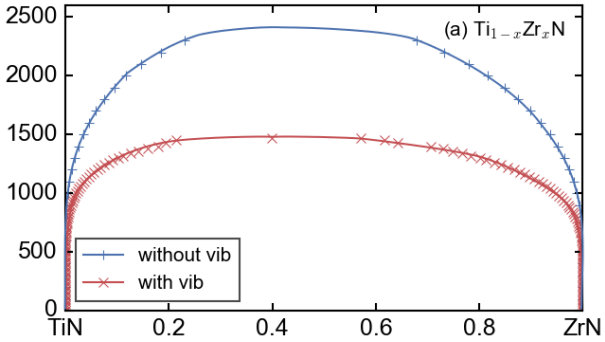

Monte Carlo simulation cells of $Ti_{0.5}Zr_{0.5}N$ at:

- 3000 K (far above the miscibility gap)
- 1500 K (just above the miscibility gap 1400 K)
- 1200 K, 900 K and 300 K (within miscibility gap)

Blue and green balls are Ti and Zr atoms. N atoms are omitted from the display for clarity. Increasing tendency towards separation is clearly visible with lowering temperature.

Z. T. Y. Liu, B. P. Burton, S. V. Khare, and D. Gall, *J. Phys. Condens. Matter* **29**, 35401 (2017).

Projected Density of States

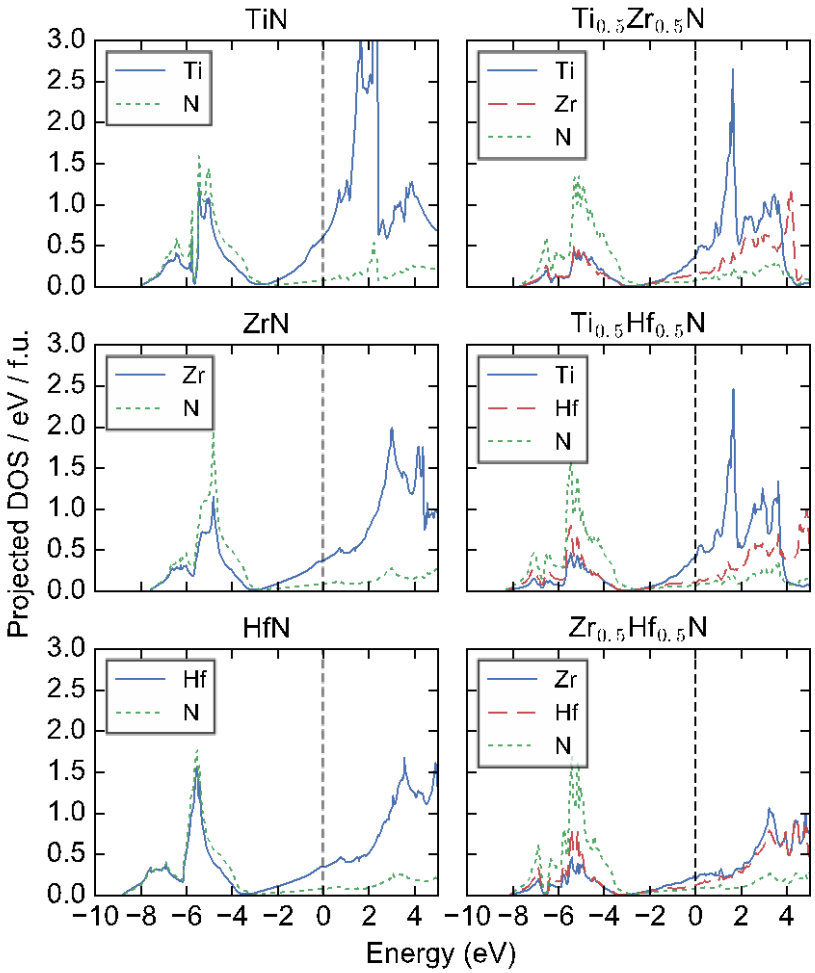

Projected density of states of TiN, ZrN, HfN and three solid solutions with composition $A_{0.5}B_{0.5}N$ where *A* and *B* are transition metals. The Fermi energy is set to 0.

- Fermi energy (E_F) is in the middle of a slope, indicating metallic behavior.
- Overlap between the transition metal d-states and nitrogen p-states, especially below E_F, indicates strong bonding.
- Ti in TiN has a higher peak between 0-2 eV in the conduction band than Zr and Hf in their respective nitrides.
- This difference persists in their solid solutions $Ti_{0.5}Zr_{0.5}N$, $Ti_{0.5}Hf_{0.5}N$ and $Zr_{0.5}Hf_{0.5}N$.

Published work: Z.T.Y. Liu, B.P. Burton, S. V Khare, and D. Gall, *J. Phys. Condens. Matter* **29**, 35401 (2017).

Volume Deviations

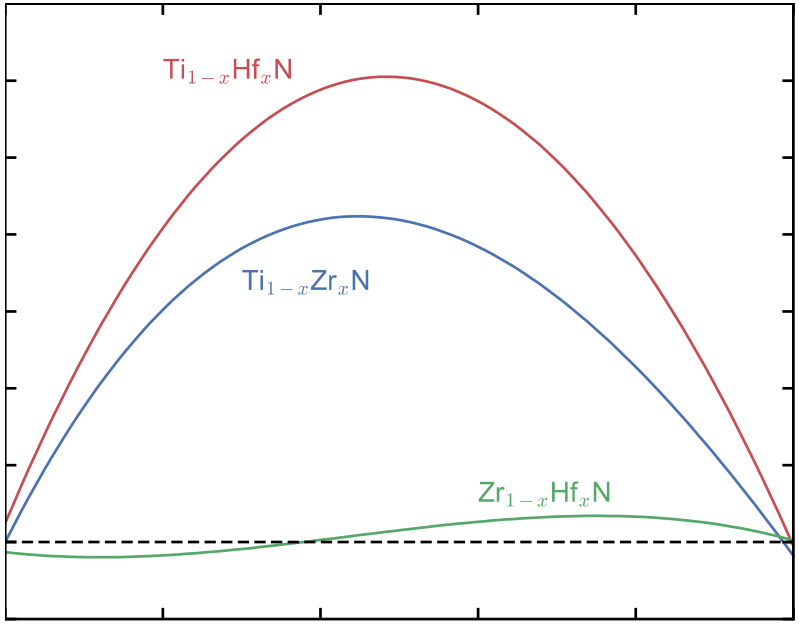

Volume deviations from linearity of $Ti_{1-x}Zr_xN$, $Ti_{1-x}Hf_xN$ and $Zr_{1-x}Hf_xN$. Curves indicate CE-fitted values of the random solid solution configurations.

Published work: Z.T.Y. Liu, B.P. Burton, S. V Khare, and D. Gall, *J. Phys. Condens. Matter* **29**, 35401 (2017).

Volume Change and Exchange-Relaxation Energies

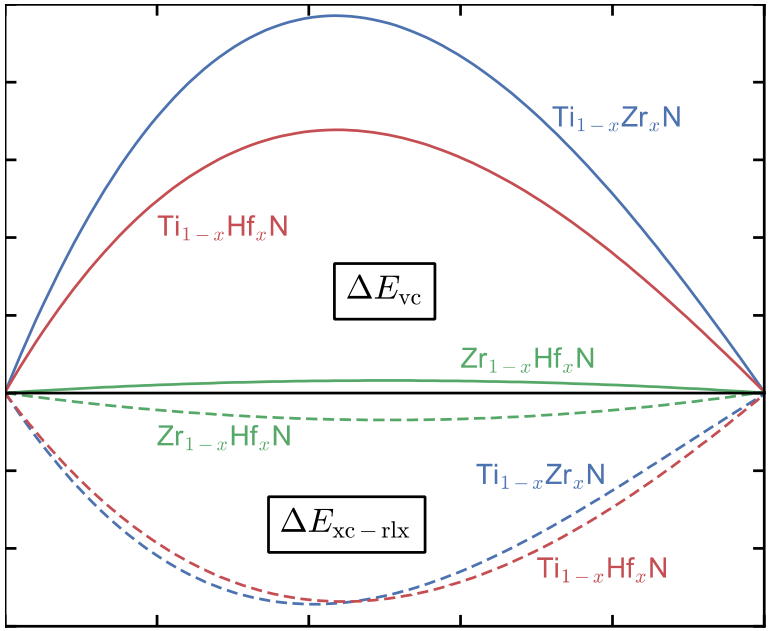

- ΔE_{vc} meansures energies during volume change.
- ΔE_{xc-rlx} measures the energies during chemical exchange and cell shape and ionic relaxation.
- A large part of the ΔE_{vc} is canceled out by ΔE_{xc-rlx}.
- ΔE_{vc} of $Ti_{1-x}Hf_xN$ is only ¾ of that of $Ti_{1-x}Zr_xN$, despite the almost identical cation radii of Ti and Zr. ΔE_{xc-rlx} are similar in magnitude.
- ΔE_{vc} is the main reason for the difference in magnitude of ΔE_f and the consolute temperatures.

	a (Å)	*V*/f.u. (Å³)	*E*/f.u. (eV)	*B* (GPa)
TiN	4.25	19.2	-19.63	259
	4.241[a]	19.1[a]		318[b]
ZrN	4.60	24.3	-20.38	240
	4.578[a]	24.0[a]		285[c]
HfN	4.54	23.4	-21.76	247
	4.525[a]	23.2[a]		276[c]

Volume change and exchange-relaxation energies of $Ti_{1-x}Zr_xN$, $Ti_{1-x}Hf_xN$ and $Zr_{1-x}Hf_xN$. Values are per formula unit, i.e. per exchangeable site. Curves indicate CE-fitted values of the random solid solution configurations.

Published work: Z.T.Y. Liu, B.P. Burton, S. V Khare, and D. Gall, *J. Phys. Condens. Matter* **29**, 35401 (2017).

Volume Change and Exchange-Relaxation Energies

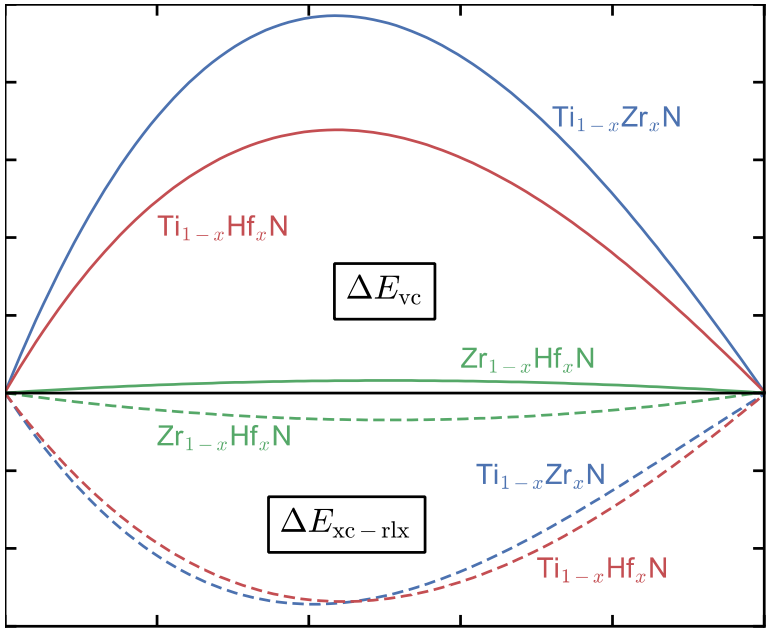

Volume change and exchange-relaxation energies of $Ti_{1-x}Zr_xN$, $Ti_{1-x}Hf_xN$ and $Zr_{1-x}Hf_xN$. Values are per formula unit, i.e. per exchangeable site. Curves indicate CE-fitted values of the random solid solution configurations.

- ΔE_{vc} meansures energies during volume change.
- ΔE_{xc-rlx} measures the energies during chemical exchange and cell shape and ionic relaxation.

- In $Ti_{1-x}Zr_xN$ and $Ti_{1-x}Hf_xN$ the ΔE_{vc} curves exhibit asymmetry, both with maxima on the smaller cation TiN-side. It takes more energy to insert a larger ion into a smaller-volume crystal, than vice versa.
- The ΔE_{xc-rlx} curve maximum for $Ti_{1-x}Hf_xN$ is less close to the TiN-side than $Ti_{1-x}Zr_xN$, resulting in more asymmetry of the final ΔE_f curve for $Ti_{1-x}Hf_xN$ than $Ti_{1-x}Zr_xN$.
- ΔE_{xc-rlx} is responsible for the asymmetry.

Published work: Z.T.Y. Liu, B.P. Burton, S. V Khare, and D. Gall, *J. Phys. Condens. Matter* **29**, 35401 (2017).

Phase Separation Discussion

- Experimental endeavors, including cathodic arc plasma deposited [1] and dc reactive magnetron sputtered [2] $Ti_{1-x}Zr_xN$ samples remained single-phase without decomposition after anealing at 600-1200 °C for hours. Only a slight broadening of an X-ray powder diffraction (XRD) peak was observed after a sample, with x = 0.53, was annealed at 1200 ºC [1]. This observation is consisitent with the initial stage of spinodal decomposition. Apparently, the experimental anealing temperature range 600-1200 °C is not sufficient in undercooling, or atomic mobility is too low for $Ti_{1-x}Zr_xN$ to phase segregate.

- In addition, the bond dissociation energies for Ti-C (423 ± 30 kJ/mol) and Zr-C (495.8 ± 38.6 kJ/mol) are smaller than the corresponding Ti-N (476 ± 33 kJ/mol) and Zr-N (565 ± 25 kJ/mol)[90], so movement of transition metals in nitrides is probably slower than in carbides.

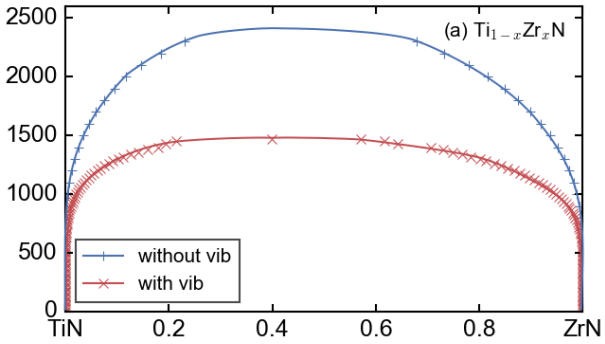

[1] Hoerling, A. *et al.*, *Thin Solid Films* **516**, 6421–6431 (2008).
[2] Abadias, G., Ivashchenko, V. I., Belliard, L. & Djemia, P. Structure, *Acta Mater*. **60**, 5601–5614 (2012).

Z. T. Y. Liu, B. P. Burton, S. V. Khare, and D. Gall, *J. Phys. Condens. Matter* **29**, 35401 (2017).

Elastic Constants

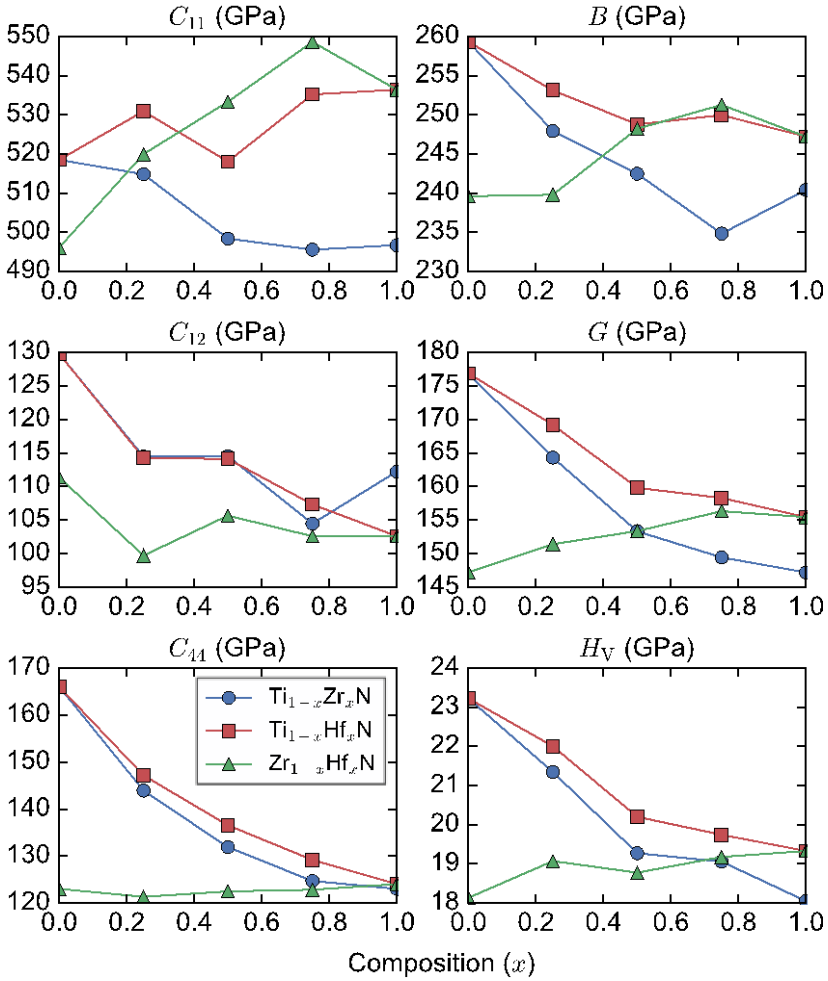

Elastic constants C_{11}, C_{12}, C_{44}, bulk moduli (B), shear moduli (G) and Vickers hardness (H_V) of the SQS's of $Ti_{1-x}Zr_xN$, $Ti_{1-x}Hf_xN$ and $Zr_{1-x}Hf_xN$

Published work: Z.T.Y. Liu, B.P. Burton, S. V Khare, and D. Gall, *J. Phys. Condens. Matter* **29**, 35401 (2017).

Answers to the Driving Questions from MGI

Transition Metal Nitrides (M_xN_y)

- Can we obtain predictive physical understanding of stable, hard and tough materials for coatings from first-principles calculations? **Yes**
- Thermodynamically (multiple-phase stability)?
- Mechanically (single-phase stability)?

- Can we identify trends of properties and possible correlations between them to restrict the parameter search space? **Yes, to some degree**

- How much can we reduce the time and expense for discovering new materials with computational work? **Yes, significantly**

- Can we construct T-x phase diagrams from purely *ab initio* techniques? **Yes, but not easy for complex crystals**

Thank You!

$CaCO_3$-$ZnCO_3$, $CdCO_3$-$ZnCO_3$, $CaCO_3$-$CdCO_3$ and $MgCO_3$-$ZnCO_3$

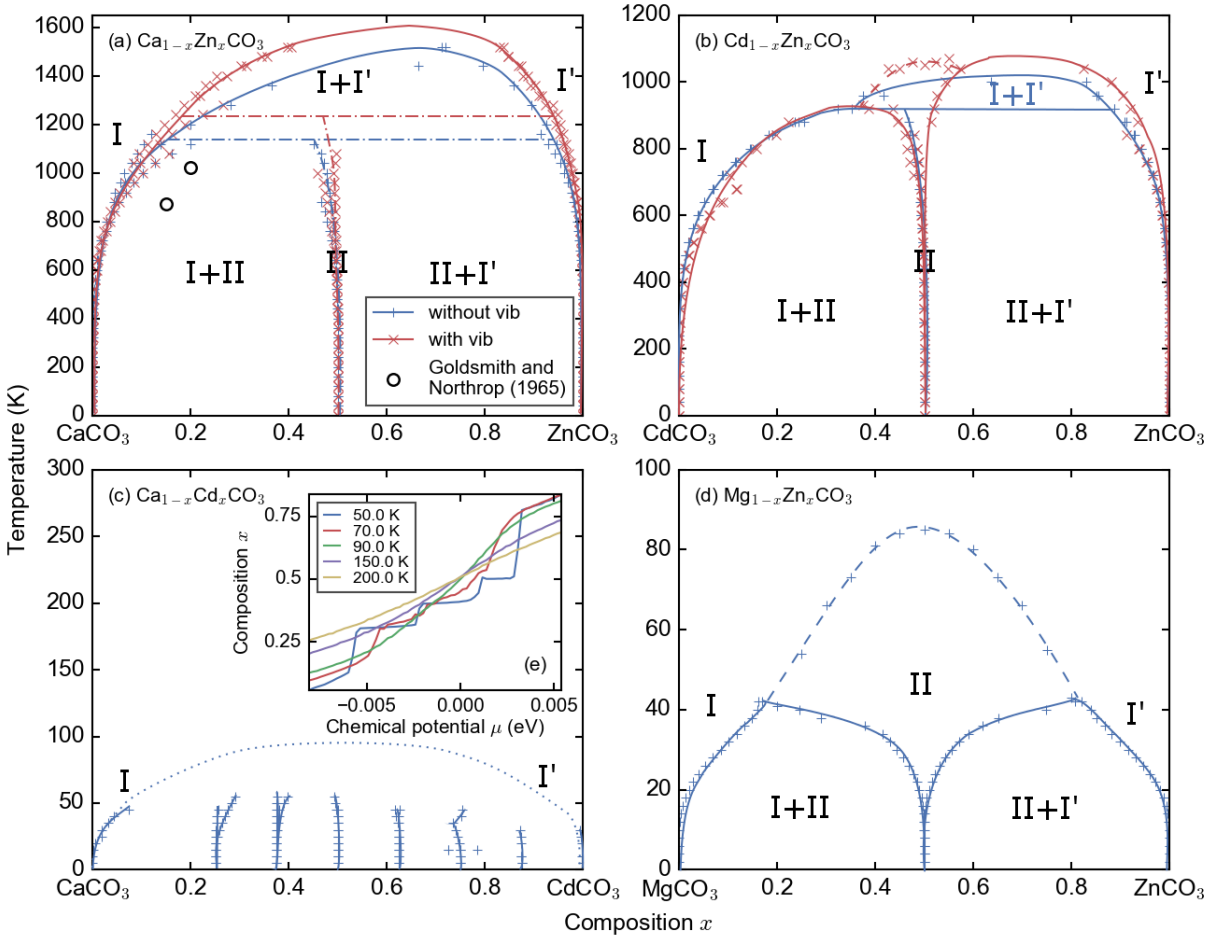

Z. T. Y. Liu, B. P. Burton, S. V. Khare, and P. Sarin, *Chem. Geol.* **443**, 137 (2016).

Thermal Equation of State of Silicon Carbide

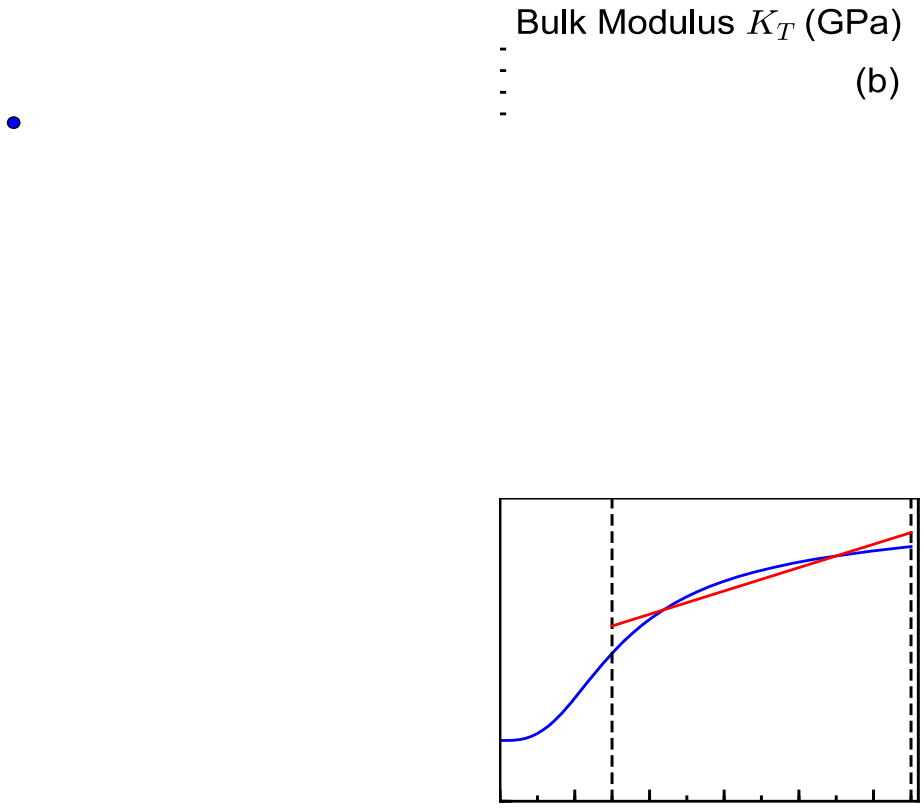

Y. Wang, Z. T. Y. Liu, S. V. Khare, S. A. Collins, J. Zhang, L. Wang, and Y. Zhao, *Appl. Phys. Lett.* **108**, 61906 (2016).

$ZnCr_2Se_4$ and $CdCr_2Se_4$

DOS (States / eV)

clinic 20 GPa

Cr-t_{2g}
Cr-e_g

Se-p
Zn-d

Energy (eV)

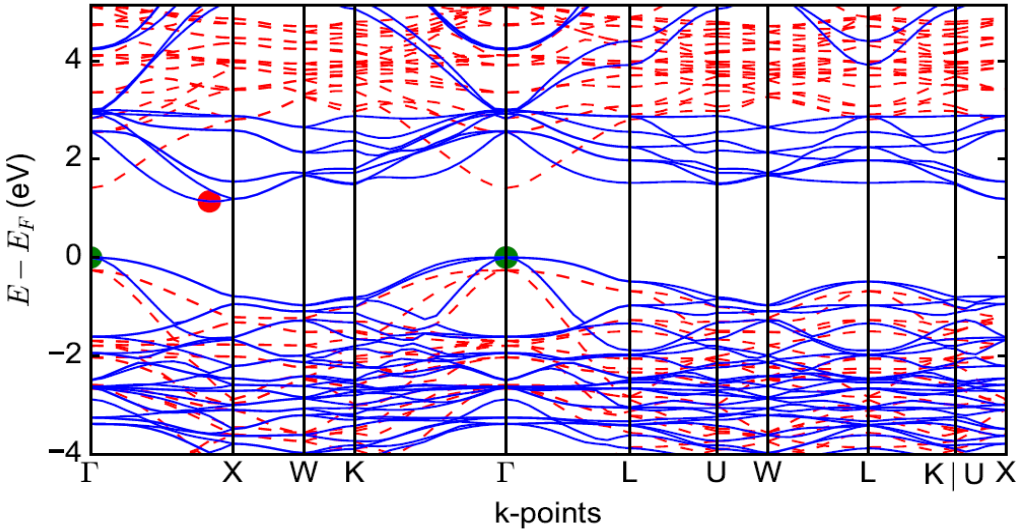

I. Efthimiopoulos, Z. T. Y. Liu, S. V. Khare, P. Sarin, V. Tsurkan, A. Loidl, D. Popov, and Y. Wang, *Phys. Rev. B*, **93**, 174103 (2016).
I. Efthimiopoulos, Z. T. Y. Liu, M. Kucway, S. V. Khare, P. Sarin, V. Tsurkan, A. Loidl, and Y. Wang, *Phys. Rev. B* **94**, 174106 (2016).
I. Efthimiopoulos, Z. T. Y. Liu, S. V. Khare, P. Sarin, T. Lochbiler, V. Tsurkan, A. Loidl, D. Popov, and Y. Wang, *Phys. Rev. B* **92**, 64108 (2015).

pydass_vasp (or, badass wasp)

Convenient Python modules and wrapping script executables.

Example: plotting band structure

pydass_vasp.electronic_structure.get_bs(plot=True, ylim=[-4,6])

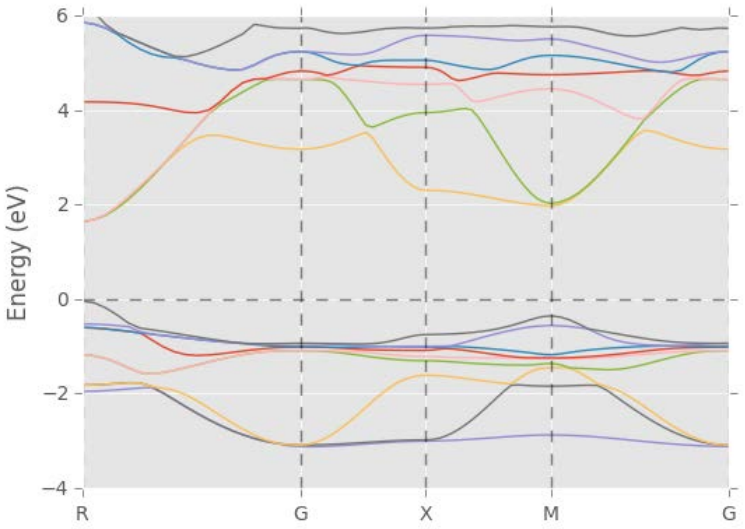

figure output

```
{'data': {'columns': ['k_points',
             'band_1', 'band_2', 'band_3', 'band_4', 'band_5', 'band_6', 'band_7', 'band_8',
             'band_9', 'band_10', 'band_11', 'band_12', 'band_13', 'band_14', 'band_15', 'band_16',
             'band_17', 'band_18', 'band_19', 'band_20', 'band_21', 'band_22', 'band_23', 'band_24',
             'band_25', 'band_26', 'band_27', 'band_28', 'band_29', 'band_30', 'band_31', 'band_32'],
          'data': array(
            [[  0.        , -20.342219  , -16.616756  , ...,   5.849101  ,
                5.855091  ,   6.074841  ],
             [  0.04558028, -20.342181  , -16.616823  , ...,   5.811826  ,
                5.815311  ,   6.060851  ],
             [  0.09116057, -20.34223   , -16.617067  , ...,   5.730248  ,
                5.734556  ,   5.80481   ],
             ...,
             [  2.49869989, -20.343194  , -16.628521  , ...,   5.172637  ,
                5.204402  ,   5.711173  ],
             [  2.53591604, -20.343228  , -16.6286    , ...,   5.219897  ,
                5.226956  ,   5.730676  ],
             [  2.57313218, -20.34319   , -16.628622  , ...,   5.234177  ,
                5.234205  ,   5.726715  ]])},
 'reciprocal_point_locations': array([ 0.        ,  0.8660254 ,  1.3660254 ,  1.8660254 ,  2.57313218]),
 'reciprocal_point_labels': ['R', 'G', 'X', 'M', 'G'],
 'ax': <matplotlib.axes._subplots.AxesSubplot at 0x108b95110>}
```

data output

https://github.com/terencezl/pydass_vasp
https://github.com/terencezl/ScriptsForVASP

pydass_vasp (or, badass wasp)

Example: plotting total density of states with spin polarization

pydass_vasp.electronic_structure.get_tdos(plot=True, xlim=[-15, 15], ylim_upper=40)

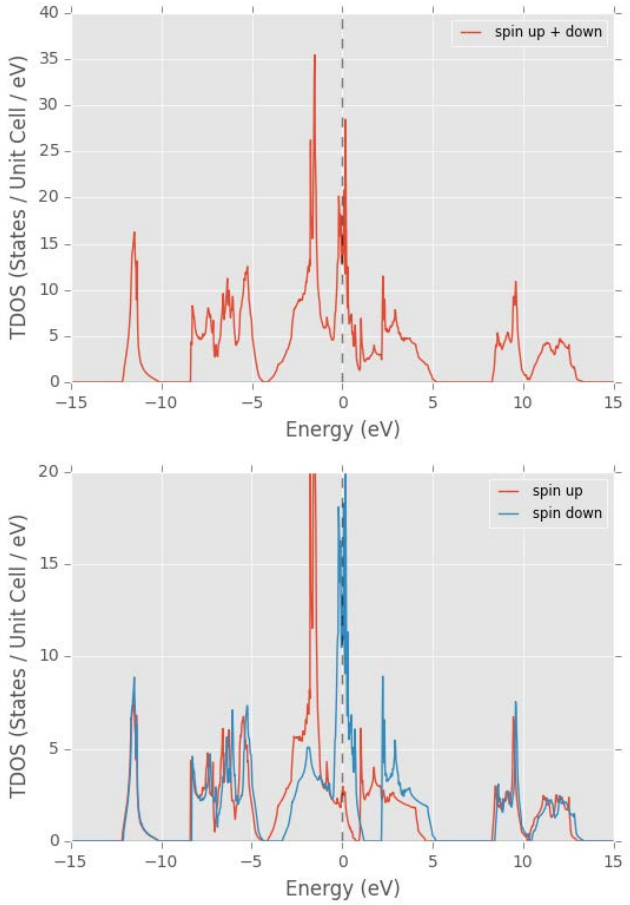

figure output

https://github.com/terencezl/pydass_vasp
https://github.com/terencezl/ScriptsForVASP

```
{'ax_spin_combined': <matplotlib.axes._subplots.AxesSubplot at 0x108b95110>,
 'ax_spin_overlapping': <matplotlib.axes._subplots.AxesSubplot at 0x10b0f5fd0>,
 'data_spin_down': {'columns': ['E', 'tot_down', 'tot_integrated_down'],
  'data': array([[-22.63140452,   0.        ,   0.        ],
                 [-22.60640452,   0.        ,   0.        ],
                 [-22.58040452,   0.        ,   0.        ],
                 ...,
                 [ 15.05159548,   0.        ,  56.        ],
                 [ 15.07659548,   0.        ,  56.        ],
                 [ 15.10159548,   0.        ,  56.        ]])},
 'data_spin_up': {'columns': ['E', 'tot_up', 'tot_integrated_up'],
  'data': array([[-22.63140452,   0.        ,   0.        ],
                 [-22.60640452,   0.        ,   0.        ],
                 [-22.58040452,   0.        ,   0.        ],
                 ...,
                 [ 15.05159548,   0.        ,  56.        ],
                 [ 15.07659548,   0.        ,  56.        ],
                 [ 15.10159548,   0.        ,  56.        ]])}}
```

data output

pydass_vasp (or, badass wasp)

Example: fitting & plotting the equation of state

pydass_vasp.fitting.eos_fit(V, E, plot=True)

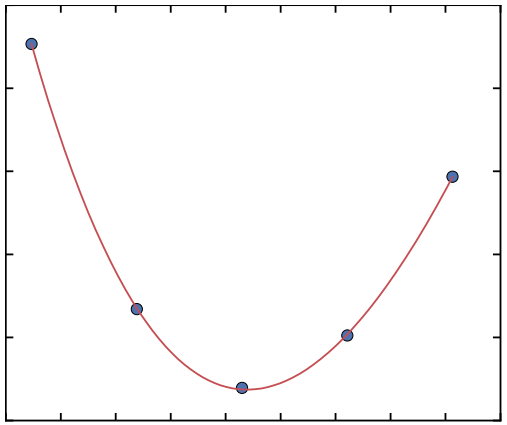

Equation of State (EOS) of TiN

```
Signature: pv.fitting.eos_fit(V, Y, eos='birch_murnaghan', B0_prime=None, plot=False, on_figs=None)
Docstring:
Fit the volume and total energy, or pressure to the Birch-Murnaghan equation of state.

Note: bulk modulus B0 will be returned in the unit of GPa.

Parameters
----------
V: array
    volume (Angstrom^3)
Y: array
    total energy (eV), or pressure (GPa) if eos has '_p'
eos: string
    chosen from ['birch_murnaghan', 'vinet']. Default to 'birch_murnaghan'
B0_prime: float
    Keep B0_prime fixed to a given value or not. Default to None
plot: bool
    whether to plot the data, default to False.
on_figs: list/int
    the current figure numbers to plot to, default to new figures

Returns
-------
a dict, containing
    'params': fitting parameters
    'r_squared': value for evaluating error
    'fitted_data': a dict that has 2D array of fitted data
        easily to Pandas DataFrame by pd.DataFrame(**returned_dict['fitted_data'])
```

https://github.com/terencezl/pydass_vasp
https://github.com/terencezl/ScriptsForVASP

pyvasp-workflow

A simple yet flexible programmatic workflow of describing, submitting and analyzing VASP jobs.

Example: fitting & plotting the equation of state

INPUT/deploy INPUT/run_relax.py INPUT/run_relax-spinel.yaml

```
run_dir: spinel/single_points
pot_type: PAW_PBE
incar:
  ENCUT: 360
  PREC: Normal
  ISPIN: 2
  ISMEAR: 0
  SIGMA: 0.05
  EDIFF: 1e-05
  NSW: 40
  IBRION: 2
  ISIF: 4
  POTIM: 0.2
  EDIFFG: -0.01
  KPAR: 4
  NPAR: 1
  LCHARG: False
  LWAVE: False
  LREAL: A
  LORBIT: 10
kpoints:
  density: 1000
  force_gamma: true
poscar:
  template: POSCAR-spinel
repl_elems: {'Cr': 'Cr_pv'}
volume: 0
```

Output:

stdout
vasprun.xml
OUTCAR
DOSCAR
PROCAR
EIGENVAL
CONTCAR
XDATCAR
OSZICAR
PCDAT
IBZKPT
CHG
WAVECAR
CHGCAR
POTCAR
POSCAR
KPOINTS
INCAR
run_relax-spinel

```
Working directory: /tmppanfshome/psarin/terencezl/CdCr2Se4/spinel/single_points/321.338
 running on   16 total cores
 distrk:  each k-point on    4 cores,    4 groups
 distr:  one band on    4 cores,    1 groups
 using from now: INCAR
 vasp.5.3.3 18Dez12 (build Oct 15 2013 21:29:38) complex

 POSCAR found type information on POSCAR  Cd Cr Se
 POSCAR found :  3 types and      14 ions
 scaLAPACK will be used

 LDA part: xc-table for Pade appr. of Perdew
 POSCAR, INCAR and KPOINTS ok, starting setup
 WARNING: small aliasing (wrap around) errors must be expected
 FFT: planning ...
 WAVECAR not read
 entering main loop
       N       E                     dE             d eps       ncg     rms          rms(c)
DAV:   1     0.920037757382E+03    0.92004E+03   -0.49985E+04  2984   0.110E+03
DAV:   2     0.879159688530E+01   -0.91125E+03   -0.86483E+03  2712   0.333E+02
DAV:   3    -0.760675799379E+02   -0.84859E+02   -0.82173E+02  3056   0.990E+01
DAV:   4    -0.785305371842E+02   -0.24630E+01   -0.24450E+01  2976   0.155E+01
DAV:   5    -0.785818351583E+02   -0.51298E-01   -0.51269E-01  3329   0.222E+00    0.288E+01
DAV:   6    -0.917251139107E+02   -0.13143E+02   -0.11403E+02  2893   0.519E+01    0.517E+01
DAV:   7    -0.738587310148E+02    0.17866E+02   -0.74822E+01  2918   0.565E+01    0.174E+01
DAV:   8    -0.755871488879E+02   -0.17284E+01   -0.99887E+00  2790   0.868E+00    0.767E+00
DAV:   9    -0.752980986066E+02    0.28905E+00   -0.13399E+00  2884   0.529E+00    0.225E+00
DAV:  10    -0.753137482954E+02   -0.15650E-01   -0.28875E-01  2878   0.187E+00    0.834E-01
DAV:  11    -0.753171309590E+02   -0.33827E-02   -0.12503E-02  2830   0.469E-01    0.415E-01
DAV:  12    -0.753181817101E+02   -0.10508E-02   -0.24324E-03  2879   0.163E-01    0.195E-01
DAV:  13    -0.753187152859E+02   -0.53358E-03   -0.69474E-04  2758   0.949E-02    0.806E-02
DAV:  14    -0.753188291361E+02   -0.11385E-03   -0.10337E-04  2939   0.405E-02    0.413E-02
DAV:  15    -0.753188735101E+02   -0.44374E-04   -0.74093E-05  2514   0.258E-02    0.164E-02
DAV:  16    -0.753188809408E+02   -0.74307E-05   -0.93285E-06  1695   0.107E-02
   1 F= -.75318881E+02 E0= -.75318881E+02  d E =-.753189E+02  mag=    12.0000
 curvature:   0.00 expect dE= 0.000E+00 dE for cont linesearch  0.000E+00
 trial: gam= 0.00000 g(F)=  0.203E-04 g(S)=  0.963E-16 ort = 0.000E+00 (trialstep = 0.100E+01)
 search vector abs. value=  0.203E-04
 bond charge predicted
       N       E                     dE             d eps       ncg     rms          rms(c)
DAV:   1    -0.753188988807E+02   -0.25371E-04   -0.33602E-04  2356   0.421E-02    0.913E-03
DAV:   2    -0.753189009312E+02   -0.20504E-05   -0.19619E-05  2048   0.132E-02
   2 F= -.75318901E+02 E0= -.75318901E+02  d E =-.199904E-04  mag=    12.0000
 trial-energy change:   -0.000020  1 .order   -0.000017   -0.000020   -0.000014
 step:   3.1592(harm=  3.1592)  dis= 0.00070  next Energy=   -75.318913 (dE=-0.321E-04)
 reached required accuracy - stopping structural energy minimisation

----------
real     0:38.12
```

Fan Page

Stargazers

All 4 | You know 0

Jianxing
Xiamen
Follow

keke
Joined on Feb 8, 2015
Follow

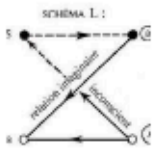

keeeto
Joined on Feb 25, 2013
Follow

jtsun
Joined on Apr 15, 2013
Follow

Asif Iqbal
Grenoble
Follow

keke
Joined on Feb 8, 2015
Follow

addbook
Joined on Mar 23, 2013
Follow

Marco Santia
Joined on Jan 13, 2017
Follow

indi-ras
Joined on Jan 6, 2017
Follow

nicheal
Joined on Apr 27, 2016
Follow

ATAT-tools

```
--> print-as-df.py -h
usage: print-as-df.py [-h] [-c [columns [columns ...]]] [--sortby SORTBY]
                      [--special SPECIAL] [-T from to] [--mu from to]
                      [-x from to] [--reflect] [-p] [-s savefig_name] [-t T]
                      [--trans] [--var VAR] [--thres THRES]
                      [--min_dist MIN_DIST] [--thres_abs THRES_ABS]
                      [--bd_tol BD_TOL] [--return_single]
                      filetype filename [filename ...]

Print the output of a file generated by a program in ATAT.

positional arguments:
  filetype              supports outputs of emc2 and phb. Also can be gs
                        (gs.out), fit (fit.out), predstr (predstr.out), and
                        the mmaps counterparts mgs, mfit, mpredstr
  filename              the actual file name, can be 1 or more.

optional arguments:
  -h, --help            show this help message and exit
  -c [columns [columns ...]]
                        the columns of the dataframe
  --sortby SORTBY       the column name to sort
  --special SPECIAL     generated by mmaps? emc2 canonical mode? emc2 innerT?
```

```
--> print-as-df.py clusters clusters.out
                  d  multi                                          coords       eci
n_pts idx
0     1   0.000000      1                                              []  0.026182
1     1   0.000000      2                                  [[1.0, 1.0, 1.0]] -0.000163
2     1   2.625000      4        [[1.0, 1.0, 1.0], [0.75, 0.75, 1.25]] -0.001730
      2   4.286607     12  [[0.25, 0.25, 0.25], [-0.25, -0.25, 0.25]]  0.000287
      3   5.026492     12      [[0.25, 0.25, 0.25], [-0.5, 0.0, 0.5]] -0.000716
      4   6.062178      6   [[0.25, 0.25, 0.25], [-0.75, 0.25, 0.25]] -0.000851
      5   6.606105     12     [[0.25, 0.25, 0.25], [-0.5, -0.5, 0.0]]  0.000105
      6   7.424621     24  [[0.25, 0.25, 0.25], [-0.75, -0.25, 0.75]] -0.000490
      7   7.875000     12      [[0.25, 0.25, 0.25], [-1.0, 0.0, 0.0]] -0.000237
      8   7.875000      4     [[0.25, 0.25, 0.25], [-0.5, -0.5, 1.0]] -0.000224
      9   8.573214     12  [[0.25, 0.25, 0.25], [-0.75, -0.75, 0.25]]  0.000019
      10  8.966082     24     [[0.25, 0.25, 0.25], [-1.0, -0.5, 0.5]] -0.000128
      11  9.585145     24  [[0.25, 0.25, 0.25], [-1.25, -0.25, 0.25]]  0.000300
```

plot-maps.py

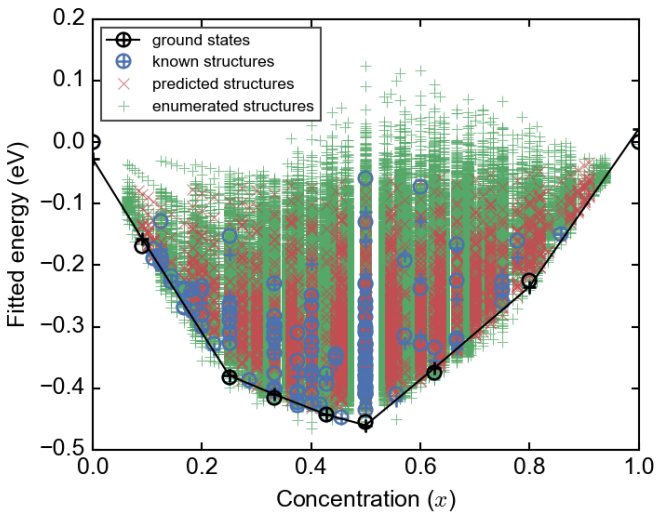

plot-phb.py phb-*.out

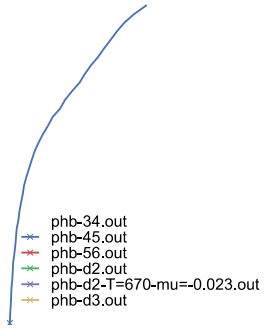

Rocksalt-structure TMNs Comparison

M	*a* (Å)	C_{11} (GPa)	C_{12} (GPa)	C_{44} (GPa)	Mechanical Stability	E_{coh} (eV/atom)
Sc	4.543	399.3	95.9	157.6	S	6.5
	4.516[a]	390[a]	105[a]	166[a]		
	4.516[b]	354.06[b]	100.20[b]	170.00[b]		
	4.44[c]					
Ti	4.258	603	118.7	159.6	S	7.01
	4.253[a]	560[a]	135[a]	163[a]		
	4.250[b]	534.67[b]	117.70[b]	175.42[b]		
	4.241[c]	625[d]	165[d]	163[d]		
		507[e]	96[e]	163[e]		
V	4.133	620.5	166.8	116.5	S	6.08
	4.127[a]	660[a]	174[a]	118[a]		
	4.119[b]	628.70[b]	144.63[b]	147.41[b]		
	4.139[c]	533[d]	135[d]	133[d]		
Cr	4.064	569.2	209	4.6	S	4.58
	4.063[b]	502.77[b]	214.23[b]	4.05[b]		

[a] D. Holec, M. Friák, J. Neugebauer, and P. H. Mayrhofer, Phys. Rev. B **85**, 64101 (2012). (GGA)
[b] M. G. Brik and C. G. Ma, Comput. Mater. Sci. **51**, 380 (2012). (GGA)
[c] Powder Diffraction Files: 03-065-0565 (TiN), 00-035-0753 (ZrN), 00-033-0592 (HfN), (International Center for Diffraction Data) PDF-2 (Expt.)
[d] J. O. Kim, J. D. Achenbach, P. B. Mirkarimi, M. Shinn, and S. A. Barnett, J. Appl. Phys. **72**, 1805 (1992). (Expt.)
[e] W. J. Meng and G. L. Eesley, Thin Solid Films **271**, 108 (1995). (Expt.)

Pyrite-structure TMNs Comparison

	a (Å)	*x*	C_{11} (GPa)	C_{12} (GPa)	C_{44} (GPa)	*B* (GPa)
PtN_2 This work	4.877	0.416	661.9	69.3	128.8	266.9
PtN_2 LAPW-GGA [a]	4.862	0.415	668	78	133	272
PtN_2 PP-PW91 [b]	4.877	0.417	713	90	136	298
PtN_2 PP-PBE [c]	4.848	0.415	696	83	136	288
PtN_2 PAW-PW91 [d]	4.875					278
PtN_2, Exp. [e]	4.804					372

[a] R. Yu, Q. Zhan, and X. F. Zhang, Appl. Phys. Lett. **88**, 51913 (2006).
[b] H. Gou, L. Hou, J. Zhang, G. Sun, L. Gao, and F. Gao, Appl. Phys. Lett. **89**, 141910 (2006).
[c] A. F. Young, J. A. Montoya, C. Sanloup, M. Lazzeri, E. Gregoryanz, and S. Scandolo, Phys. Rev. B **73**, 153102 (2006).
[d] J. C. Crowhurst, A. F. Goncharov, B. Sadigh, C. L. Evans, P. G. Morrall, J. L. Ferreira, and A. J. Nelson, Science **311**, 1275 (2006).
[e] E. Gregoryanz, C. Sanloup, M. Somayazulu, J. Badro, G. Fiquet, H. K. Mao, and R. J. Hemley, Nat. Mater. **3**, 294 (2004).

Calculation Parameters

We performed *ab initio* DFT computations using the Vienna Abinitio Simulation Package (VASP) with the projector-augmented wave method (PAW) and Purdew–Burke–Ernzerhoff (PBE) generalized gradient approximation (GGA). We selected the potentials of Ti_sv, Zr_sv, Hf_pv and N, where "_sv" denotes that the semi-core s and p electrons are also included, while "_pv" specifies the semi-core p electrons. The plane wave energy cutoff was chosen to be 520 eV to ensure correct cell volume and shape relaxations. The k-point meshes were created with k-points per reciprocal atom (KPPRA) of 4000. Methfessel-Paxton order 1 smearing was used with a sigma value as small as 0.1 eV. The convergence criterion was set to 10^{-5} eV in energy during the electronic iterations. For structural optimization, the cell volume, shape and atomic positions were allowed to relax until stress was minimized and forces on any atom were below 0.02 eV/Å.

Published work: Z.T.Y. Liu, B.P. Burton, S. V Khare, and D. Gall, *J. Phys. Condens. Matter* **29**, 35401 (2017).

Calculation Parameters

Phase diagrams were generated for $Ti_{1-x}Zr_xN$, $Ti_{1-x}Hf_xN$ and $Zr_{1-x}Hf_xN$ using the Alloy Theoretic Automated Toolkit (ATAT). Included in ATAT, the MIT Ab-initio Phase Stability (maps) code was used to generate the energy landscapes and CEs. The Easy Monte Carlo Code (emc2 and phb) was used to perform MC simulations to obtain the phase diagrams. With well-converged CEs, a box of 12 × 12 × 12 2-atom unit cells (1728 exchangeable sites) was chosen in the semi-grand canonical (SGC) ensemble simulations, in which chemical potential and temperature (T) can be given as external conditions. Chemical potential is defined as $\mu_i = \left({}^{\partial G}/_{\partial n_i}\right)_{T,n_{j\neq i}}$, where G is the Gibbs free energy, n_i is the number of atoms of species i in the simulation cell. In a binary system $A_{1-x}B_x$, $\mu = \mu_A - \mu_B$ is used as the input. For each μ and T point, sufficient MC passes were used to make sure the composition (x) reached a precision of 0.01. In a SGC ensemble the composition jumps from one boundary to another, skipping the two-phase region in response to the change in μ. This jumping prevents the determination of spinodal curves in this ensemble.

Published work: Z.T.Y. Liu, B.P. Burton, S. V Khare, and D. Gall, *J. Phys. Condens. Matter* **29**, 35401 (2017).

Vickers Hardness

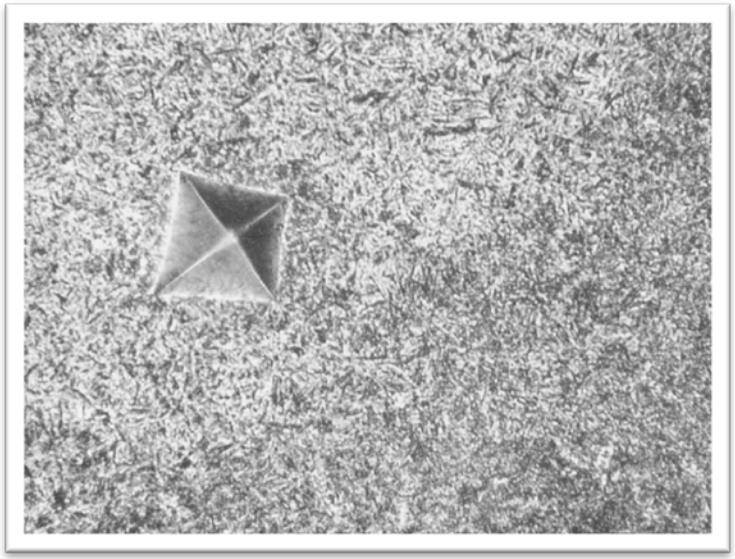

http://en.wikipedia.org/wiki/Vickers_hardness_test

Brittleness/Ductility

brittle

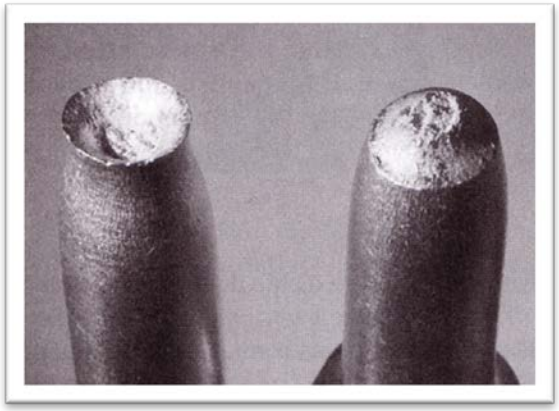

ductile

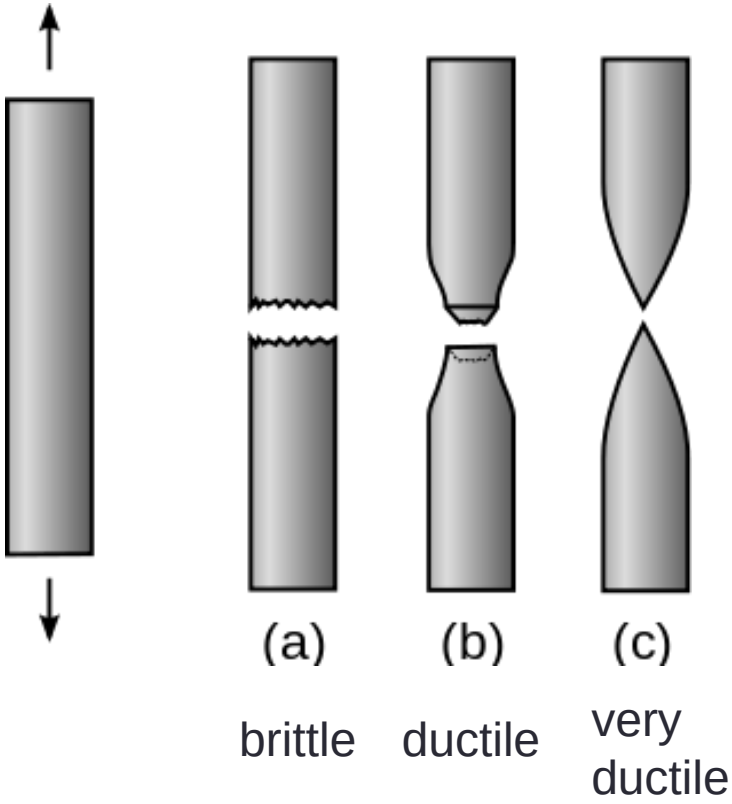

http://oregonstate.edu/instruct/engr322/Homework/AllHomework/S09/ENGR322HW7.html
http://en.wikibooks.org/wiki/Advanced_Structural_Analysis/Part_I_-_Theory/General_Properties_of_Materials

Elastic Constants

- There are two ways to determine the elastic constants.
  - Energy-strain
  - Stress-strain
- Here we employed the energy-strain method, which requires fitting the relation to a 2nd order polynomial. The strain tensor has the general form below.
- There are three independent elastic constants, C_{11}, C_{12} and C_{44} for the cubic crystallographic system. Therefore, we applied three sets of strains to the unit cell.

$$\varepsilon_{ij} = \begin{pmatrix} e_1 & \frac{e_6}{2} & \frac{e_5}{2} \\ \frac{e_6}{2} & e_2 & \frac{e_4}{2} \\ \frac{e_5}{2} & \frac{e_4}{2} & e_3 \end{pmatrix}$$

Strain	Non-zero Strain Elements	$\Delta E/V_0$
1	$e_1=e_2=e_3=\delta$	$3/2\ (C_{11}+2C_{12})\delta^2$
2	$e_1=\delta$, $e_2=-\delta$, $e_3=\delta^2/(1-\delta^2)$	$(C_{11}-C_{12})\delta^2$
3	$e_6=\delta$, $e_3=\delta^2/(4-\delta^2)$	$1/2\ C_{44}\delta^2$

Equation for Calculating Vickers Hardness (H_V)

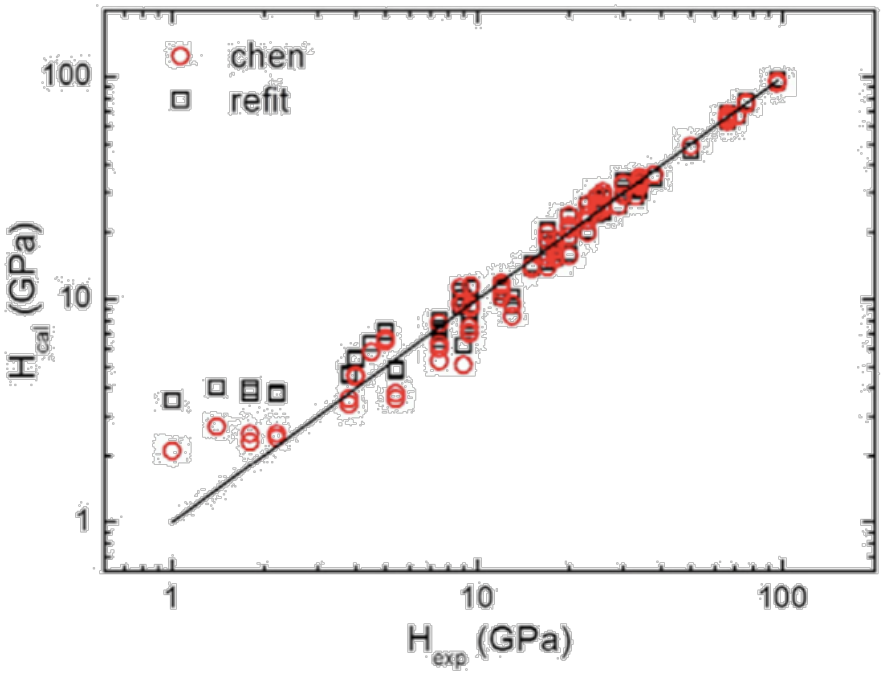

$$H_V = 0.92k^{1.137}G^{0.708}$$

$k = G/B$

k - Pugh's ratio
G - shear modulus

Data points (40+ compounds):

Covalent: C, Si, BN…
Ionic: NaCl, KBr…
Metallic glasses

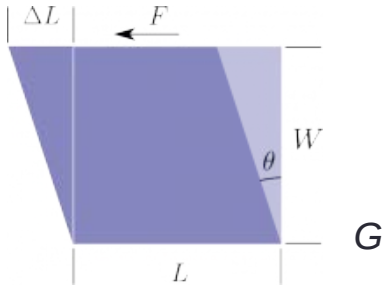

Figure adapted from Tian et al.
Y. Tian, B. Xu, and Z. Zhao, Int. J. Refract. Met. Hard Mater. 33, 93 (2012).
X. Q. Chen, H. Y. Niu, D. Z. Li and Y. Y. Li, *Intermetallics* 19, 1275 (2011).

Anti-Correlation

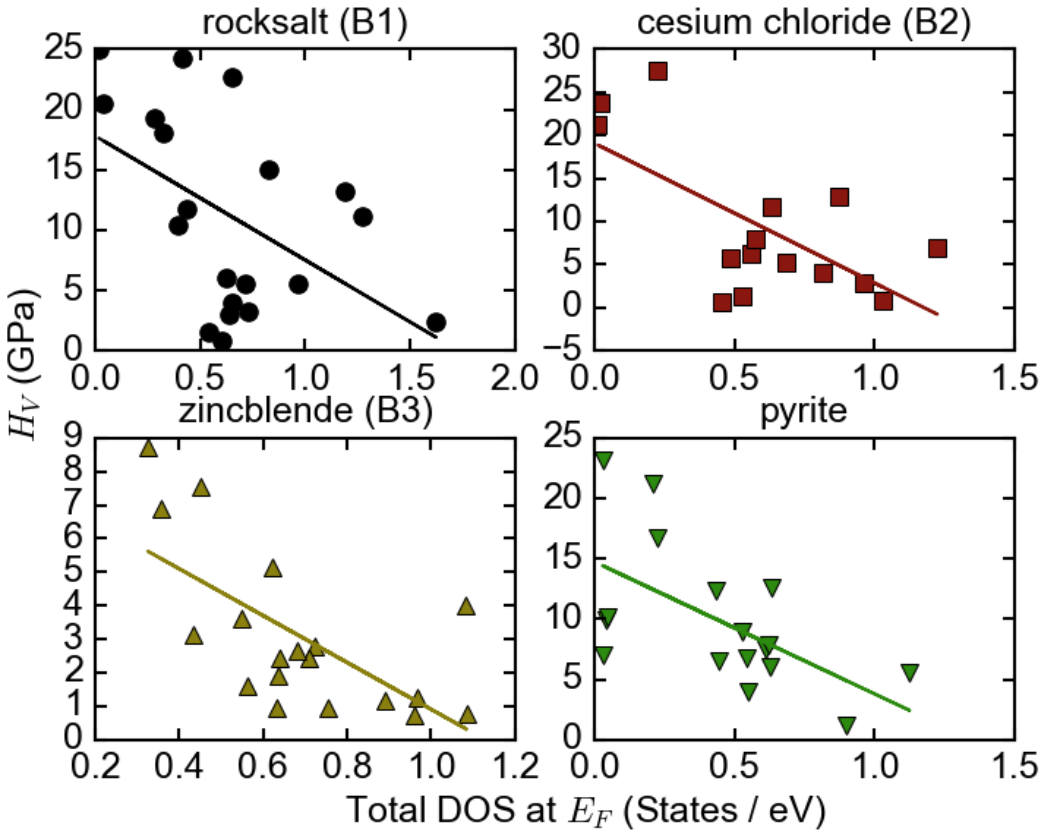

Difference in B and G

$B = (C_{11} + 2C_{12})/3$

$G_v = [(C_{11} - C_{12}) + 3C_{44}]/5$

$G_R = [5(C_{11} - C_{12})C_{44}]/[4C_{44} + 3(C_{11} - C_{12})]$

$G = G_{VRH} = (G_v + G_R)/2$

$k = G/B$

Difference in *B* and *G*

Bulk modulus (*B*) only measures the resistance to isotropic hydrostatic pressure, while shear modulus (*G*) measures the resistance to anisotropic shear strain.

TiN (*G*: 187.2 GPa, *B*: 318.3 GPa, H_V: 23 GPa)

β-SiC (*G*: 191.4 GPa, *B*: 224.7 GPa, H_V: 34 GPa)

Gao FM, He JL, Wu ED, Lu SM, Yu LD, Li DC, et al. Phys Rev Lett 2003;91: 015502.
Gou HY, Hou L, Zhang JW, Gao FM. Appl Phys Lett 2008;92:241901.

Formulation for H_V (Vickers Hardness)

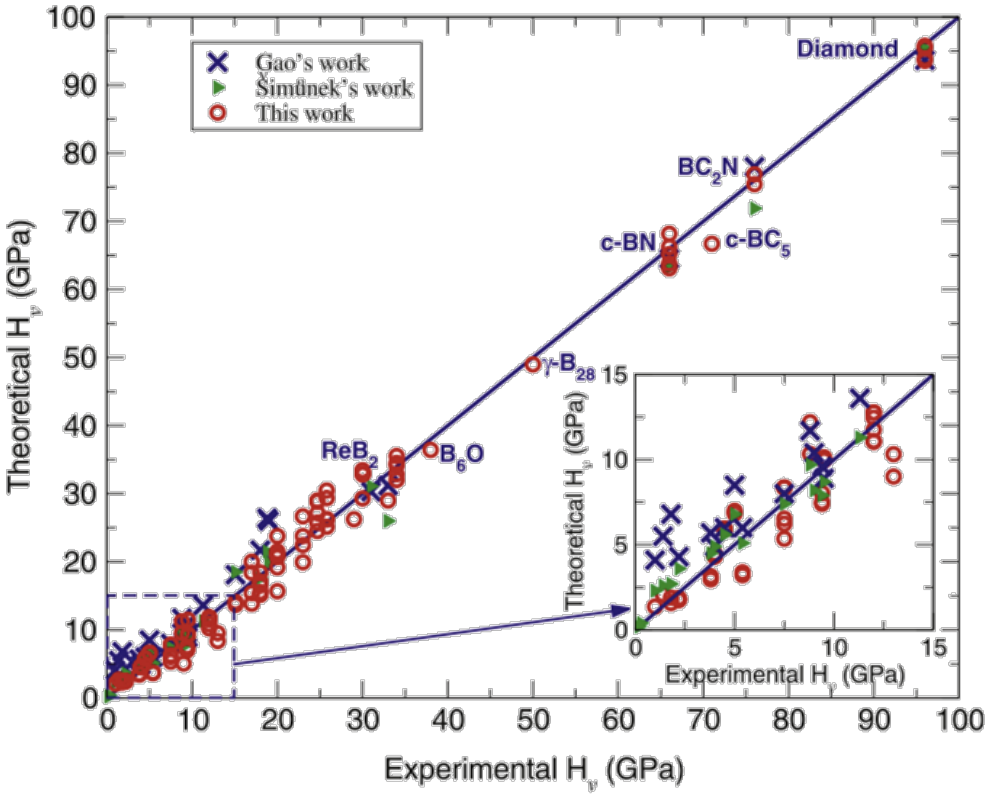

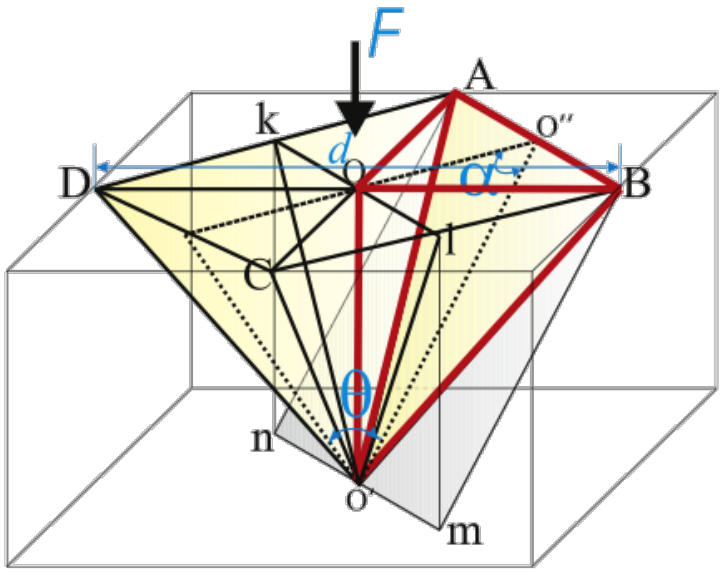

$$H_V = 2\left(k^2 G\right)^{0.585} - 3$$

X. Q. Chen *et al.*, Intermetallics **19**, 1275 (2011)

Crystal	H_{Exp} (GPa)	H_{Tian} (GPa)	$H_{Simunek}$ (GPa)	H_{Xue} (GPa)	H_{Chen} (GPa)
C	96[a]	93.6	95.4[b]	90[e]	94.6[f]
Si	12[a]	13.6	11.3[b]	14[e]	11.2[f]
Ge	8.8[b]	11.7	9.7[b]	11.4[e]	10.4[f]
SiC	31[b]	30.3	31.1[b]	27.8[e]	33.8[f]
BN	63[a]	64.5	63.2[b]	47.7[e]	65.3[f]
BP	33[a]	31.2	26[b]	24.9[e]	29.3[f]
BAs	19[b]	26	19.9[b]	21.1[e]	–
AlN	18[a]	21.7	17.6[b]	14.5[e]	16.8[f]
AlP	9.4[a]	9.6	7.9[b]	7.4[e]	7.2[f]
AlAs	5.0[a]	8.5	6.8[b]	6.3[e]	6.6[f]
AlSb	4.0[a]	4	4.9[b]	4.9[e]	4.4[f]
GaN	15.1[a]	18.1	18.5[b]	13.5[e]	13.9[f]
GaP	9.5[a]	8.9	8.7[b]	8[e]	9.9[f]
GaAs	7.5[a]	8	7.4[b]	7.1[e]	7.8[f]
GaSb	4.5[a]	6	5.6[b]	4.5[e]	5.8[f]
InN	9[a]	10.4	8.2[b]	7.4[e]	7.4[f]
InP	5.4[a]	6	5.1[b]	3.9[e]	3.7[f]
InAs	3.8[a]	3.8	5.7[b]	4.5[e]	3.3[f]
InSb	2.2[a]	4.3	3.6[b]	2.2[e]	2.4[f]
ZnS	1.8[b]	6.8	2.7[b]	2.4[e]	2.4[f]
ZnSe	1.4[b]	5.5	2.6[b]	1.8[e]	2.7[f]
ZnTe	1[b]	4.1	2.3[b]	0.9[e]	2.1[f]
TiC	32[c]	34	18.8[b]	23.9[e]	27[f]
TiN	20.6[c]	21.6	18.7[b]	23.8[h]	23.3[f]
ZrC	25[c]	21	10.7[g]	15.7[h]	27.5[f]

Y. Tian *et al.*, Int. J. Refract. Met. Hard Mater. **33**, 93 (2012).

Crystal	H_{Exp} (GPa)	H_{Tian} (GPa)	$H_{Simunek}$ (GPa)	H_{Xue} (GPa)	H_{Chen} (GPa)
ZrN	15.8[c]	16.7	10.8[g]	15.9[h]	–
HfC	26.1[c]	26.8	10.9[g]	15.6[h]	–
HfN	16.3[c]	18	10.6[g]	15.2[h]	19.2[f]
VC	27.2[c]	23	25.2[g]	17.5[h]	26.2[f]
VN	15.2[c]	14.9	26.5[g]	16.5[h]	–
NbC	17.6[c]	16.1	18.3[b]	12.8[h]	15.4[f]
NbN	13.7[c]	13.6	19.5[b]	12[h]	14.7[f]
TaC	24.5[c]	26	19.9[g]	14.7[h]	–
TaN	22[c]	20	21.2[g]	14.3[h]	–
CrN	11[c]	11	36.6[g]	19.2[h]	–
WC	30[c]	31	21.5[b]	20.6[e]	31.3[f]
Re_2C	17.5[j]	19.7[j]	11.5[g]	16.2[h]	26.4[i]
Al_2O_3	20[c]	18.8	13.5[g]	18.4[h]	20.3[i]
MgO	3.9[d]	4.5	4.4[g]	5.4[h]	24.8[i]
LiF	1[d]	0.8	2.2[g]	–	8.5[i]
NaF	0.6[d]	0.85	1[g]	–	5.7[i]
NaCl	0.2[d]	0.4	0.4[b]	–	2.4[i]
KCl	0.13[d]	0.18	0.2[b]	–	2.3[i]
KBr	0.1[d]	0.23	0.2[g]	–	0.1[i]

[a] Reference [34].
[b] Reference [37].
[c] Reference [32].
[d] Reference [60].
[e] Reference [58].
[f] Reference [30].
[g] Calculated by authors using method [36].
[h] Caculated using [35].
[i] Calculated with [30].
[j] Referenece [52].

k vs P_C

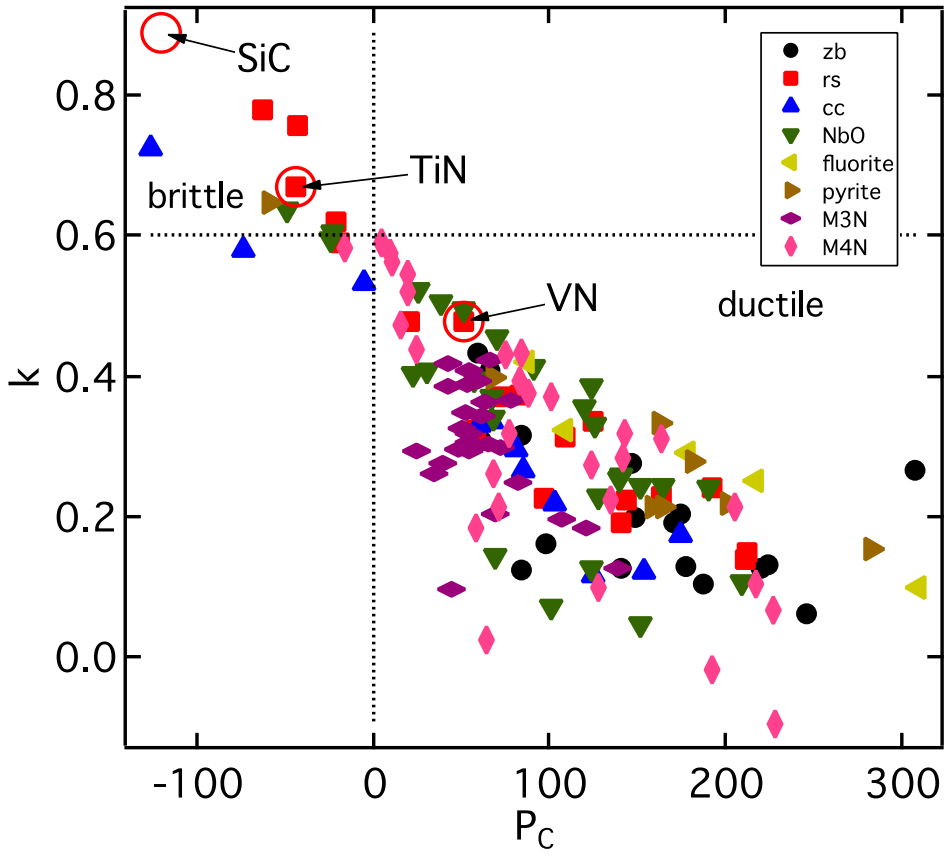
SiC
TiN
VN
brittle
ductile
zb
rs
cc
NbO
fluorite
pyrite
M3N
M4N
0.8
0.6
0.4
0.2
0.0
κ
-100
0
100
200
300
P_C

Chen's formulation for calculating H_V (Vicker's Hardness)

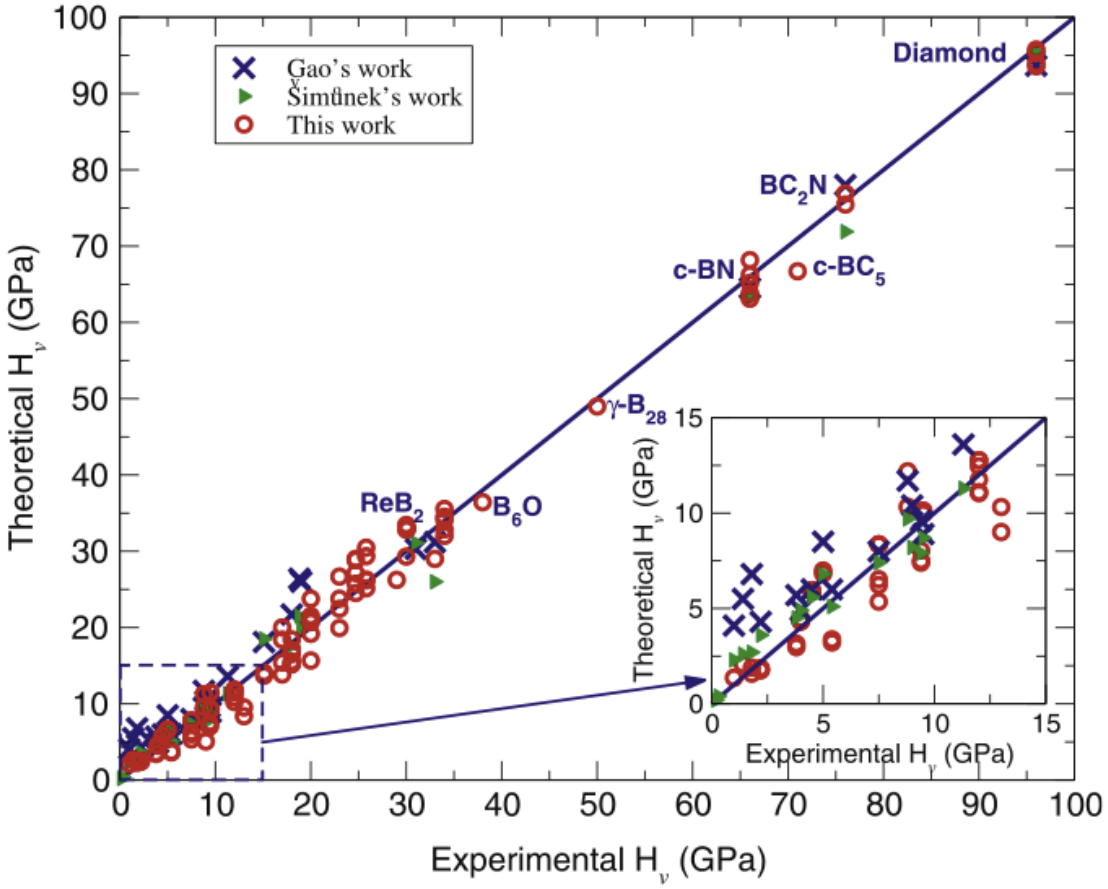

$$B = (C_{11} + 2C_{12})/3$$

$$G_v = [(C_{11} - C_{12}) + 3C_{44}]/5$$

$$G_R = [5(C_{11} - C_{12})C_{44}]/(4C_{44} + 3C_{11} - 3C_{12})$$

$$G = G_{VRH} = (G_v + G_R)/2$$

$$k = G/B$$

$$H_v = 2\left(k^2 G\right)^{0.585} - 3$$

X. Q. Chen *et al.*, Intermetallics **19**, 1275 (2011)

Equation for Calculating Vickers Hardness (H_V)

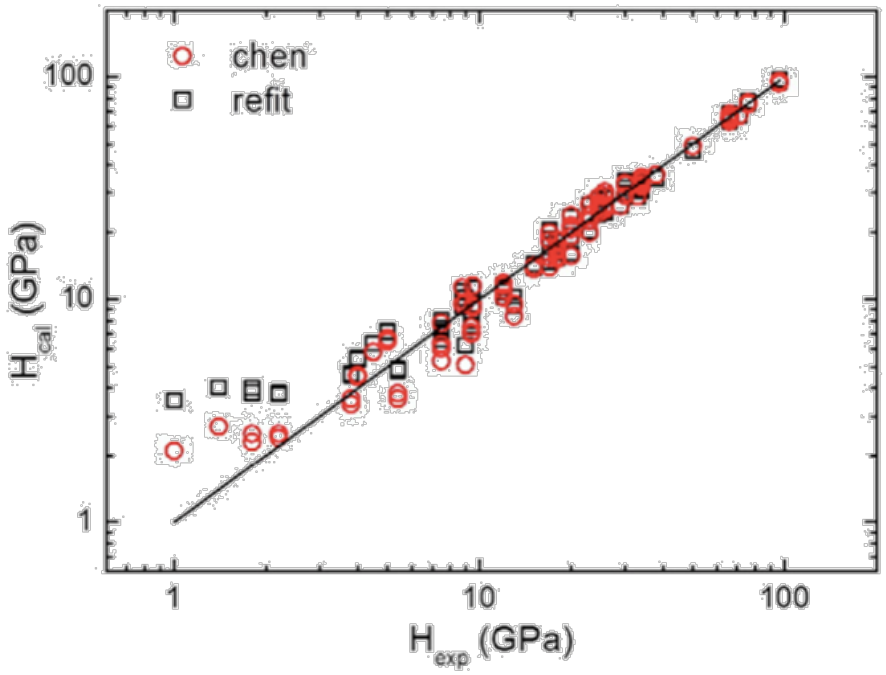

$$H_V = 0.92k^{1.137}G^{0.708}$$

$k = G/B$

k - Pugh's ratio
G - shear modulus

Data points (40+ compounds):

Covalent: C, Si, BN…
Ionic: NaCl, KBr…
Metallic glasses

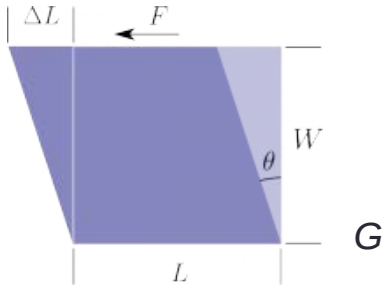

Figure adapted from Tian et al.
Y. Tian, B. Xu, and Z. Zhao, Int. J. Refract. Met. Hard Mater. 33, 93 (2012).
X. Q. Chen, H. Y. Niu, D. Z. Li and Y. Y. Li, *Intermetallics* 19, 1275 (2011).